Coupled tectonic evolution of Andean orogeny and global climate

Rolando Armijo, Robin Lacassin, Aurélie Coudurier-Curveur, Daniel Carrizo

Earth-Science Reviews 143 (2015) 1–35

Contents lists available at ScienceDirect

Earth-Science Reviews

journal homepage: www.elsevier.com/locate/earscirev

Coupled tectonic evolution of Andean orogeny and global climate

Rolando Armijo [a,c,*], Robin Lacassin [a,c], Aurélie Coudurier-Curveur [a,c], Daniel Carrizo [b,c]

[a] Institut de Physique du Globe de Paris, Sorbonne Paris Cité, Univ Paris Diderot, UMR 7154 CNRS, F-75005 Paris, France
[b] Advanced Mining Technology Center, Universidad de Chile, Tupper 2007, Santiago, Chile
[c] Laboratoire International Associé Montessus de Ballore (LIA MdB) CNRS (France)-CONICYT Chile

ARTICLE INFO

Article history:
Received 28 March 2014
Accepted 19 January 2015
Available online 29 January 2015

Keywords:
Orogeny
Climate
Andes
Subduction
Tectonics
Geomorphology

ABSTRACT

The largest tectonic relief breaking the Earth's surface (13 km vertically) is at the subduction margin of the Andes, which generates routinely megathrust earthquakes (Mw > 8.5) and drives the paradigmatic Andean orogen. Here we present key geologic evidence to reassess first-order features of geomorphology and tectonics across the Central Andes, where the orogen includes the Altiplano Plateau and attains its maximum integrated height and width. The Andean subduction margin has a stepped morphology dominated by the low-relief Atacama Bench, which is similar to a giant uplifted terrace, slopes gently over a width of 60–100 km from the Andes to the Pacific, and runs over more than 1000 km of coastal length. We find that the genesis of stepped morphology at the Andean seaboard is due to concomitant development of large west-vergent thrusts parallel to the subduction interface and increasing aridity in the Atacama Desert, which keeps an unprecedented large-scale record of interplaying tectonics and Cenozoic climate change. Incorporating our results with published geological knowledge demonstrates that Andean orogeny is characterized by trench-perpendicular (bivergent) and trench-parallel (bilateral) growth over the past 50 Myr, associated with positive trench velocity toward the continent (trench advance) and subduction of a wide slab under South America. We hypothesize that a global plate tectonic reorganization involving long-lasting viscous mantle flow has probably forced both, Andean orogeny and global climate cooling since ~50 Ma. In contrast, two important stepwise pulses of increasing aridity and trench-perpendicular Andean growth appear to be results of changes in erosion rates due to global Late Eocene and Middle Miocene cooling events.

Contents

* Corresponding author. Tel.: +33 1 83957607.
E-mail address: armijo@ipgp.fr (R. Armijo).

http://dx.doi.org/10.1016/j.earscirev.2015.01.005

1. Introduction

The Himalayas–Tibet and the Andes–Altiplano – the largest active mountain belts creating relief in our planet – have been caused by radical changes in plate-boundary conditions. In both cases, subduction of oceanic lithosphere beneath an initially flat continental margin, close to sea-level, evolved to critical tectonic conditions triggering substantial shortening and thickening of marginal continental lithosphere, either by continental collision or by an equivalent process producing similar effects. Therefore, deformation should be similarly partitioned between elastic deformation generating routinely megathrust earthquakes and distributed deformation accumulating over millions of years in the marginal continent. Mechanical coupling and structure of the plate interface in the two cases should be comparable as well. However, while the India–Asia continental collision zone appears to be a structurally complex interface between subducting continental lithosphere and a deforming continental region (e.g. Molnar and Lyon-Caen, 1988; Avouac, 2003; Grandin et al., 2012), the subduction margin of South America is generally assumed to be a simple subduction interface between a plunging oceanic slab and a non-deforming continental forearc (e.g. Uyeda and Kanamori, 1979; Isacks, 1988).

Here we present results from a study of the Andean subduction margin and its evolution to conditions sustaining the Andean orogeny, over a range of scales in space and time. Our approach integrates key geomorphological and geological observations along the Central Andean subduction margin with a critical review of the literature. It is aimed at solving three first-order problems. The first one is to define specific structural characteristics and degree of complexity of the Andean subduction margin (representing 13 km of vertical tectonic relief), enabling us to establish a tectonic comparison with the Himalayan margin, and to elucidate how the growing marginal relief of the Andes can be supported by crustal shortening and thickening in the overriding South America plate. The second objective is to use first-order constraints obtained from the climatically-controlled aspects of the geomorphology and geology of the subduction margin – which is characterized by the imprint of the Andean tectonic landscape in the Atacama Desert – to reconstruct an overall section of the Andean orogen, allowing us to elucidate its tectonic and morphologic growth processes over the continent. Our third goal is to address possible relationships of Andean orogeny with plate-scale tectonic evolution and global climate change.

Earlier studies of upper crustal structure (down to ~15 km depth and mainly conducted with seismic sounding approaches) demonstrate that the Central Andes (Andes–Altiplano Plateau, core of the Andean orogen) have grown during the Cenozoic by crustal shortening (of up to ~ > 300 km) and thickening processes, associated with significant east-directed thrusting along its east flank, toward the continent (e.g. Suárez et al., 1983; Sheffels, 1990; Kley et al., 1999; Elger et al., 2005; McQuarrie et al., 2005; Barnes and Ehlers, 2009; Whipple and Gasparini, 2014) (Figs. 1 and 2). The surface geology shows also that crustal shortening started at ~50–30 Ma close to the subduction zone associated with west-directed thrusting in the Western Cordillera, then propagated progressively away from the subduction zone, first by a jump (at ~40 Ma) to the Eastern Cordillera, then since ~10 Ma to the easternmost Subandes Belt (Sempere et al., 1990; Allmendinger et al., 1997; Gregory-Wodzicki, 2000; McQuarrie et al., 2005; Oncken et al., 2006; Arriagada et al., 2008; Barnes and Ehlers, 2009; Carrapa et al., 2011; Charrier et al., 2013). Shortening of the Altiplano Plateau occurred later (since ~30 Ma: Sempere et al., 1990; Elger et al., 2005; Oncken et al., 2006) – and is less (as shown by crustal thickness of ~70 km) – than in the two flanking Western Cordillera and Eastern Cordillera belts, which are both sustained by deeper crustal roots (~74–80 km thickness) (Yuan et al., 2000; Wölbern et al., 2009). The most accepted view of Andes crustal thickening describes the orogen as a large back-arc thrust wedge transported upon the adjacent continent (South America), with subsidiary tectonic activity – accretionary or non-accretionary – in the fore-arc (e.g. Stern, 2002; Lamb and Davis, 2003; McQuarrie et al., 2005). That view is readily comparable to the paradigmatic description of the Cordilleran Belt of North America. However, it has been recently argued that much like the Himalaya–Tibet Plateau (core of the Himalayan orogen), the structure of the Central Andes is symmetrically bivergent (Armijo et al., 2010a), as suggested earlier by (Sheffels, 1990; Haschke and Gunther, 2003; Elger et al., 2005). In this work, we explore the hypothesis that continued support of the Andean orogen, particularly the uplift and crustal thickening processes under the Western Cordillera, could be kinematically coupled with the subduction interface, with the same westward vergence. That hypothesis differs from current kinematic models suggesting that deformation of the Andean subduction margin would depend only upon processes at the eastern flank of the orogen (e.g. Isacks, 1988; McQuarrie et al., 2005; Jordan et al., 2010; Lamb, 2011). Another accepted description states that Andean deformation has progressed by widespread synchronous pulses (or phases: e.g. Noble et al., 1979; Coira et al., 1982; Mégard, 1984; Charrier et al., 2007). However, crustal contraction has propagated not only across the Andean belt, but also laterally by southward trench-parallel growth of the Western Cordillera, as indicated by ages of deformation younging southwards to the latitude of Santiago, where shortening started at ~25 Ma (e.g. Armijo et al., 2010a) (Fig. 1). In this work, we explore the hypothesis that shortening processes in the Andean orogen are basically diachronic.

Our study strategy starts by analysing first-order features at the leading edge of the Andean subduction margin, where the Cenozoic geology and morphology are marked by the widespread occurrence of the Atacama Desert (here the Atacama Desert concept includes the Sechura Desert of southern Peru). The approach is centred on determining the

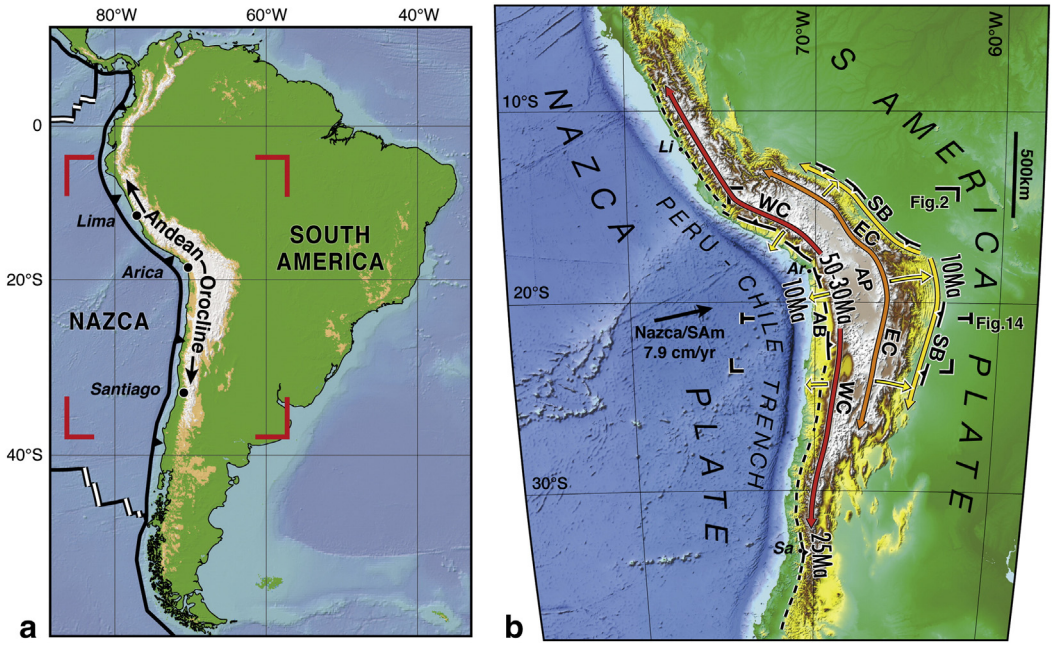

Fig. 1. The Andean orogen. (a). Tectonic framework of Central Andes, with bend at Arica marking the hinge of Andean Orocline (Isacks, 1988)). Extent of orocline is outlined (between 7°S and 33°S). (b). Enlarged topography of orocline region (located by red corners in a) with outline of main mountain belts. Trench-parallel double arrows indicate location and easterly decreasing extent of Western Cordillera (WC, red), Eastern Cordillera (EC, orange) and Subandes Belt (SB, yellow), associated with development of Andean Orocline. AP is Altiplano Plateau. The bivergent trench-perpendicular orogenic growth (yellow arrows) is constrained by the decreasing age of shortening across the orogen: compare the main shortening ages at the centre of the WC (50–30 Ma, in Mega Annum) with the age of shortening propagation to the SB (10 Ma) and the coeval initiation of the uplift of the Atacama Bench (AB). The trench-parallel (lateral) orogenic growth is indicated by the southward and northward decrease in the amount of shortening across the orogen (with respect to the Andean Orocline hinge) and by the southward decrease of shortening initiation age along the WC: compare ages at the central WC (50–30 Ma at 20°N) with ages in the southern WC (25 Ma at 35°S). Segmented black lines with triangular ticks represent main bivergent mountain fronts. The trace of the section in Fig. 14 is given. The Nazca/South America horizontal convergence vector is from NUVEL-1A model (DeMets et al., 1994). Li is Lima; Ar, Arica; Sa, Santiago. (For interpretation of the references to colour in this figure legend, the reader is referred to the web version of this article.)

processes that developed a large-scale, low-relief surface perched on the west flank of the Western Cordillera, along the Andean margin (Fig. 3), which we denote here as the Atacama Bench.

Morphologically, the Atacama Bench has the shape of a giant terrace 1–2 km high that stretches over a length of more than 1000 km, mantled by sediment and sloping gently oceanward (<1°) (Figs. 2 and 3). The northern part of the Atacama Bench is incised by deep canyons, suggesting substantial tectonic land uplift (Mortimer, 1973; Tosdal et al., 1984; Sébrier et al., 1988; Schlunegger et al., 2006; Schildgen et al., 2007; Thouret et al., 2007). However, it has for long been believed that tectonic uplift of coastal regions, as described in north Chile, is relatively old (of Oligocene–early Miocene age) and de-correlated from younger incision processes, which would be controlled by wetter climate conditions (Mortimer and Saric, 1975; García et al., 2011). Here we analyse the morphological and structural characteristics of the Atacama Bench, to distinguish first-order observations and revise interpretations to characterize the interplay of tectonic evolution with Cenozoic climate change throughout the Pacific seaboard of the growing Andean orogen.

Structurally, the Atacama Bench appears to be bounded by fault systems at the flank of the Western Cordillera and offshore near the coastline (Fig. 2), but the nature and significance of those structures are unclear and a subject of controversy (e.g. see Astini and Dávila (2010) vs. Armijo et al. (2010b)). Here we analyse the structure of the Western Cordillera, which encompasses what appears to be its hidden backbone (an earlier mountain range called "Incaic" range (Charrier et al., 2013)) that is truncated by a widespread erosion surface (Choja Pediplain (Galli-Olivier, 1967)) and covered by unconformable younger deposits (~ ≤ 30 Ma) (Fig. 4). We hypothesize that the Atacama Bench and the hidden structure of the Western Cordillera are to scale with the subduction margin of the Central Andes and so can help retrieving primary quantitative constraints on the Andean orogeny and climate change.

We use the high-resolution coverage of topography provided by the Shuttle Radar Topography Mission (standard SRTM3 with 90 m resolution) and recent compilations of topography with bathymetry compilation designated SRTM 30+ with 900 m resolution (Becker et al., 2009), allowing us to define major morphological units composing the subduction margin of the Central Andes and to elucidate the structural framework of the Atacama Bench explaining its uplift. Then, we incorporate geomorphic results with a review of geological information and with new field-based observations of structure targeted at key areas of the hidden "Incaic" backbone of the Western Cordillera.

The second step of our strategy is to incorporate our results on the Andean subduction margin with relevant data on Andean geology and geomorphology, which enables us to conduct a reassessment of the tectonic–climatic evolution of the Andean subduction margin throughout the late Cenozoic and to construct a simple 2D section of modern structural features at latitude 21°S to scale with crustal shortening and thickening throughout the core of Andean orogen. An important condition for that model is consistency with present-day coupling processes across the plate boundary and generation of megathrust earthquakes.

Finally, at the larger scale, we discuss how our 2D evolutionary results on the subduction margin and across the core of the Andean orogen can be extended latitudinally over the deforming margin of South America, then incorporated with a selective review of current knowledge of Andean boundary conditions, plate-scale tectonics and climate change. With this approach, we propose a new unifying concept of Andean orogeny.

2. The Atacama Bench

2.1. Topography and morphology of the Andean margin: Atacama Bench and major structural discontinuities

The Central Andes form a characteristic bend, named here Andean Orocline (Bolivian orocline of Isacks (1988)), which is marked on the coastline of South America by a kink at Arica, close to the Peru–Chile

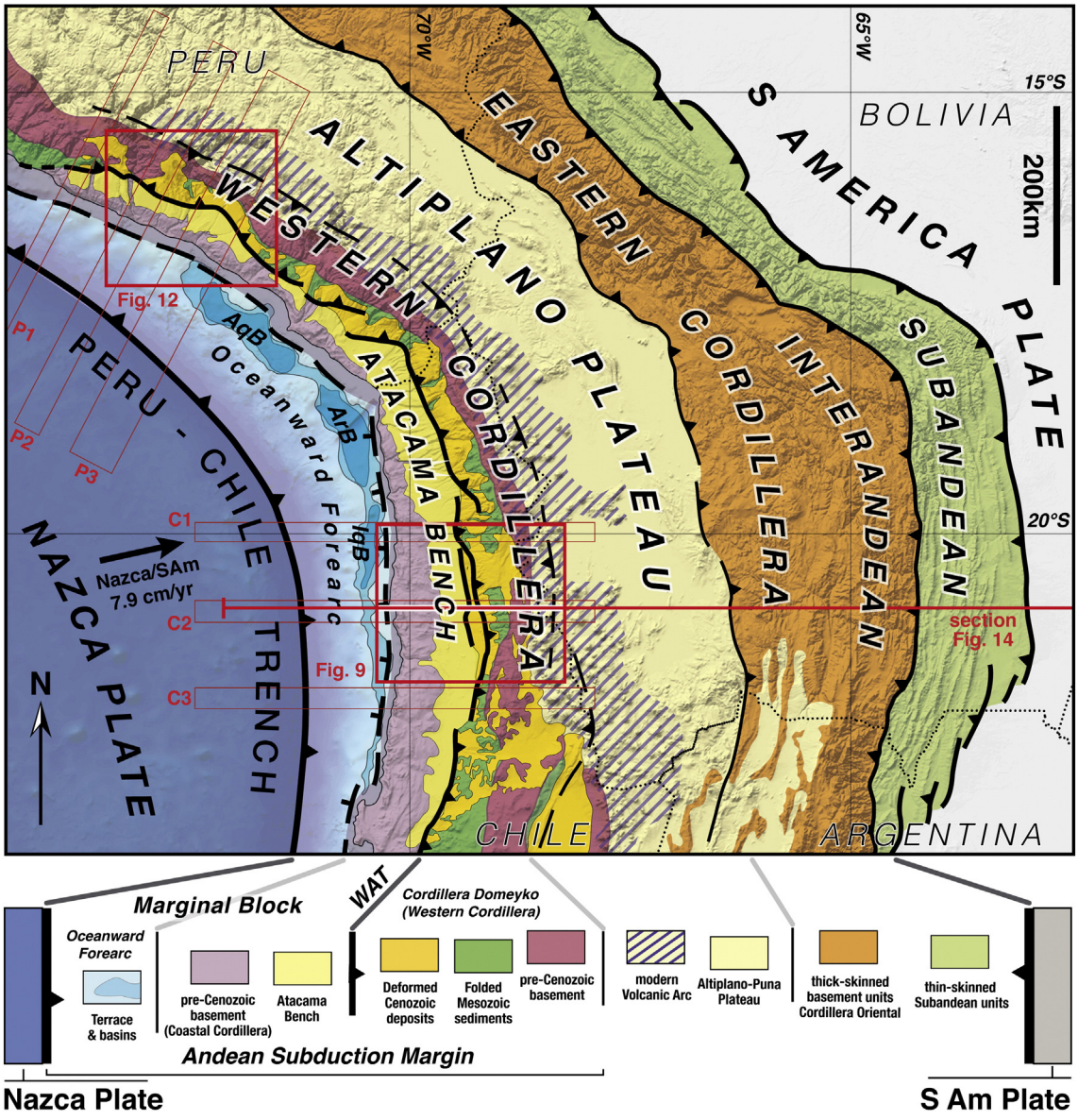

Fig. 2. Geological sketch map of Andean orogen. The main morphological–structural units of the bivergent Central Andes (continental region with over-thickened crust constituting the core of the Andean orogen) are represented within horizontal boundary conditions (converging Nazca and South America plates). Plate convergence vector is from NUVEL 1-A model (DeMets et al., 1994). Tectonic units of the trenchward verging Andean Subduction Margin (fore-arc) are specified. The Atacama Bench is on top of the pre-Cenozoic basement of the rigid Marginal Block. The Atacama Bench is bounded to the East by the West Andean Thrust (WAT), which flanks the Western Cordillera and is a major mechanical boundary with the same vergence as the subduction zone (Armijo et al., 2010a). To the West of the Atacama Bench are the Arequipa Basin (AqB), Arica Basin (ArB) and Iquique Basin (IqB), which form a trench-parallel string on the oceanward forearc (Coulbourn and Moberly, 1977). The overall structure across the orogen (displaying all units and structures depicted here) is shown in the section displayed in Fig. 14. Its trace is indicated here in red at 21°S latitude. Also, the imprint of trench-perpendicular swath profiles and interpretations discussed in Fig. 7 (P1–P3; C1–C3) are located by elongated rectangles labelled in red. Finally, the bold red rectangles locate the detailed tectonic maps (Figs. 9 and 12). (For interpretation of the references to colour in this figure legend, the reader is referred to the web version of this article.)

border (Figs. 1, 2 and 3). To examine the morphological features of the Andean margin (Figs. 5–7), our analysis of topography uses swath-profiles constructed along and across the strike of the two limbs of the Andean Orocline (North Chile and South Peru). The two sides of the Arica bend are covered conveniently, enhancing features at the larger scale, by constructing "wide-swath" images (Figs. 5b-c and 6b-c) composed of a series of ≥500 km-long trench-parallel profiles scanning the land and seafloor topography over a significant width of the margin (~≥ 350 km), using SRTM 30+ data (incorporating bathymetry) with resolution of 30 arc seconds (~900 m) (Becker et al., 2009). The same "wide-swath" technique is applied to capture details of the onshore morphology with trench-parallel profiles scanning a width of ~≥200 km (Figs. 5d and 6d) and using more accurate SRTM3 data with 3 arc seconds resolution (~90 m). To crosscut information, a series of trench-perpendicular ~500 km long swath-profiles (Fig. 7) are focused on selected sections (see location in Fig. 2) across the Andean margin over a reduced width of a few tens of km in the SRTM 30+ data.

Broad orogen-scale characteristics of the topography (Figs. 5–7) are as follows: (1) The total relief of more than 13 km from the summits of the Western Cordillera (≥5000 m elevation) to the depths of the trench axis (~8000 m depth) appears to be a 250-km-wide upwarping of the wholesale Andean margin (with ~3° of average slope). That upwarping represents a large-scale steep gradient, comparable to the (8 km high, 150-km-wide, also with ~3° of average slope) topographic scarp flanking the Himalayas. (2) The west Andean upwarping is however broken into a flight of steps, which represent low-relief morphologies,

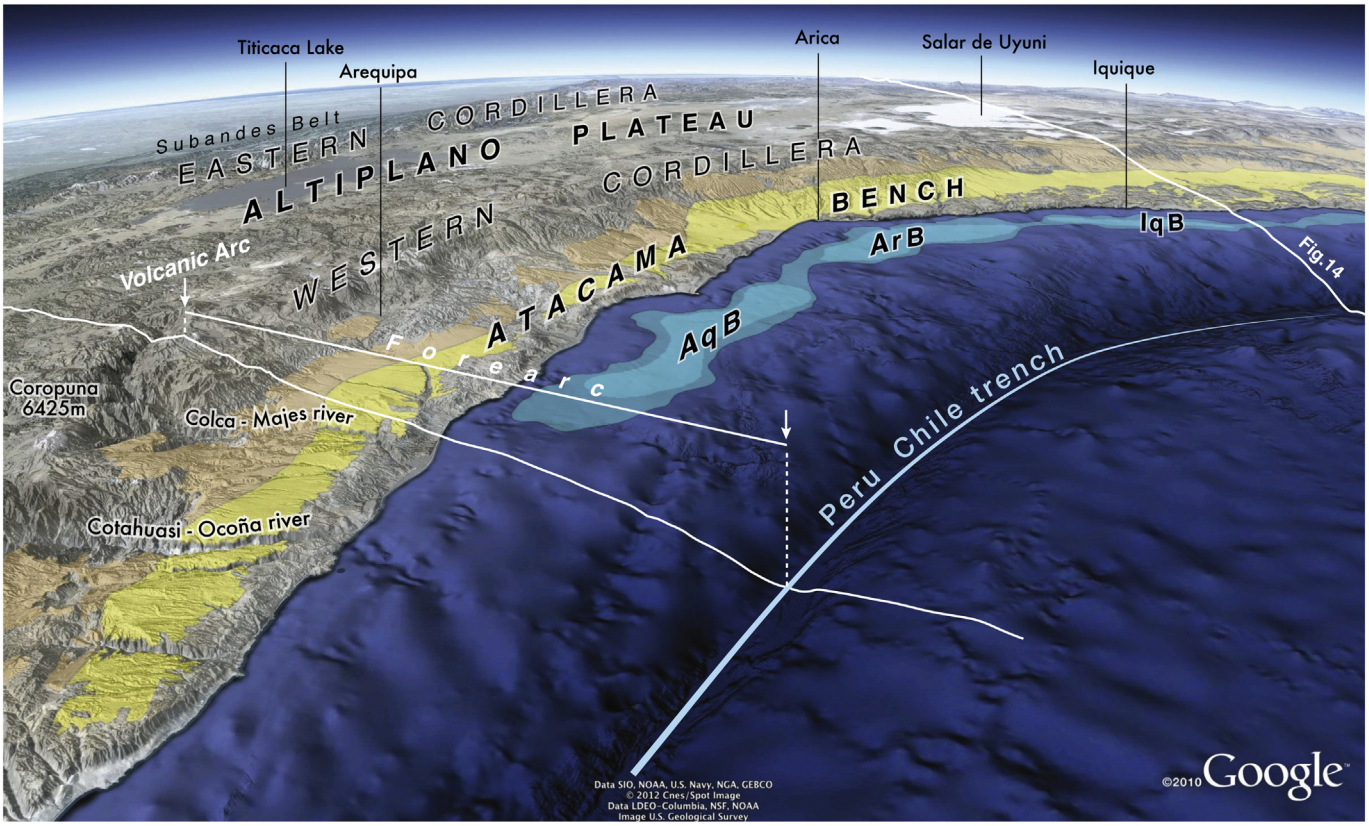

Fig. 3. Atacama Bench within over Andean subduction margin. Oblique 3-D display (GoogleEarth) of main units of the Andean orogen emphasizing the trenchward downwarping and stepped morphology of the subduction margin. View is southeastward. The position of the modern volcanic arc and the extent of the forearc are outlined. On the landward forearc, the flat Atacama Bench (yellow) is geologically similar to a giant terrace, overprinting the warped Central Depression Basin (brown), which extends farther inland and drapes the flanks of the Western Cordillera. The oceanward forearc is characterized by a terrace over a string of basins (Arequipa, ArB; Iquique, IqB; and Arica, ArB) (Coulbourn and Moberly, 1977), represented by two tones of light blue. A quantitative analysis of the margin's topography is given in Figs. 5–7. (For interpretation of the references to colour in this figure legend, the reader is referred to the web version of this article.)

having evolved for a significant period of time with a stable base level. The two most prominent steps are the onshore Altiplano Plateau and Atacama Bench, respectively at ~4000–4500 m and ~1000–2000 m elevation. (3) The Atacama Bench emerges clearly as a fundamental tectonic unit at the same scale as the Altiplano Plateau and the Andean Orocline. (4) The third step is a terrace on the oceanward forearc at ~400–1600 m depth, beneath which modern sedimentation has accumulated in back-tilted basins forming a trench-parallel string (Coulbourn and Moberly, 1977). (5) As demonstrated later (Sections 3 and 4), two major structural discontinuities, or fault systems, appear to form the main boundaries (between the Altiplano Plateau and the Atacama Bench, as well as between the Atacama Bench and the terrace in the oceanward forearc) and control the development of the flight of steps.

2.2. Late Cenozoic evolution of the Atacama Bench: central depression basin between two pediplains

Using the available geological evidence, it is possible to define basic features of the Atacama Bench down to some depth and to decipher its structural evolution (Fig. 8), which appears closely associated with the Cenozoic evolution from semi-arid to extremely arid conditions in the Atacama Desert (e.g. Jordan et al. (2014)). The top of the Atacama Bench corresponds to the flat west part of an extensive climatically-controlled erosion surface called Atacama Pediplain (e.g. (Hartley and Evenstar, 2010)), which slopes down westwards from elevations of ~ ≥3000 m on the flank of the Western Cordillera to elevations of ~ ≤1000 m atop the Coastal Cordillera. Beneath the Atacama Pediplain is a continental wedge-shaped forearc basin, called the Central Depression Basin (CDB), which has formed over the west piedmont of the Andes in the Late Eocene–Late Miocene (from ~30 to ~10 Ma) and is considered of foreland type (Victor et al., 2004; Hartley and Evenstar, 2010). The CDB is filled with a sedimentary pile (up to ~1.5 km thick) grading eastward into coarse grained alluvium derived from the Western Cordillera and large ignimbrite flows erupted from the Miocene volcanic arc (Farías et al., 2005; Hartley and Evenstar, 2010; Schlunegger et al., 2010).

In more stratigraphic detail, the Central Depression Basin started to develop with deposition of the Oligocene Azapa formation (Charrier et al., 2007), roughly correlated with the late Eocene–early Miocene Moquegua group in South Peru (Sébrier et al., 1988; Thouret et al., 2007). It has been shown that in some places the latter group may extend up through the late Miocene or even the Pliocene (Roperch et al., 2006). However, most of the sediments associated with the Azapa formation and the Moquegua group (units designated Moquegua A and Moquegua B by (Roperch et al., 2006)) appear clearly followed by dominant emplacement of volcanic ashes and lava flows that cover much of the landscape, which generally group into the late Oligocene–middle Miocene Oxaya formation (also termed Oxaya ignimbrites) (Muñoz and Charrier, 1996; Charrier et al., 2007; Schlunegger et al., 2010), and roughly correlated with plateau-forming ignimbrites called collectively Huaylillas ignimbrites in South Peru (Sébrier et al., 1988; Thouret et al., 2007). Then, over the large ignimbrite units is the early-middle Miocene El Diablo formation (Charrier et al., 2007), which may extend up into the late Miocene (Schlunegger et al., 2006). The El Diablo Formation of northern Chile can be roughly correlated with the Chuntacala Formation in South Peru, (Sébrier et al., 1988). Since ~14 Ma (middle Miocene), deposition of gravels associated with minor fluvial reworking and climate change (Evenstar et al., 2009) appears to have led to progressive

Fig. 4. Hidden "Incaic" structure of Western Cordillera under flexured Choja and Atacama Pediplains. Oblique 3-D display (GoogleEarth) showing the "frozen" folded structure of the Western Cordillera (northern Cordillera Domeyko area) under the west Andean monocline flexure affecting the pediplains. The Atacama Pediplain tops the Early Oligocene–Late Miocene sedimentary/volcanic pile deposited in the Central Depression Basin (see Fig. 8). Under those deposits is Choja Pediplain marking the sharp unconformity over the west-vergent folded Mesozoic rocks of the composite early Jurassic–late Palaeocene Andean Basin. Three first-order features of Andean orogeny are identified spectacularly: (1) The main period of tectonic shortening and basement exhumation across the Western Cordillera (late Palaeocene–Eocene, between 50 Ma and 30 Ma); (2) The effects of increased aridity in the earliest Oligocene (~33 Ma) throughout the Pacific seaboard of central South America; (3) The effects of hyper-aridity since the Late Miocene abandonment of Atacama Pediplain (~10 Ma). View is northward. Chacarilla Canyon is in the middle ground; Pica and Atacama Bench in the background to the left. Geology of the area is depicted in Figs. 9 and 10.

completion and eventual abandonment of the Atacama Pediplain (e.g. Evenstar et al. (2009); Jordan et al. (2014)). Dated ashes intercalated within the uppermost gravels reworking the El Diablo Formation indicate ages as young as 5–6 Ma, both in northern Chile and South Peru (Sáez et al., 1999; Hoke et al., 2007; Schildgen et al., 2009). However, in contrast with the climatically-controlled development of the Atacama Pediplain, its abandonment appears to be associated with a significant tectonic change, involving canyon incision and land uplift (which is discussed later in this section).

The evolution of the Central Depression Basin and the eventual establishment of the Atacama Bench recorded the climate evolution toward the present-day hyper-aridity in the Atacama Desert (≤5 mm/yr of precipitation) and more generally the climate change over the western seaboard of central South America (see section 2.3 and discussions by Hartley and Chong (2002); Hartley et al. (2005); Rech et al. (2006); Rech et al. (2010); Amundson et al. (2012); Jordan et al. (2014)). An important piece of evidence on the passage from aridity to hyper-aridity comes from studies of supergene enrichment in porphyry-copper deposits in North Chile (Alpers and Brimhall, 1988; Sillitoe and McKee, 1996; Arancibia et al., 2006), which indicate erosion and thus precipitation rates significantly decaying after 14 Ma, coevally with a global cooling event of the Cenozoic (Zachos et al., 2008) and with the intensification of a cold upwelling Peru–Chile Current between 15 and 10 Ma (see discussions by Gregory-Wodzicki (2000); Houston and Hartley (2003)). That correlation would be stratigraphically signed by the end of significant sediment deposition (El Diablo formation)

Fig. 5. Trench-parallel topography along Andean subduction margin — North Chile. Figs. 5 and 6 are intended to describe the major morphological features of the Central Andes margin on the two limbs of the Andean Orocline (Isacks, 1988) (covering the two sides of the Arica bend, see Figs. 1, 2 and 3). So, the continuity of those features can by visualized. (a). 3D front view to the East of the area described, using Shuttle Radar Topography Mission SRTM 30+ data (Becker et al., 2009) to produce the N–S wide-swath profile below. The Arica bend is to the left. The upwarping of the Andean margin is clearly visible, as well as its main steps, indicated with red characters: Altiplano Plateau and Atacama Bench. An overlay with two tones of light blue (according to sediment thickness) indicates the offshore step constituted by a terraced string of basins including the Arica Basin. (b). Wide-swath profile scanning systematically the topography shown in the 3D view. The image is obtained by stacking a series of N–S profiles sampling at full resolution (each 30 arc seconds) between 18°S–25°30′S and 72°W–67°26′W). Vertical exaggeration is VE = 7.5. (c). The interpretation of the image in (b) describes the main morphological features of the margin extending down to latitude 23°S (Mejillones Peninsula–Salar de Atacama), south of which variations in the structural style of the Central Andes, clearly distinguishable in the topography, are beyond the scope of this study. The Mejillones Peninsula is a morphological singularity of the margin, representing a structural complexity of the overriding continental plate associated with segmentation of earthquake rupture at the subduction interface (Béjar-Pizarro et al., 2010). Red characters indicate Altiplano Plateau (AP), Atacama Bench (AB, in yellow), Arica Basin (ArB) and Iquique Basin (IqB). Features below sea level are in dark blue, except basins in the step close to the coastline (light blue). The warped sedimentary and volcanic units of the Central Depression Basin (in orange) conceal largely the flank of the Western Cordillera, except in Cordillera Domeyko. The red frame indicates the location of the close-up below. (d). Close-up of onshore topography using the same wide-swath technique and SRTM3 data (with 3 arc seconds resolution). The stacked image includes most of the area covered by the map in Fig. 9. The red trapezoid encompasses approximately the aerial view displayed in Fig. 11a. The modern volcanic arc is clearly seen in the background, above the flat surfaces of the Altiplano Plateau and the Atacama Bench (yellow enhancement). The canyons flowing down from the Altiplano Plateau (Chacarilla, Guatacondo and Mani) cut across the west flank of Cordillera Domeyko, where the west-vergent thrust structure crops out (Figs. 4 and 9-11). At the lower course of Loa river a 1-kilometre deep canyon is incised across the Atacama Bench. The equally high area of the image facing the sea in the foreground (in shade) is the Coastal Scarp (CS). (For interpretation of the references to colour in this figure legend, the reader is referred to the web version of this article.)

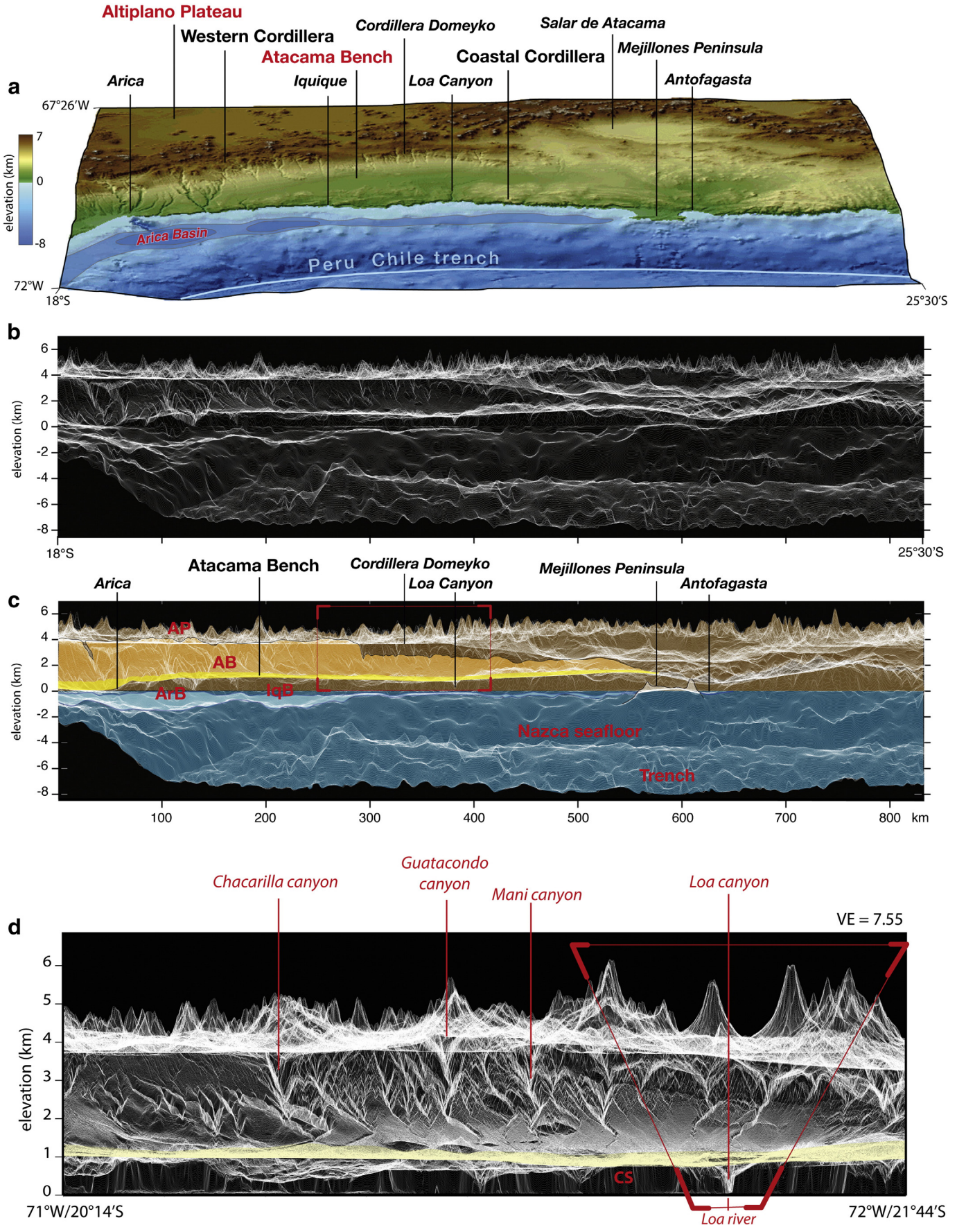
a
Altiplano Plateau
Western Cordillera
Atacama Bench
Cordillera Domeyko
Coastal Cordillera
Salar de Atacama
Mejillones Peninsula
Arica
Iquique
Loa Canyon
Antofagasta
67°26'W
72°W
18°S
25°30'S
elevation (km)
7
0
-8
Arica Basin
Peru Chile trench
b
elevation (km)
18°S
25°30'S
c
Arica
Atacama Bench
Cordillera Domeyko
Loa Canyon
Mejillones Peninsula
Antofagasta
AP
AB
ArB
IqB
Nazca seafloor
Trench
elevation (km)
100
200
300
400
500
600
700
800 km
d
Chacarilla canyon
Guatacondo canyon
Mani canyon
Loa canyon
VE = 7.55
CS
Loa river
elevation (km)
71°W/20°14'S
72°W/21°44'S

and pedimentation processes (Atacama Pediplain) topping the CDB, before its entrenchment by canyons (see Fig. 8). However, the gradual evolution to hyper-aridity starting in the Middle Miocene appears to include fluctuations and a further Pliocene hyper-aridity increase (Hartley and Chong, 2002; Allmendinger et al., 2005; Hartley et al., 2005; Rech et al., 2006; Rech et al., 2010; Amundson et al., 2012; Jordan et al., 2014), which could be associated with a relatively warm Pliocene sea surface temperature along the Peruvian coast (Dekens et al., 2007; Jordan et al., 2014).

At the base of the Central Depression Basin is a regional erosion surface named Choja Pediplain (Galli-Olivier, 1967) (see Section 2.3). Under that surface are previously deformed sedimentary and magmatic rocks associated with a thick (≥10 km thick) proto-Andean Mesozoic arc and back-arc basin system (early period of the Andean cycle) deposited on top of Palaeozoic and Precambrian metamorphic rocks (Mpodozis and Ramos, 1989; Sempere et al., 2002; Charrier et al., 2007; Schildgen et al., 2009) (Fig. 8). It has been suggested that the ensemble formed by the Mesozoic magmatic arc embedded in Palaeozoic and older basement rocks constitute the cold rigid basement of the crustal-scale Marginal Block flanking the Western Cordillera for several thousand kilometres (Armijo et al., 2010a) (Figs. 2 and 7). The structure defining the boundary between the Western Cordillera and the Marginal Block (so possibly explaining the topographic step between the Altiplano Plateau and the Atacama Bench, see Figs. 7 and 8) would correspond to the major West Andean Thrust (WAT) (Armijo et al., 2010a, 2010b). However, the topography of the Central Andes margin indicates another continuous step near the coastline between the Atacama Bench and the oceanward forearc (Fig. 7), which calls for a structural explanation.

Basic features to constrain evolution of the Central Depression Basin are the following. In South Peru, the CDB preserves an intercalated marine sediment layer 25 Myr old (Thouret et al., 2007), indicating sedimentation at that time in the Andes piedmont has occurred at low level, close to the oceanic base level. The marine layer is now found close to the flank of the Western Cordillera ~50 km inland from the coast, at ~2000 m elevation (Tosdal et al., 1984; Sébrier et al., 1988; Thouret et al., 2007; Schildgen et al., 2009) (location in Fig. 12), beneath the surface of the Atacama Bench, which is now incised by a series of deep canyons grading down to the Ocean from headwaters in the Altiplano Plateau and the Western Cordillera (Figs. 3–6). $^{40}Ar/^{39}Ar$ age determinations (Thouret et al., 2007) and apatite (U–Th)/He thermochronology data (Schildgen et al., 2009) imply at least 2.4–3 km of river incision by those canyons after ~9 Ma (in the Cotahuasi-Ocoña river) (Schildgen et al., 2009; Schildgen et al., 2010). Those observations require a minimum of 1.4–2 km of differential uplift of the Western Cordillera with respect to the Atacama Bench and ~1 km of overall land uplift with respect to the oceanic base level (Atacama Bench coupled with Western Cordillera and Altiplano Plateau) (Schildgen et al., 2009), driving the incision of canyons. Schildgen et al. (2009) discussed two distinct phases of incision, the first through the Western Cordillera, and the later through the Atacama Bench and the coastal region. In North Chile, similar canyons have been incised headwards from the Pacific across the Atacama Bench as much as 1 km after 11 Ma, or more recently (Schlunegger et al., 2006; Schlunegger et al., 2010; García et al., 2011; Kirk-Lawlor et al., 2013), suggesting significant (~0.6 to 1 km) land uplift relative to the oceanic base level, consistent with the occurrence of the spectacular 1-km-high Coastal Scarp (Armijo and Thiele, 1990) (Fig. 10), and with observations of lower-level sets of glacio-eustatic marine platforms and terraces testifying to late Pleistocene coastal uplift (e.g. Armijo and Thiele (1990); Ortlieb et al. (1996); Marquardt et al. (2004); Regard et al. (2010)).

In stark contrast with the evidence in South Peru, it has for long been considered that uplift of coastal regions in North Chile would be independent and much older (Cretaceous–Palaeocene; ~ ≥ 25 Ma) than the post-Late Miocene (~ ≤ 11 Ma) incision of canyons (Mortimer and Saric, 1975; Farías et al., 2005; García et al., 2011). However, the hypothesis of old uplift (~ ≥ 25 Ma) appears controversial (Schildgen et al., 2007; Schlunegger et al., 2010). In principle, the onset of incision is not necessarily triggered by surface uplift, because it could be also a response to climatic change (Alpers and Brimhall, 1988; Gregory-Wodzicki, 2000). Following the hypothesis of old uplift (~ ≥ 25 Ma) and subsequent incision, García et al. (2011) suggested that canyon incision across the Atacama Bench could have been triggered during the Late Miocene–Pleistocene (~ ≤ 11 Ma), which would be a period of prevalent hyper-aridity, by a runoff increase associated with possible local pulses of semi-aridity. There is limited geological evidence for such scenario, although (as stated above) a Pliocene period of relative warmth, consistent with a warmth at global scale, appears warranted (e.g. Dekens et al. (2007); Jordan et al. (2014); Molnar and Cane (2007)). Alternatively, Armijo and Thiele (1990) suggested that the large-scale uniformity of the Atacama Bench (see Figs. 3, 5 and 6) can be explained simply by an evolution in the opposite order: first, pediment formation by planation processes (sedimentary and erosional) grading to the ocean, then tectonic uplift. Here we prefer to take the latter scenario, as it appears now founded upon both, geologic–paleoclimatic evidence and well-dated morphologic evidence constraining tectonic uplift: First, since ~14 Ma, evolution of climate passing gradually from aridity to hyper-aridity (Alpers and Brimhall, 1988; Gregory-Wodzicki, 2000; Jordan et al., 2014), coeval with the gradual end of sediment deposition in the CDB of the early-late Miocene El Diablo formation (Sáez et al., 1999; Charrier et al., 2007; Hoke and Lamb, 2007; Schildgen et al., 2009; Jordan et al., 2014). Second, since ~10–7 Ma, relatively uniform surface uplift of the wholesale Western Cordillera together with the Atacama Bench in both South Peru and North Chile, which has triggered the ~1 km headward incision of canyons across the Atacama Bench (Schildgen et al., 2007; Jordan et al., 2010; Schlunegger et al., 2010; Jeffery et al., 2013; Kirk-Lawlor et al., 2013). In that case, the Pliocene warmth could have contributed by increasing precipitation and enhancing the incision process, before conditions returned to hyper-aridity since ~ ≤3 Ma.

A clear feature of the morphology is that deposits of the Central Depression Basin (particularly ignimbrite units forming an extensive caprock) cover largely the Western Cordillera's slopes, in some places up to the Altiplano Plateau, so concealing the Andes frontal structure (e.g. Schildgen et al. (2009))(see Fig. 4). However, it has been shown that the development of the CDB is associated with relatively small west-vergent thrust deformation (representing ~3 km of shortening (Victor et al., 2004)) producing a vast monocline flexure at the flank of the Western Cordillera and its uplift (with respect to the CDB), associated with discrete localized thrusts and smaller flexures at its base (Mpodozis and Ramos, 1989; Muñoz and Charrier, 1996; Pinto et al., 2004; Victor et al., 2004; Farías et al., 2005; García and Hérail, 2005; Hoke et al., 2007; Jordan et al., 2010; Pinto et al., 2010; Hall et al., 2012) (Figs. 3, 8, 9 and 13).

Summarizing, the Atacama Bench results from evolution during the past 30 Myr of a flat-topped, wedge-shaped, foreland-type Central Depression Basin, formed probably close to sea level, on the west piedmont of the growing Andes, intercalated between two pediplains (Fig. 8).

Fig. 6. Trench-parallel topography along Andean subduction margin - South Peru. The approach is the same as in Fig. 5. (a). 3D front view to the North-East of the area covered by the NW-SE wide-swath profile below (corner points: 17°41′S/76°30′W; 13°29′S/74°14′W; 16°27′S/68°33′W; 20°38′S/70°52′W). The Arica bend is to the right. (b). Wide-swath profile using SRTM 30+ data. (c). Interpretation of the image in (b), with same colours and symbols as in Fig. 4. Frame indicates location of the close-up below. (d). Close-up of onshore topography using SRTM3 data. The stacked image includes most of the area covered by the map in Fig. 12. The high Coropuna volcano emerges above the Altiplano Plateau, as the Atacama Bench (yellow enhancement) is entrenched by the Ocoña and Majes river canyons. (For interpretation of the references to colour in this figure legend, the reader is referred to the web version of this article.)

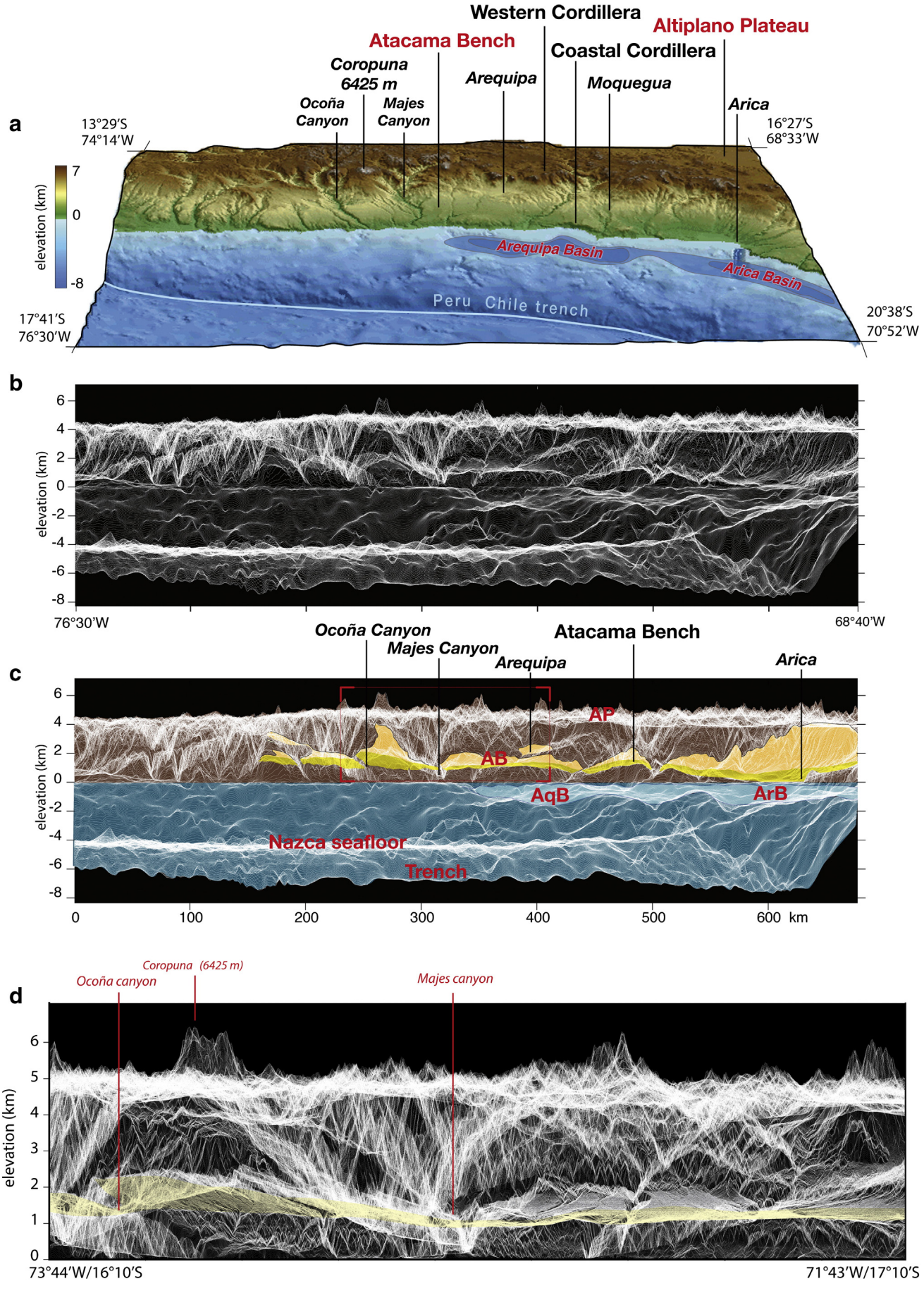
a
Western Cordillera
Altiplano Plateau
Atacama Bench
Coastal Cordillera
Coropuna
6425 m
Arequipa
Moquegua
Ocoña
Canyon
Majes
Canyon
Arica
13°29'S
74°14'W
16°27'S
68°33'W
elevation (km)
7
0
-8
Arequipa Basin
Arica Basin
Peru Chile trench
17°41'S
76°30'W
20°38'S
70°52'W
b
elevation (km)
6
4
2
0
-2
-4
-6
-8
76°30'W
68°40'W
c
Ocoña Canyon
Majes Canyon
Arequipa
Atacama Bench
Arica
AP
AB
AqB
ArB
Nazca seafloor
Trench
elevation (km)
0
100
200
300
400
500
600 km
d
Coropuna (6425 m)
Ocoña canyon
Majes canyon
elevation (km)
6
5
4
3
2
1
0
73°44'W/16°10'S
71°43'W/17°10'S

Under concomitant action of tectonics and increasing aridity, the slowly deforming CDB received relatively little sediment fill and was gradually bevelled by erosion and eventually abandoned by ~10 Ma. As a result, the west sloping, concave-upwards shaped Atacama Pediplain grading to the Pacific has formed, and the Atacama Bench corresponds to its flat undeformed part (Fig. 8). Since ~10–7 Ma, the abandoned Atacama Pediplain under hyper-arid conditions and its rigid basement have been incised by deep canyons carved headwards from the ocean as a response to a ~1 km baselevel drop associated with bulk Andean uplift (Schlunegger et al., 2010; Kirk-Lawlor et al., 2013).

2.3. Climatic change indicated by Choja Pediplain, at the base of the CDB

The overall process of formation of the Atacama Bench (starved CDB and development of the Atacama Pediplain) occurred coevally with the evolving arid to hyper-arid conditions that have prevailed in the Atacama Desert probably since ~30 Ma (after completion of the Choja Pediplain, see Fig. 8) or earlier, throughout the Pacific seaboard of central South America (Garreaud et al., 2010). Indeed, aridity to semi-aridity may have dominated climate to the west of the continent, at low latitudes (equatorial to subtropical), since ~150 Ma (Late Jurassic, see Hartley et al. (2005)). However, as seen in Figs. 4, 11b–c and schematised in Fig. 8, the Choja Pediplain coincides with the basal unconformity beneath the eastward-thinning stratigraphic units of the CDB, nearly undeformed and devoid of significant erosion, on top of deformed and eroded earlier structures, which we interpret as a first-order feature of the Andes (see earlier discussions of that feature, often denoted "post-Incaic" surface, e.g. Noble et al. (1979); Tosdal et al. (1984); Hartley and Evenstar (2010)). Regardless of a possible change of tectonic activity and of other structural and mechanical consequences (analysed later), this major feature is indicative of a change of erosive power at about ~30 Ma, over a region to scale with the western seaboard of the Central Andes. Some inferences can be retained: (1) Reduction of erosive power at large scale would be consistent with a substantial reduction of precipitation, increase of aridity and desertification in Atacama. (2) Such a change at the scale of the Central Andes (Montgomery et al., 2001) would be indicative of a climatic change throughout South America associated with global changes (e.g. Zachos et al. (2001)). (3) Regardless of the latter inference, the inferred climatic change must have occurred after a significant episode of efficient erosion of strongly deformed tectonic features of the Western Cordillera. Climatic implications (including a possible interplay between tectonics and increasing aridity) are further discussed along with the tectonic evidence in Sections 3.3.3, 5 and 6 of this paper.

3. Hidden structure of Western Cordillera: "Incaic" backbone under Choja Pediplain

3.1. Structure at west flank of the Andes: Pre-Andean, Early Andean and Late Andean tectonics

Clearly, the modest deformation (~3 km of shortening) observed across the CDB in North Chile using shallow penetration seismic profiles (Victor et al., 2004) is not to scale with the structural relief of the Western Cordillera and crustal thickness beneath. Most of the deformation at the boundary between the Marginal Block and the Western Cordillera and responsible of the Western Cordillera's structure is older than 30 Ma and concealed unconformably by the CDB sediments and ignimbrites (Haschke and Gunther, 2003). However, key observations can be gathered in the northern Cordillera Domeyko region, and especially south of Chacarilla Canyon (Fig. 9; see the location of the area in the interpreted wide-swath topography in Fig. 5, detailed maps in Figs. 9–10 and field photographs in Fig. 11). There, an overall section of a west-vergent fold-thrust belt bounded to the East by an exhumed basement backstop that reveals the backbone of the Western Cordillera is well exposed and can be determined in some detail (Fig. 13). Yet, the geology of Cordillera Domeyko displays also evidence of geological features of its earlier tectonic evolution. Those features appear fundamental to our understanding of the Andean orogeny. Main facts of pre-Andean and Andean structural cycles, described summarily hereafter, are associated with evolution of global-scale mantle convection cells that drove the assembly (concomitant with pre-Andean cycles) and subsequent dispersal (concomitant with the Andean cycle) of Pangaea and Gondwana continental fragments (Dalziel and Forsythe, 1985; Collins, 2003).

3.2. Accretion of Andean structural basement during assembly of Gondwana

The Andean structural basement was shaped in pre-Andean times by a protracted late Proterozoic–Palaeozoic process of docking and progressive accretion of various terranes to the Amazonian craton (Ramos, 1988; Bahlburg and Hervé, 1997; Rapela et al., 1998; Lucassen et al., 2000). The overall global-scale result of that process is the assembly of the South America realm of Gondwana and the Pangaea super continent (Ramos, 1988; Bahlburg and Hervé, 1997; Lucassen et al., 2000). Gondwanan basement rocks in Cordillera Domeyko are exposed along its high structural backbone, including mica-schists of the Choja formation of Proterozoic age (or pre-Silurian, see Charrier et al. (2007)), which are considered to be part of the Arequipa–Antofalla terrane (Ramos et al., 1986). That terrane includes also other Proterozoic rocks well exposed in the Western and Coastal Cordillera of southwest Peru, as well as in northwest Argentina (Shackleton et al., 1979; Loewy et al., 2004; Ramos, 2008; Casquet et al., 2010). Altogether, the Arequipa–Antofalla ensemble would have been accreted to Gondwana during the Ordovician (Charrier et al., 2007; Ramos, 2008). Closing the Gondwanan cycle of subduction and continental accretion is the intense late Carboniferous–early Permian magmatic activity documented by volcanism and major granite intrusions, basically the Collahuasi formation in the north Domeyko region (Vergara and Thomas, 1984). That magmatism is followed by a process of crustal extension during the Triassic (Sempere et al., 2002; Charrier et al., 2007), characterized by interruption or little subduction at the South America margin and development of a continental rift system associated with sedimentation in half-grabens (mostly represented in north Chile and the Domeyko region by the El Profeta and La Ternera formations (Charrier et al., 2007)).

Fig. 7. Trench-perpendicular topography and basic geology across Andean subduction margin -South Peru (P1–P3) and North Chile (C1–C3). The major features of morphology and structure are illustrated using discrete transverse profiles along a ~1000 km stretch of margin, sampling the two limbs of the Andean Orocline. The swath profiles (located in Fig. 2) are constructed using the same SRTM 30+ data as in Figs. 5–6. Distance from trench in km. Vertical exaggeration VE = 8.33. Beneath the Atacama Bench (yellow) and the Atacama Pediplain (reddish brown), is the Late Eocene–Late Miocene (from ~40 to ~10 Ma) Central Depression basin (brown) corresponding stratigraphically to the Azapa and El Diablo Formations in North Chile (Farías et al., 2005; García et al., 2011; Charrier et al., 2013) and to the Moquegua Group in South Peru (Thouret et al., 2007; Schildgen et al., 2009; Decou et al., 2011) (see Fig. 8). The major breaks in the topography of the forearc mark fault boundaries separating main basement units (represented schematically by grey stripes). The break at the foot of the Andes (Western Cordillera) corresponds (as discussed in the text, Section 2.2 and 3.4) to the West Andean Thrust (WAT, see Fig. 8). The Marginal Block (Armijo et al., 2010a), located between the Andes and the trench, is broken into two parts by an offshore fault system located relatively close to the coastline. The Atacama Bench tops the uplifted piedmont region (dark violet) of the Marginal Block's basement, while the subsiding region of the Marginal Block's basement (light violet) underlies the oceanward forearc, over which are the Arequipa and Iquique basins, forming in map view a string of basins (see Figs. 2 and 4–6). (For interpretation of the references to colour in this figure legend, the reader is referred to the web version of this article.)

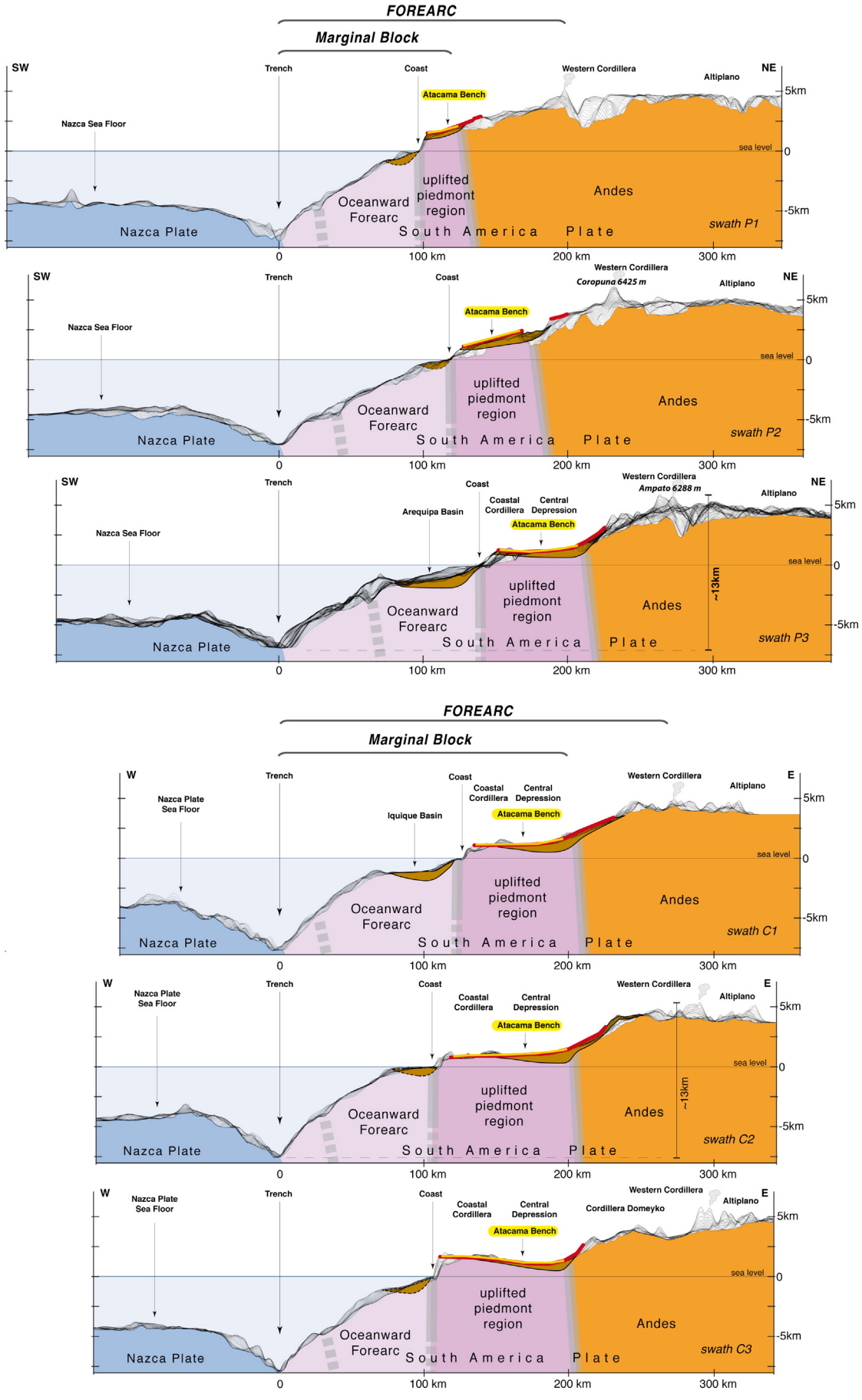
FOREARC
Marginal Block
SW
NE
Trench
Coast
Western Cordillera
Altiplano
Atacama Bench
Nazca Sea Floor
sea level
5km
0
-5km
uplifted piedmont region
Oceanward Forearc
Andes
Nazca Plate
South America Plate
swath P1
0
100 km
200 km
300 km
Coropuna 6425 m
swath P2
Arequipa Basin
Coastal Cordillera
Central Depression
Ampato 6288 m
~13km
swath P3
FOREARC
Marginal Block
W
E
Nazca Plate Sea Floor
Iquique Basin
Cordillera Domeyko
swath C1
swath C2
swath C3

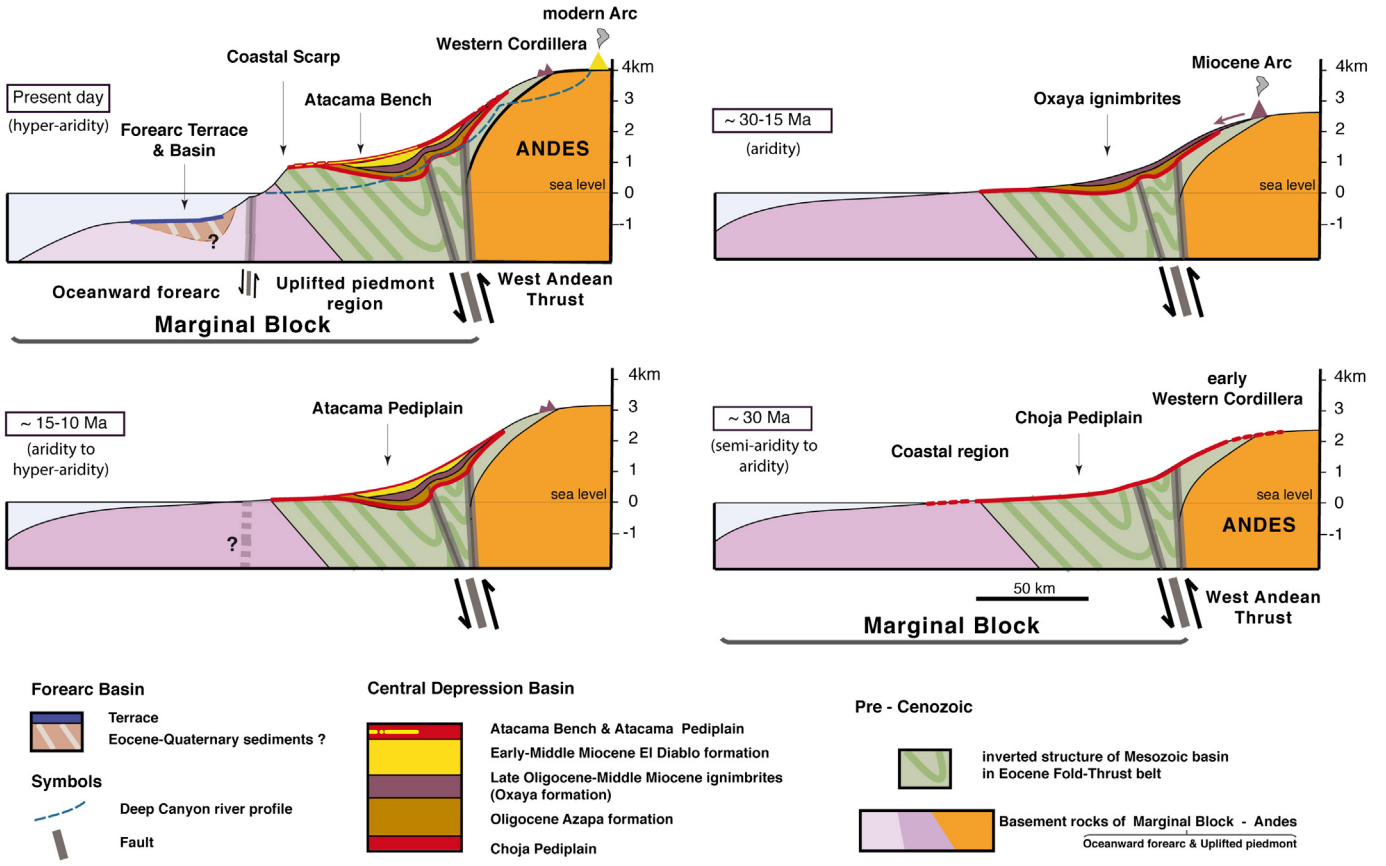

Fig. 8. Cenozoic evolution (post 30 Ma) of west flank piedmont of Central Andes: evidence for increasing aridity. The figure describes schematically the late evolution of the piedmont, after completion of the main tectonic pulse of shortening and mountain building associated with significant erosion and basement exhumation of the Western Cordillera between ~50 Ma and 30 Ma, which is well exposed in the Cordillera Domeyko area (see text, Section 3.4, and Figs. 4 and 9–11). The early deformation has occurred by inversion of a proto-Andean (Mesozoic) volcanic arc and back-arc basin system, which had previously formed at the subduction margin of South America. The best evidence for the shortening has occurred by development of a west-vergent fold-thrust belt (light green adorned with contorted stripes in darker green) associated with activity of the West Andean Thrust, indicated by double arrows beneath the boundary between Mesozoic rocks and the Andean (Western Cordillera) basement. The overall geometry of the present-day stage is represented without vertical exaggeration by the section in Fig. 13. The names of stratigraphic formations are those used for units defined in North Chile. The four panels are intended to describe the main features of the piedmont evolution while the Western Cordillera has been slowly rising above it since 30 Ma, developing a vast monocline at its flank (Isacks, 1988; Hoke et al., 2007; Jordan et al., 2010; Decou et al., 2011), associated with discrete localized thrusts at its base (Muñoz and Charrier, 1996; Victor et al., 2004; Farías et al., 2005; García and Hérail, 2005). The relative degree of aridity for each panel is shown in parentheses. Erosion since 30 Ma is much less than immediately after the previous tectonic pulse. Lower-right panel (snapshot at ~30 Ma): An erosion surface (designated Choja Pediplain: Galli-Olivier (1967)) has formed over the truncated fold-thrust structure, as well as over exhumed basement rocks of the early Western Cordillera and the coastal region. Upper-right panel (evolution from ~30 Ma to 15 Ma): The Central Depression Basin starts with deposition of Oligocene Azapa formation (correlated with Moquegua group in South Peru (Sébrier et al., 1988; Thouret et al., 2007)) followed by series of volcanic ashes and lava flows (mainly the Oxaya ignimbrites (Muñoz and Charrier, 1996; Schlunegger et al., 2010), correlated with the Huaylillas ignimbrites in South Peru (Sébrier et al., 1988; Thouret et al., 2007) fed by the nearby Miocene volcanic arc. Lower-left panel (evolution from ~15 Ma to 10 Ma): End of development and abandonment of the Central Depression Basin. As the Miocene volcanism stops, the El Diablo formation is deposited (Chuntacala formation in South Peru, see Charrier et al. (2007)), followed by formation of the Atacama Pediplain (Evenstar et al., 2009). Note that formation of the Choja Pediplain completed by ~30 Ma and the Atacama Pediplain completed by ~15–10 Ma appear to mark important steps during progressive increase of aridity in Atacama, the earlier possibly representing transition from semi-aridity to aridity; the later transition from aridity to hyper-aridity (see text, Section 2.3). Question marks associated with fault and basin in the oceanward forearc express their unknown age. Upper-left panel (snapshot of present day): Uplift of the Atacama Bench (in yellow, identified on the flat western part of the warped Atacama Pediplain) with respect to the oceanic base level (documented by incision of deep canyons; dashed blue). The modern volcanic arc is located 10–20 km east of the extinct Miocene volcanoes. The ~2 km vertical separation of the Atacama Bench (and the Central Depression Basin) from the offshore terrace (and the oceanward forearc basin) is largely, but possibly not entirely, attributable to the post-10 Ma overall Andean uplift with respect to the oceanward forearc. (For interpretation of the references to colour in this figure legend, the reader is referred to the web version of this article.)

3.3. Andean structural cycle during dispersal of Gondwana: from spreading to contraction of Andean subduction margin

The Andean cycle is associated with the oceanic–continental Andean subduction process that developed throughout the past ~190 Myr (Early Jurassic to Present), which in turn is associated with the early Jurassic fragmentation of Pangaea, followed by the long-lasting fragmentation of Gondwana, the opening of the Atlantic, and the westward drift of South America (Russo and Silver, 1996; Collins, 2003; Husson et al., 2008). The Andean orogeny is the ultimate result of the Andean structural cycle, which is driven by subduction of the eastern plates of the Pacific Ocean (Farallon and Nazca) under Gondwanan basement at the west margin of South America. The first half of the Andean cycle, during most of the Mesozoic, occurred under extension across the subduction margin probably associated with negative trench rollback velocity (trench retreat relative to SouthAmerica) (Husson et al., 2008; Ramos, 2010). The second half, mostly during the Cenozoic, is characterized by a long transitional period (null trench rollback velocity, unstable trench) followed by the Andean orogeny, characterized by increasing contraction across the margin and progressive mountain building, associated with positive trench rollback velocity (trench advance relative to SouthAmerica) (Husson et al., 2008; Ramos, 2010). During the Andean cycle, the subduction process is characterized by progressive continent-ward migration of a conspicuous magmatic arc, which is

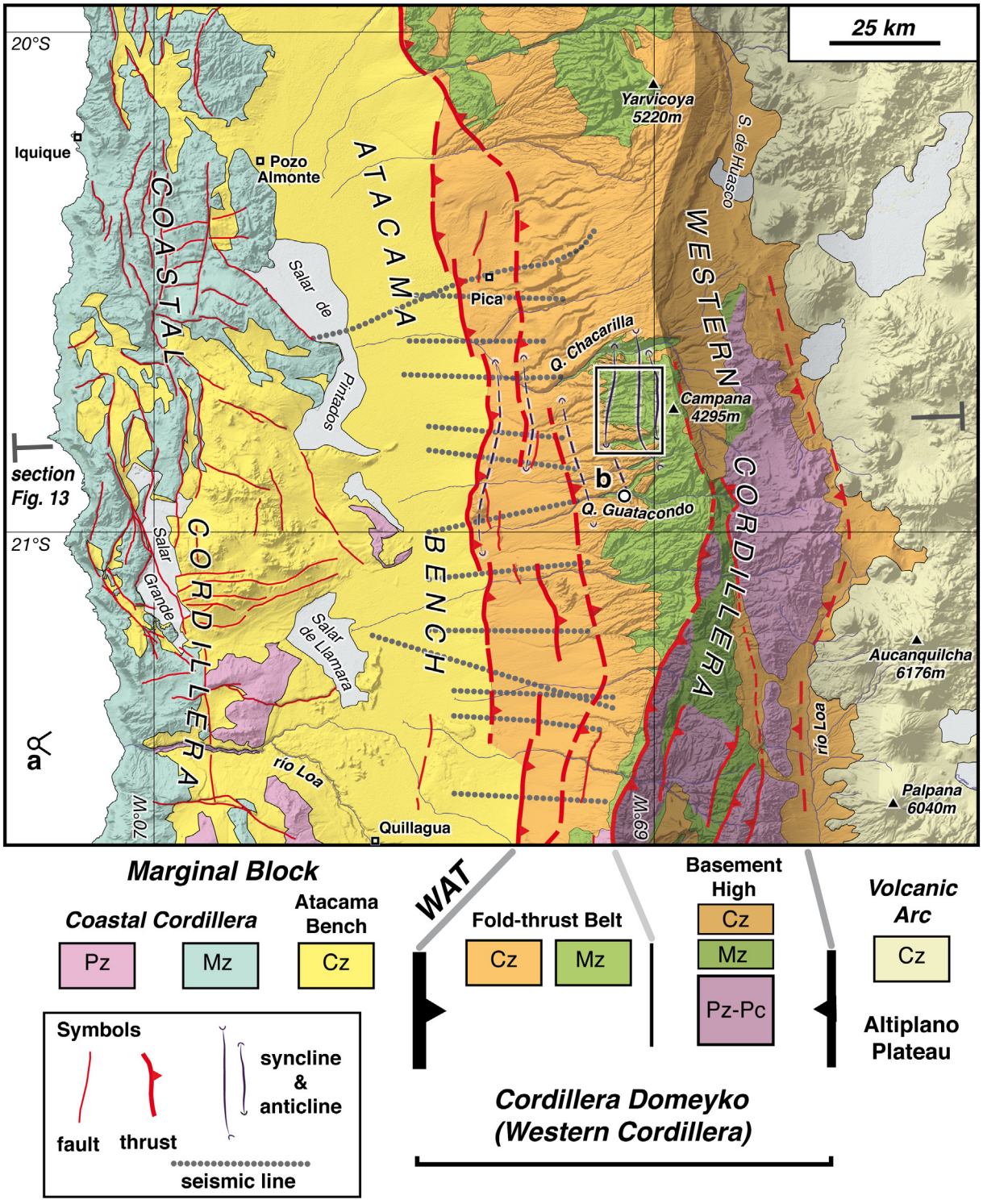

Fig. 9. Tectonics of landward forearc–Andean subduction margin — North Chile. Simplified Geological Map (see location within the large-scale regional context in Fig. 2) based on Carta Geológica de Chile (Vergara and Thomas, 1984) and other 1:250000, 1:100000 and 1:50000 scale maps (Tomlinson et al., 2001), Empresa Nacional del Petróleo (ENAP) seismic sections analysed by (Nester, 2008) and our own field observations. The trace of the tectonic section shown in Fig. 13 (which discusses main implications) is indicated. The structure of the Western Cordillera, bounded by large bivergent thrusts, crops out in the Cordillera Domeyko from an extensive cover of Cenozoic sediments (particularly ignimbrite flows) of the Central Depression Basin (compare with Figs. 4, 7 and 8). Significant exhumation and erosion of the Western Cordillera structure, associated with the late Palaeocene – Eocene pulse of crustal thickening and uplift (50–30 Ma), has occurred before the regional blanketing by the late Cenozoic cover (30 Ma to Present). The rectangle shows the well-exposed area enlarged in Fig. 10. Labels (a), (b) indicate location of corresponding views presented in Fig. 11. The coloured boxes indicate the age of corresponding rocks in the map: Precambrian (Pc), Paleozoic (Pz), Mesozoic (Mz) and Cenozoic (Cz). WAT indicates the location of the frontal east-dipping trenchward-vergent West Andean Thrust. Location of Quebrada Chacarilla (= Chacarilla Canyon) helps to locate oblique northward view in Fig. 4.

probably associated with subduction erosion (Kukowski and Oncken, 2006). As a consequence, the arc and back-arc formed under extension during the early Andean cycle are found largely in forearc position and under contraction during the late Andean cycle. In more detail, the tectonic evolution of the subduction margin during the Andean cycle can be described in three main periods, as follows.

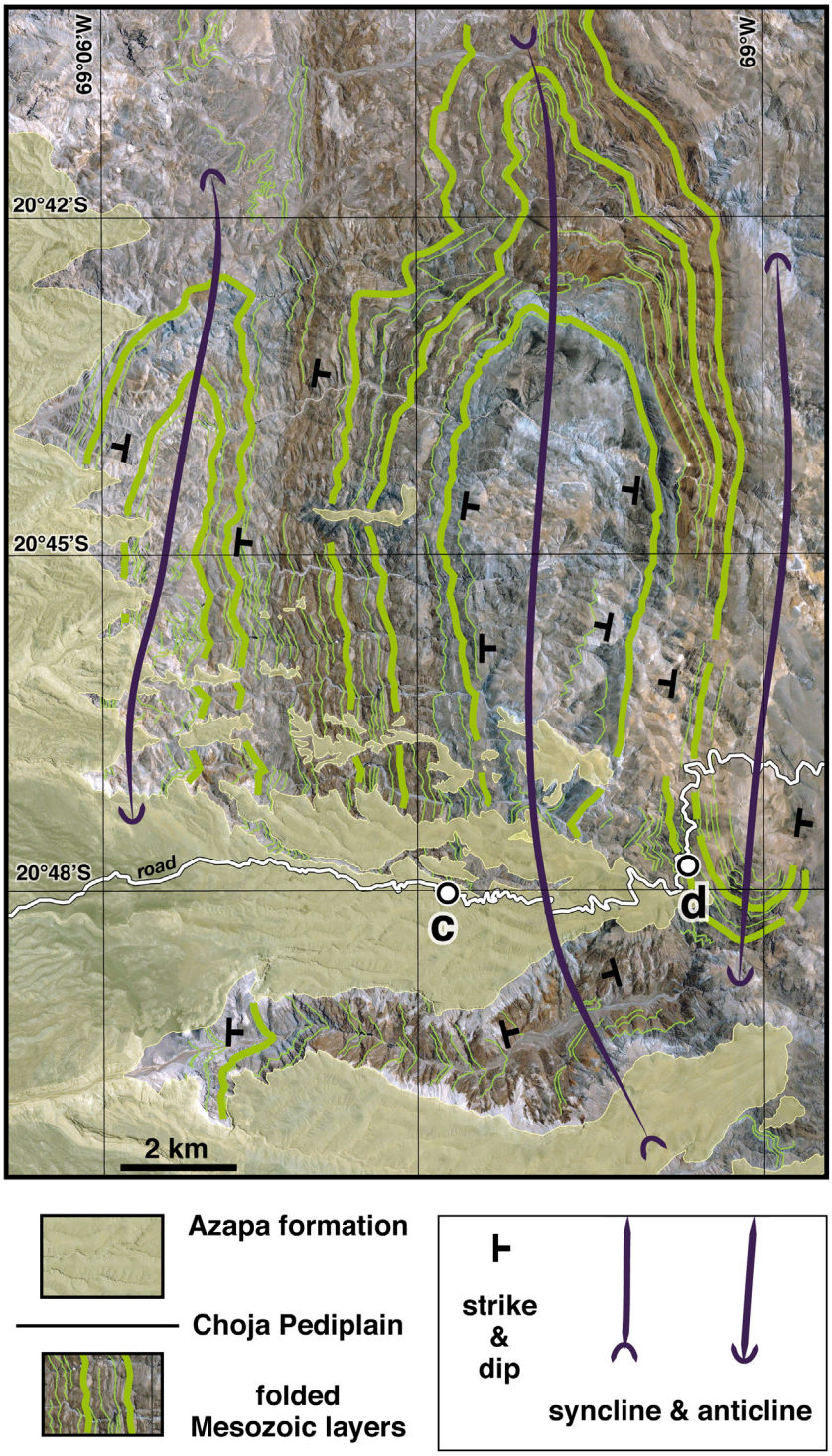

Fig. 10. Detailed structural map in Western Cordillera (Cordillera Domeyko). The trace of folded layers (in green) are enlarged and overlaid on GoogleEarth map view covering the rectangular area indicated in Fig. 9. Most of the folded structure mapped here is seen south of Chacarilla Canyon in Fig. 4. A series of two large anticlines with a syncline in the middle, are strongly inclined (slightly overturned by places) to the West. Both the length (measured along strike) of the structures (~ ≥ 25 km) and the wave-length dimensions (measured across strike) indicate that significant westward-vergent shear has occurred across the thick Mesozoic sediment pile. That strong deformation has been followed by significant erosion of the Western Cordillera and subsequent deposition of the very shallow westward-dipping layers of the Cenozoic Azapa formation. The erosion surface named Choja Pediplain (Galli-Olivier, 1967), carved across the already deformed and overthickened Western Cordillera, is clearly visible in the area. Labels c and d indicate location of corresponding views in Fig. 11. Road (in white) goes from Pintados to Quebrada Blanca (small localities not shown in our maps). (For interpretation of the references to colour in this figure legend, the reader is referred to the web version of this article.)

3.3.1. Early period

The early period of the Andean cycle, from early Jurassic to early Cretaceous (190 Ma–100 Ma), is associated with margin-perpendicular extension localized for at least 3000 km alongside the west margin of South America, on a paired arc and back-arc basin system (Coira et al., 1982; Mpodozis and Ramos, 1989; Ardill et al., 1998; Charrier et al., 2007). Geographically, in north Chile and south Peru, the Jurassic–early Cretaceous arc follows mostly the present-day Coastal Cordillera (La Negra arc in north Chile, see Charrier et al. (2007)). The thick deposits of the arc and back-arc system (possibly exceeding 10 km

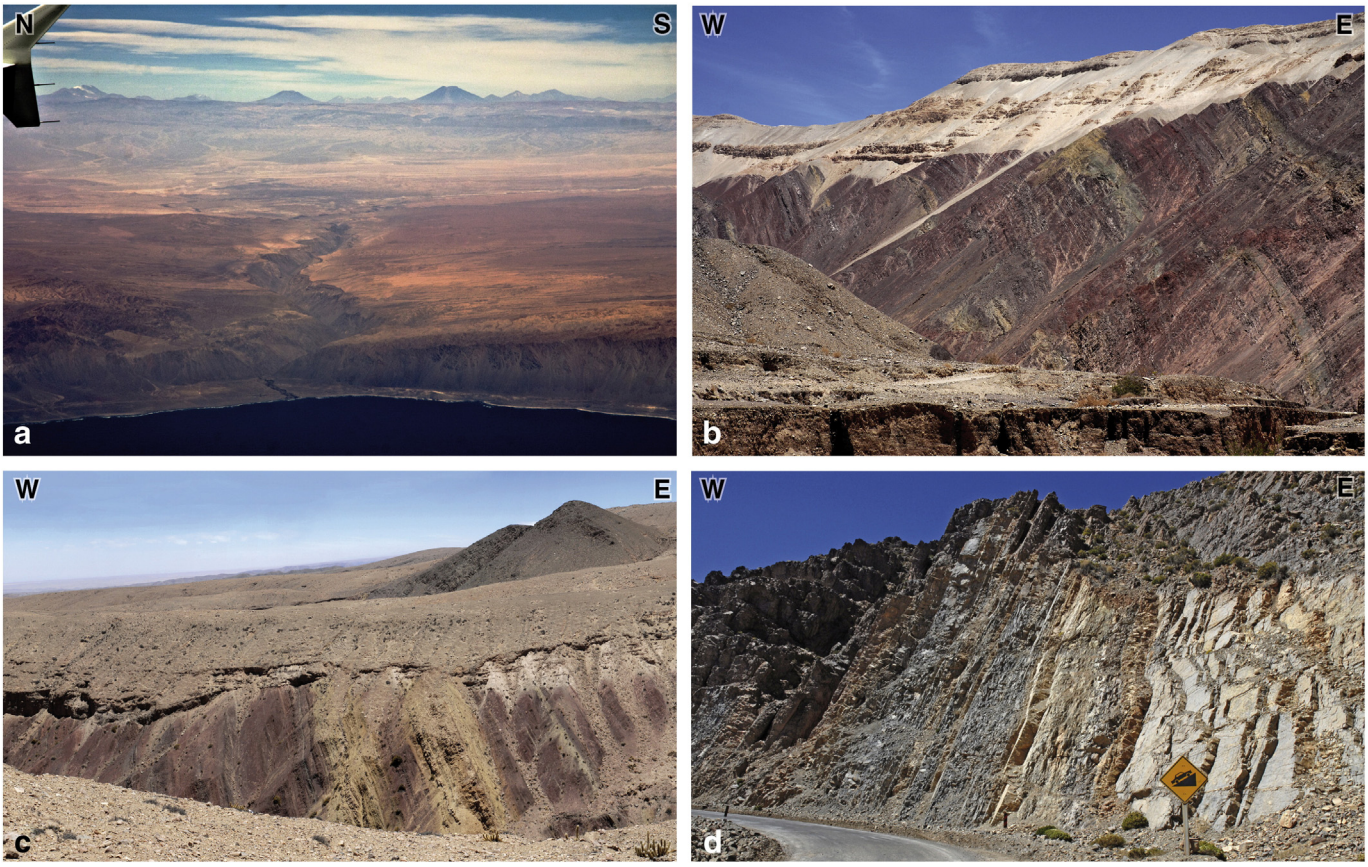

Fig. 11. Field views. For locations see Figs. 9 and 10. (a). Eastward view (from aircraft liner) of (in the foreground) the Atacama Bench incised ~800 m by the Loa river canyon and cut along the shoreline by the N–S oriented Coastal Scarp. The Western Cordillera (locally named Cordillera Domeyko) and the flat Altiplano Plateau topped by the Volcanic Arc are distinguishable in the background. Compare with the similar view of the topography in the lower panel of Fig. 5. (b–c). Views of the basal unconformity of the Central Depression basin sediments deposited over east-dipping Mesozoic sediments at the west flank of Cordillera Domeyko. The Azapa formation (on top) covers an erosion surface (Choja Pediplain) carved previously on the already deformed structure, see Fig. 8). (d). Steeply west-dipping (>80°) Mesozoic sediments at the east flank of the large syncline seen in Figs. 4 and 9–10.

thickness in main localized depocentres) appear superimposed on the earlier Triassic half-grabens (Sempere et al., 2002; Charrier et al., 2007; Mpodozis and Ramos, 2008; Ramos, 2010) and are located beneath what is now the area between the Coastal Cordillera, the Central Depression and the west flank of the Western Cordillera. During this period, as a result of progressive eastward arc migration, part of the back-arc became an intra-arc basin, denoted locally in north Chile as Tarapacá Basin (Charrier et al., 2007). Extensional processes during the Mesozoic possibly associated with fragmentation of Gondwana and the opening of the Atlantic also affected more internal regions of continental South America, particularly in the Salta Rift extensional province (Kley et al., 1997; Kley et al., 2005; Insel et al., 2012). Many of the extensional features of western South America appear reactivated by structural inversion during later shortening and thickening processes of the Andean cycle (Elger et al., 2005; Charrier et al., 2007; Barnes and Ehlers, 2009).

3.3.2. Transitional period

The transitional period from middle Cretaceous to late Palaeocene (100 Ma–50 Ma) is marked by further eastward arc migration and a partial initiation of basin inversion during two short pulses, one in the early-middle Cretaceous (customarily correlated with the "Peruvian phase" in Peru, see (Mégard, 1984; Coira et al., 1982)) and the other one close to the Cretaceous–Palaeocene boundary (Mpodozis et al., 2005; Arriagada et al., 2006; Charrier et al., 2007; Amilibia et al., 2008). In north Chile, the Cretaceous–Palaeocene magmatic arc appears shifted about 60–80 km eastward with respect to the initial Jurassic arc and is roughly aligned with the west flank of the present Western Cordillera. Deposition in basins in a correspondingly shifted back-arc position has continued (mainly Tolar, Cerro Empexa and Tambillos formations in the north Domeyko area) and has been interpreted as persisting back-arc extension (Charrier et al., 2007). This regime would have been followed perhaps more locally, by establishment since the Maastrichtian–Danian (70–64 Ma) of a Palaeocene foreland basin tectonic environment controlled by progressive shortening, as observed in the Salar de Atacama basin, which is located in atypical tectonic environment (Mpodozis et al., 2005; Arriagada et al., 2006; Charrier et al., 2007; Jordan et al., 2007; Amilibia et al., 2008).

An important consequence of the early Jurassic–late Palaeocene eastward migration of the magmatic arc (during a protracted period of 140 Myr covering the early and transitional periods of the Andean cycle) was the formation of a distinct Andean structural fabric along the western margin of continental South America, which clearly obliterates contacts between different terranes that comprised the earlier accretionary Gondwanan fabric (Ramos and Aleman, 2000). The newly created Andean fabric is characterized by significant crustal thinning and structural damage of the earlier continental basement. The damage process is associated with accumulation of a thick pile of sediments and volcanic rocks in the dominantly extensional environment of a composite basin, which has evolved from back-arc to intra-arc, then to forearc conditions. This large-scale feature of the Andes orogen (long ago recognized as the "Andean Geosyncline", see Aubouin et al. (1973)) is the equivalent of the continuous basin described from north to central Chile by (Mpodozis and Ramos, 1989) and denoted for simplicity hereafter in this paper as the "Andean Basin" (as proposed by Armijo et al. (2010a)).

3.3.3. Late period: overview of Andean orogeny at subduction margin

The Andean orogeny properly (50 Ma to Present) is the late period of the Andean cycle, dominated by major margin-perpendicular shortening, crustal thickening, mountain building and exhumation of basement rocks by erosion. The observed shortening implies substantial basin inversion at upper crustal levels (Haschke and Gunther, 2003; Charrier et al., 2007; Barnes and Ehlers, 2009), which suggests that the initial localization of margin-perpendicular shortening process was controlled by the crustal-scale structural fabric beneath the Jurassic–Palaeocene Andean Basin. Shortening initiated regionally all over the Western Cordillera of the Central Andes by deformation of mostly late Palaeocene–Eocene age, corresponding to the so-called "Incaic phase" (Noble et al., 1979; Coira et al., 1982; Mégard, 1984; Charrier et al., 2007). The "Incaic" shortening appears associated with subsidiary arc-parallel strike–slip faulting along Cordillera Domeyko and along the south Peru forearc, which in turn explains the initiation of rotation (correspondingly clockwise and counter-clockwise) of the two limbs forming the Andean Orocline, as documented by paleomagnetism (Roperch et al., 2006; Arriagada et al., 2008).

The "Incaic" deformation in the Western Cordillera is characterized by exhumation of at least 4–5 km between 50 Ma and 30 Ma, as documented by apatite fission track thermochronology in Palaeozoic crystalline basement rocks sampled along Cordillera Domeyko (Maksaev and Zentilli, 1999). That amount of exhumation has been enough to remove entirely by erosion the Mesozoic cover deposited on top of the Domeyko basement during earlier periods of the Andean cycle. So, probably no significant basement upheaval had occurred during earlier tectonic pulses, which corroborates the idea that the Andean orogeny has started principally at ~50 Ma in the Central Andes by significant shortening and crustal thickening under the present-day Western Cordillera (Figs. 1–2 and 4).

The 50–30 Ma uplift and mountain building of Cordillera Domeyko and the Western Cordillera (denoted "Incaic Range", see Charrier et al. (2007)), has produced important changes in the paleogeography and sedimentation pattern (Mpodozis et al., 2005). It has been suggested that the emergence of a basement high (which we denote here as the "Incaic" backbone of the Western Cordillera) bounded by bivergent trench-ward and continent-ward thrusts, has controlled development of two flanking basins fed by sediments eroded from the growing mountain range (Mpodozis and Ramos, 1989; Charrier et al., 2007; Hartley and Evenstar, 2010; Decou et al., 2011). Fig. 8 shows that the Central Depression Basin has developed lately within that framework, with sharp truncation of the "Incaic" backbone by an erosion surface (Choja Pediplain in north Chile: Galli-Olivier (1967); Altos de Camilaca surface in south Peru: Tosdal et al. (1984)) and a pronounced unconformity at the base of the deposited sequence (see Section 2.3 and Figs. 4, 8–11). Later contraction (30 Ma to Present) across the subduction margin of the Central Andes is relatively modest (Muñoz and Charrier, 1996; Victor et al., 2004; Farías et al., 2005; García and Hérail, 2005; Schildgen et al., 2009; Charrier et al., 2013) and has resulted in a total of 2–3 km of late Cenozoic relative uplift of the Western Cordillera with respect to the CDB, as illustrated in Fig. 8. Little erosion and basement exhumation have occurred over the Western Cordillera during the 30 Ma to Present period, compared with the exhumation by erosion during the earlier 50 Ma–30 Ma period of much stronger uplift and mountain building in the same place of the Western Cordillera (see Fig. 4). That feature appears indicative of a sharp aridity increase and desertification in Atacama possibly signaling a climatic change of continental or global scale (see Section 2.3). Those observations are consistent with the relatively sediment-starved formation of the CDB in a piedmont environment, leading ultimately to the flat morphology of the Atacama Bench. However, as shown in Fig. 1 (and further discussed in Sections 3.4 and 5.1), the larger-scale process of margin-orthogonal contraction during the late period of the Andean cycle appears to have progressively intensified as it has propagated away diachronously in two directions, perpendicularly and laterally along the Andean margin. For this reason, the concept of synchronous tectonic "phases", widely used in the Andean literature, should be taken with caution (see Sébrier et al. (1988); Pardo-Casas and Molnar (1987)).

3.4. Uncovered structures in Cordillera Domeyko: the West Andean Thrust (WAT)

Although discontinuously exposed all along the Central Andes margin, there is a ubiquitous stripe of deformed rocks of the composite early Jurassic–late Palaeocene Andean Basin which is positioned between the older Palaeozoic basement rocks of the Coastal Cordillera and the exhumed basement backbone of the Western Cordillera (see Fig. 2). In this section, following (Haschke and Gunther, 2003), we attempt to explain the observed crustal thickness of 74–80 km beneath the Western Cordillera (Yuan et al., 2000; Wölbern et al., 2009) by using structural evidence of substantial basin inversion, west-vergent folding, and thrusting collected in the Cordillera Domeyko at 21.5°–23°S (see Figs. 2, 4 and 8–11). We also proceed by testing a shortening mechanism such as that described earlier for similar structures observed 1400 km southward along the strike of the Andes at 33°–34°S (Fig. 1), where the mountain building process is in an early stage of its development (Armijo et al., 2010a). At that latitude (33.5°S, latitude of Santiago), the Andes are much younger and narrower than at 21°S, and no significant relief or mountain belt has developed yet to the east of the main structural backbone (the equivalent to the Western Cordillera basement at 21°S, which at 33°–34°S is simply designated as the Frontal Cordillera).

The west-vergent structure of Cordillera Domeyko may be reconstructed using the evidence of folded Mesozoic rocks of the Andean Basin, which was inverted mostly during the ~50–30 Ma shortening pulse, as discussed earlier. Fig. 9 shows in map view the position of the fold-thrust belt in North Chile, between the undeformed Marginal Block (topped by the Atacama Bench) and the basement high of the Western Cordillera. More precisely, the width of the belt is 30–50 km, as defined from the westernmost frontal traces of thrusts associated with the WAT (in red) crossing the Cenozoic cover, which are determined using seismic sections and topography, and the westernmost traces of basement thrusts over deformed Mesozoic cover. This width is comparable to the ~50 km width of the west-vergent thrust belt at 33.5°S (see Figs. 2 and 8 in Armijo et al. (2010a)). The west-vergent folding style (Figs. 4, 9–10 and 13) is also similar in the two cases, and both the wavelength of folds (~10 km) and their amplitude (~5 km) are comparable. The main difference is that at the latitude of Santiago the folded structure (see Fig. 3 in Armijo et al. (2010a)) affects younger strata (Oligocene–Miocene), which demonstrates the diachronism (southward younging) of the main shortening pulse along the Western Cordillera's backbone (Fig. 1) and the lateral propagation of deformation. Fig. 13 incorporates a complete geomorphologic section of the forearc at 21°S (from Fig. 7) with a structural section (derived from Figs. 9–10) showing a likely reconstruction of the fold-thrust belt geometry at depth and its relation with the Western Cordillera basement high. Because the basement high acts as a backstop (and for the same reasons as for the structure at the latitude of Santiago; see Figs. 8 and 9 in Armijo et al. (2010a)), a flat-ramp geometry is required for the main thrust under the Western Cordillera (Fig. 13).

According to our reconstruction, the total shortening across the fold-thrust belt in North Chile would not be less than ~20–30 km (Fig. 13), which is an order of magnitude larger than earlier estimates by (Victor et al., 2004; Hoke et al., 2007) and 2–3 times larger than the estimate by (Haschke and Gunther, 2003). Both approaches minimized deformation associated with the West Andean Thrust: the work by Victor et al. (2004) and Hoke et al. (2007) did not consider the uncovered "Incaic" shortening (50 Ma–30 Ma) in Mesozoic rocks of the Western Cordillera and the approach by Haschke and Gunther (2003) did not take into account the ≥4–5 km of basement exhumation by erosion during the same 50 Ma–30 Ma period (Maksaev and Zentilli, 1999).

At a larger scale, significant west-dipping backthrusting in the adjacent Altiplano of Chile and Bolivia (Charrier et al., 2013), which are now largely concealed by lava flows of the modern arc (Figs. 9 and 2), forms a wedge with the master west-vergent thrust system (see also Fig. 14). This wedge pattern is consistent with the sedimentary record in the Altiplano basin indicating rapid sedimentation close to a western source (the Western Cordillera) and west-to-east transport during deposition of the main body of the Potoco formation in the late Eocene–Oligocene (Sempere et al., 1990; Horton et al., 2001; Charrier et al., 2013). Overall, our reconstruction suggests that the total shortening under the Western Cordillera may attain ~30–50 km, sufficient to double crustal thickness over that width (Fig. 14) and consistent with geophysical estimates (Yuan et al., 2000; Wölbern et al., 2009). Note that the bivergent nature of the Western Cordillera has for long been suggested (Mpodozis and Ramos, 1989; Charrier et al., 2013), but not the dominance and the steering role of the deeply rooted west-vergent structure and its specific relation with the fundamental crustal thickening processes under the Western Cordillera. We find it reasonable to conclude that the Western Cordillera structure in North Chile is consistent with the inference of a major continuous West Andean Thrust (WAT), as proposed by Armijo et al. (2010a). Furthermore, the occurrence of an uplifted basement backstop juxtaposed with a significantly inverted Mesozoic basin under the basal unconformity of the Moquegua Group in South Peru (Schildgen et al., 2009) suggests that the same tectonic model applies on the Peruvian limb of the Andean Orocline (Fig. 12). However, the lack of any clear discontinuity in zircon (U–Th)/He ages across the margin in South Peru (Schildgen et al., 2009) could be indicative of a more discrete structural expression of the WAT. Therefore, between ~50 Ma and ~30 Ma the rigid Marginal Block as a whole (the modern forearc) appears to have been dragged by the subduction process at the plate boundary and underthrust at the WAT by tens of kilometres under the Western Cordillera. The same process has also sustained at much slower rate since ~30 Ma (age of completion of the Choja Pediplain, see section 2.3), the progressive uplifting and increasing topography of the Western Cordillera relative to the Atacama Bench (Fig. 8).

4. West of Atacama Bench: structures controlling coastline and seismic coupling

In line with the foregoing, the bulk post-10 Ma land uplift responsible of the Atacama Bench's upheaval would be controlled by another west-vergent structure breaking the modern forearc (thus separating the Marginal Block into two pieces, see Figs. 7, 8 and 13), probably reaching the Earth's surface offshore and directly associated with the subduction interface (Fig. 14). Its likely trace thus follows roughly the coastline between the Atacama Bench and the terraced string of basins on the oceanward forearc (Fig. 3). Fig. 14 illustrates the simplified geometry of structures discussed hereafter. The structure emanating upwards from the subduction interface and separating the currently uplifting piedmont region of the Marginal Block (landward forearc), probably under thickening conditions, from the subsiding oceanward forearc under tectonic erosion (von Huene and Ranero, 2003; Kukowski and Oncken, 2006; Clift and Hartley, 2007), is elusive and appears mechanically complex. In North Chile, an offshore west-dipping normal fault system associated with an abrupt change in the dip and a flat-ramp geometry of the subduction interface have been proposed to explain field observations of trench-perpendicular extension in the Coastal Cordillera, the land uplift causing the incision of canyons and the occurrence of the Coastal Scarp (Armijo and Thiele, 1990).

Those inferences appear supported by detailed seismic refraction and seismic reflection experiments in North Chile at ~22°S latitude, which show an abrupt change in the dip of the subduction interface (from less than 10° to about 22°) at about 20 km depth, a few kilometres west of the coastline (Contreras-Reyes et al., 2012). Furthermore, the analysis of surface deformation associated with the seismic cycle (co-seismic, inter-seismic and post-seismic) using GPS and InSAR data indicates down-dip segmentation of mechanical coupling across the subduction interface possibly associated with structural complexity and a flat-ramp geometry beneath the coastline (Béjar-Pizarro et al., 2010; Béjar-Pizarro et al., 2013). Specifically, the highly coupled region of the interplate during inter-seismic periods spreads mostly over the flat oceanward part of the subduction interface and main asperities there appear to correlate well with offshore terraced basins (Song and Simons, 2003; Wells et al., 2003). On the other hand, gradually lower inter-seismic coupling occurs mostly landward from the kink in the steeper transition zone, which may consist of a mosaic of regions that creep aseismically intermixed with small seismic asperities (Béjar-Pizarro et al., 2013). We suggest that structural complexity associated with an underthrust crustal wedge (such as the one depicted in Fig. 14) is a likely explanation for heterogeneity and discontinuous distribution of frictional properties in the steeper transition zone. Hence, the coastal and offshore normal faulting in North Chile would correspond to a secondary surface expression of a west-vergent thrust splay, associated with underthrusting and wedge accretion of continental material from the oceanward forearc, as suggested earlier (Armijo and Thiele, 1990; Adam and Reuther, 2000). That process would be consistent with discussions of forearc basin development by Wells et al. (2003) and Melnick et al. (2006). Concerning the earlier Andean structural fabric, however, we note that the post-10 Ma underthrusting of the oceanward forearc beneath the coastal structural high in the frontal Central Andes represents dragging by the modern subduction process of the Jurassic forearc beneath the Jurassic arc.

A consequence of the process described above is that a similar subduction process implying structural complexity and underthrusting with less or no secondary normal faulting could also explain the similar topography and tectonic features observed along the coast and offshore South Peru (see Figs. 7 and 12). We thus generalize, at least for the whole Central Andean forearc, the inference that significant subduction splay structures, yet complex and poorly described, may steer seismic loading processes at the plate interface and explain occurrence and distribution of major asperities under the oceanward forearc (Song and Simons, 2003; Wells et al., 2003), the down-dip segmentation of coupling and seismicity (Béjar-Pizarro et al., 2013) and occurrence of megathrust earthquake rupture overwhelming that segmentation (Vigny et al., 2011).

5. Discussion: evolution of the Andean orogen

5.1. Incorporating tectonic features of the subduction margin with main features of the Andean orogen

As summarized in Fig. 14, the structures at the two boundaries of the Atacama Bench appear to be first-order features controlling morphology, deformation, crustal thickening and differential land uplift processes across the Andean subduction margin. Furthermore, according to our analysis, the overall margin's style and degree of structural complexity can be described by the evolution over the past 50 Myr of two parallel flat-ramp thrust systems of similar geometry and scale, at the West Andean Thrust and at the subduction interface. That style of deformation reflects the progressive collision and eastward underthrusting of the Mesozoic arc and its continental basement beneath the Western Cordillera, sustaining its crustal thickness and high relief. We find this particular feature of Andean tectonics can be considered comparable with continental collision processes elsewhere and represents a basic element to understand Andean orogeny. To incorporate those results across the Andean subduction margin into the larger scale, Fig. 14 also compiles published knowledge of other significant large-scale structures and the timing of their deformation across the whole Andean orogen, so providing the basic elements to describe the overall tectonic evolution of the Andean orogeny since 50 Ma (covering for simplicity only the late period of the Andean cycle).

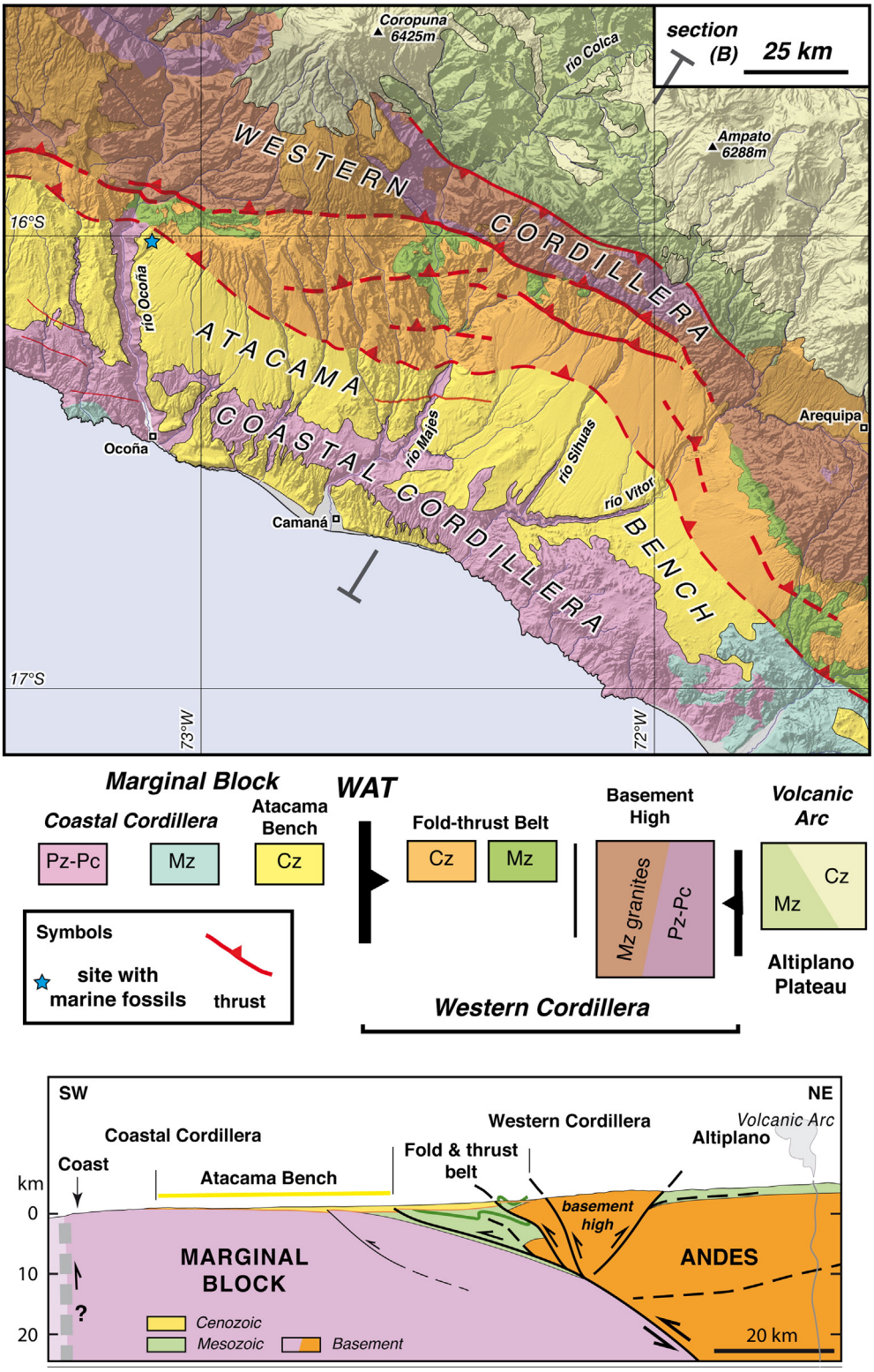

Fig. 12. Tectonics of landward forearc – Andean subduction margin – South Peru. a. Geological Map showing that, as in the similar map compiled for North Chile in Fig. 9, the same tectonic units can be recognized and mapped at the same scale, even if the structural outcrops are of less quality. Compiled from 1:100,000-scale geologic maps of southwest Peru from the Instituto Geológico Minero y Metalúrgico (INGEMMET, 2001). See the precise location within the large-scale regional context in Fig. 2. The trace of the section coincides with profile P3 in Fig. 6. The coloured boxes indicate the age of corresponding rocks in the map: Precambrian (Pc), Paleozoic (Pz), Mesozoic (Mz) and Cenozoic (Cz). WAT indicates the location of the frontal east-dipping trenchward-vergent West Andean Thrust. b. Schematic section showing the probable structure, which is comparable with the much better constrained section across Cordillera Domeyko in North Chile, shown in Fig. 13. Our section here is basically consistent with a section presented earlier in a more local study of the same region (Schildgen et al., 2009). (For interpretation of the references to colour in this figure legend, the reader is referred to the web version of this article.)

Our compilation in Fig. 14 illustrates the following implications: (1) The Andean orogen results from protracted processes of bivergent crustal shortening and thickening in the wide region (in orange) squeezed between the underthrusting South America Plate (Brazilian Shield) and the rigid Marginal Block (both in light violet). (2) The horizontal forces driving the orogeny are associated with plate convergence

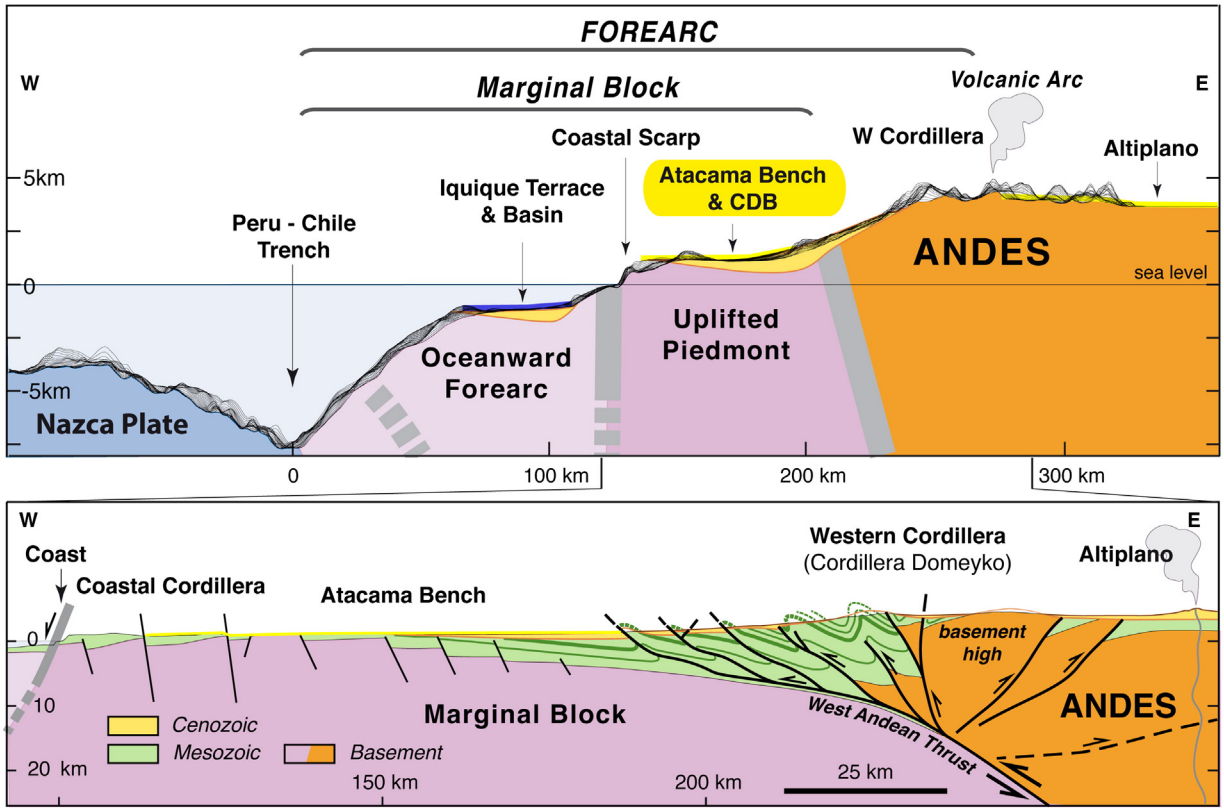

Fig. 13. Simplified geology of central Andean margin. The top panel displays morphologic steps in the forearc between the Western Cordillera and the Nazca Plate. A swath topographic profile across the Andean subduction margin (at 20°S, vertical exaggeration of 8.33) shows its trenchward downwarping and main tectonic boundaries (gray stripes, segmented where uncertain). The Atacama Bench overlaps the flat western part of the wedge-shaped Cenozoic Central Depression Basin (CDB). The eastern side of the CDB is deformed by uplift of the Western Cordillera relative to the Marginal Block. The similar offshore Iquique terrace and Iquique back-tilted oceanward forearc basin are offset vertically by ~2 km with respect to the Atacama Bench. The precise age of the possibly Late Cenozoic Iquique Basin is undetermined. In North Chile, the tectonic boundary between the uplifted region of the Marginal Block and the sinking oceanward forearc appears to be a secondary normal fault system responsible of the Coastal Scarp (Armijo and Thiele, 1990). The lower panel enlarges the corresponding structural section as reconstructed at 21°S across the Cordillera Domeyko (see Section 3.4 and Figs. 9-11). It shows without vertical exaggeration the attitude of the mildly deformed SDB over the strongly deformed west-vergent inverted structure of the earlier Mesozoic basin. The exhumed basement high constituting the structural backbone of the Western Cordillera and the role of the West Andean Thrust (WAT) (Armijo et al., 2010a), similar as that observed at 33.5°S, are specified. The Marginal Block appears underthrust beneath the WAT and Western Cordillera basement backbone.

across the subduction interface (main plate contact under fast-rate convergence), where energy is chiefly dissipated during megathrust earthquakes rupturing from depths of ~50 km up to the trench (region of coupling outlined in dark magenta). (3) The lower limit of high coupling correlates at the surface with coastal structures (Armijo and Thiele, 1990) and with the boundary between the oceanward forearc and the Marginal Block (Song and Simons, 2003; Fuller et al., 2006; Béjar-Pizarro et al., 2010; Béjar-Pizarro et al., 2013). (4) The Marginal Block appears bounded by two flat-ramp thrusts of similar scale: the West Andean Thrust (WAT) (Armijo et al., 2010a) beneath the Western Cordillera and the probably kinked subduction interface (Armijo and Thiele, 1990; Contreras-Reyes et al., 2012; Béjar-Pizarro et al., 2013). (5) The uplift of the Atacama Bench atop the Marginal Block may result from underthrusting and wedging of light continental material during bivergent growth of the Andean orogen since 10 Ma (yellow arrows). (6) The effects of an interplay between tectonics and increasing aridity governing the Cenozoic evolution of morphology over the Pacific seaboard (Western Cordillera and Atacama Bench, Figs. 3 and 4) is barely noticeable at the large scale of Fig. 14, but important tectonic constraints from that interplay are discussed along with our evolutionary reconstruction of Andean orogeny (Fig. 15).

However, Fig. 14 does not represent elements of the Andean lateral evolution along strike. As shown in Fig. 1 and mentioned earlier (Sections 3.3.3 and 3.4), the bivergent growth process is associated with bilateral propagation of deformation along the Western Cordillera, as documented by the southward decrease of shortening and shortening age (Armijo et al., 2010a; Armijo et al., 2010b), and by exhumation ages along its basement backbone. At latitude 21°S, basement exhumation has occurred mostly by 50–30 Ma, as determined with fission track thermochronology in apatites (Maksaev and Zentilli, 1999). By comparison, at latitude 33°S, the main exhumation of the equivalent basement backbone, named here the Cordillera Frontal, had started at ~25 Ma, as constrained by apatite (U/Th)/He (Hoke et al., 2014). The symmetric northward decrease of shortening age from 21°S to the north has barely been assessed specifically (Picard et al., 2008), but the process of bilateral propagation in the Andean Orocline has been implied, among others, by Kley (1999), Barnes and Ehlers (2009) and Ramos (2010). Despite the large scale considered here, the along-strike propagation associated with increasing slip on localized faults, crustal-scale thrust faults in this case, appears consistent with scaling laws in elastic fracture mechanics (e.g. see discussion by (Hubert-Ferrari et al., 2003)). We retain that the bivergent and associated bilateral growth are fundamental features of the Andean orogen allowing us to address boundary conditions at the scale of continental South America (Section 6.1.2 and Fig. 18).

5.2. Approach for reconstructing a 2D evolution

To discuss further possible implications at the scale of the orogen, Fig. 15 schematically reconstructs the same E–W section at latitude 21°S as in Fig. 14 in order to describe a first-order model of the Andean evolution during the late period of the Andean cycle by a series of discrete snapshots (every 10 Myr). As for Fig. 14, the large-scale representation of tectonic features dwarfs the more subtle implications

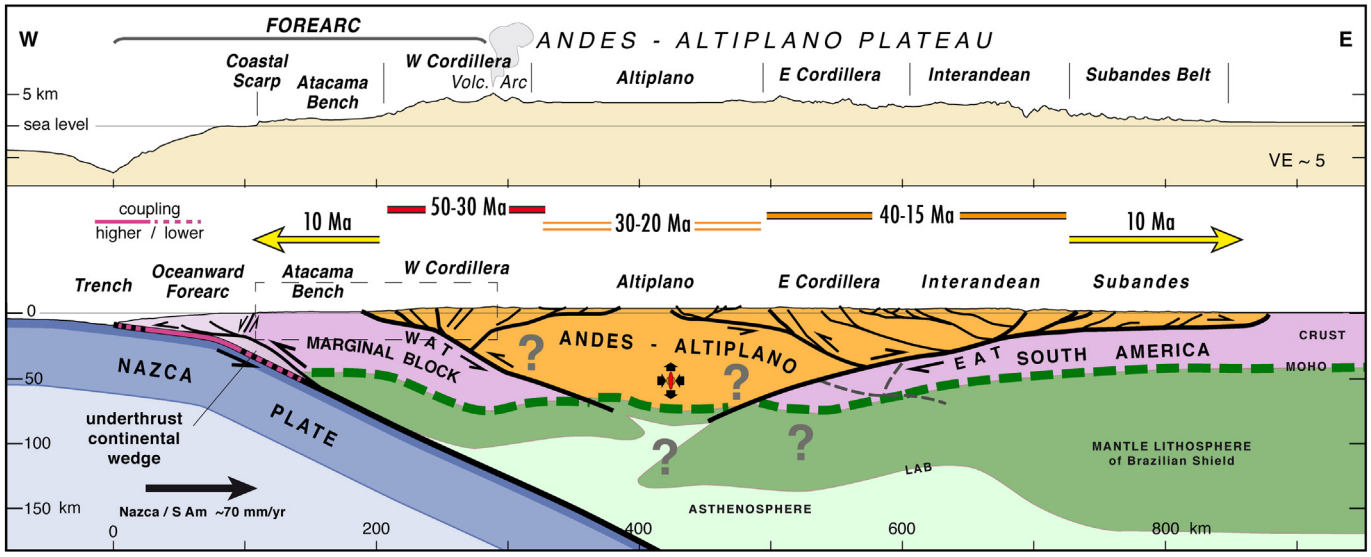

Fig. 14. Large-scale 2D structure of Andean orogen. Interpreted section at 21°S, across the southern limb of the Andean orogen (trace given in Figs. 1, 2 and 3). It superposes with the section across Cordillera Domeyko in Fig. 13 (indicated by dashed rectangle). Black arrow represents net EW Nazca/South America convergence. Upper panel is topographic profile (with vertical exaggeration of ~5). Ages of main periods of deformation across different regions of the orogen (in Ma, from Sempere et al. (1990); Maksaev and Zentilli (1999); McQuarrie et al. (2005); Oncken et al. (2006); Barnes and Ehlers (2009); Charrier et al. (2013)) are indicated by horizontal double bars (dark red, light red, orange). The divergent yellow arrows indicate frontal regions of the orogen over which deformation has propagated since 10 Ma. Positions of Moho (MOHO) and of lithosphere–asthenosphere boundary (LAB) are consistent with converted seismic phases and receiver function data (Yuan et al., 2000; Heit et al., 2007; Wölbern et al., 2009). Flexure of the Brazilian Shield is consistent with gravity anomalies as defined by Lyon-Caen et al. (1985). Gray question marks are placed where uncertainty is considerable. The structure of the Eastern Cordillera, the Interandean belt and Subandes belts is consistent with interpretations of seismic sections, as discussed by (Kley, 1996; Muller et al., 2002; Oncken et al., 2006; Barnes and Ehlers, 2009). The west-vergent West Andean Thrust (WAT) and the east-vergent East Andean Thrust (EAT) delimit the boundaries of over-thickened crust in the Andean orogen (orange), caught between the Marginal Block and the South America craton (Brazilian Shield); both in light violet. In large thrust systems as the West Andean Thrust (WAT), the East Andean Thrust (EAT) and the Eastern Cordillera Thrust (ECT), shortening is absorbed by shear and displacement (simple shear mechanism). Where fault structures are not specified (e.g. deeper crust of the Altiplano) shortening and thickening are diffuse (pure shear mechanism, represented by red deformed ellipse adorned with paired bold arrows indicating horizontal shortening and vertical lenghtening). The viability of this interpreted section is tested by the schematic reconstruction in Fig. 15 and discussed in Section 5. (For interpretation of the references to colour in this figure legend, the reader is referred to the web version of this article.)

associated with evolution of morphology, so the latter is emphasized in our written discussion, when necessary. For simplicity, our approach of the crustal structure considers only thickening processes associated with tectonic shortening and does not take into account possible magmatic contributions (e.g. Sheffels (1990); Gubbels et al. (1993)). Crustal shortening may include distributed thickening, equivalent of middle-lower crustal flow (e.g. Isacks (1988); Lamb (2011)). Other types of deep flow (e.g. Kley and Monaldi (1998); Ouimet and Cook (2010)) and mechanisms of lithospheric mantle thinning, etc. (e.g. Lamb (2011)) can be included. The attempt presented here is fairly quantitative, given the large uncertainties of the geological estimates considered, but it does not adopt the usual formalism of balanced cross sections (e.g. McQuarrie et al. (2005)), which does not allow for distributed deformation inside prescribed blocks of a given thickness. Instead, to balance our reconstructed sections, we proceed by trial and error using a backward-and-forward analysis of deformation, which allows for both internal deformation of blocks – thus also of faults – and accommodation of displacement on major fault systems. Specifically, in our sections the basement footwall blocks can undergo distributed deformation as well, in contrast with the usual formalism where the basement below a sole thrust is postulated to be rigid and undeformable, or only affected by long-wavelength flexure. Imposed simplistic constraints (derived from arguments synthesized in Fig. 14) are as follows:

(1) Concerning tectonic shortening and kinematics. We assume a total crustal shortening of 360 km, consistent (within uncertainties) with discussions, among others, by Sheffels (1990), Kley and Monaldi (1998), Elger et al. (2005), McQuarrie et al. (2005), Barnes and Ehlers (2009) and Oncken et al. (2012). So, the eastern edge of the model moves gradually westward a total of 360 km with respect to the axis of the Western Cordillera (bold red arrow to the right of lower panel). We assume a subduction erosion of 1 km/Myr, consistent with estimates by Kukowski and Oncken (2006), implying a total of 50 km of trench advance with respect to the continent (bold red arrow labelled tr in lower panel). As a result, the forearc width (bracketed in initial and final stages) has remained nearly constant. For

Fig. 15. Evolution of Andean orogeny (from 50 Ma to present). The growth process of the Central Andes is schematically represented for a section at 21°S, across the southern limb of the Andean orogen, as Fig. 14. The past geometry of the geological elements in Fig. 14 (present stage, lower panel) is reconstructed for distinct snapshots represented by superposed panels with upward growing age (labelled 10 Ma, 20 Ma, 30 Ma, Ma, 40 Ma and 50 Ma, with timing uncertainty in parenthesis). Significant features discussed in this paper are identified already in the snapshot at 50 Ma: (1) The Mesozoic arc and back-arc formed during the early Andean cycle, which is at 50 Ma largely in forearc position. (2) The main body of Mesozoic magmatism intruded at crustal scale, schematically shaded, with smoke column marking the position of the early Cenozoic arc. (3) The Andean basin represented by a wedge (shaded in brown) and its shape controlled by an asymmetrical extensional system associated with a crustal-scale normal fault dipping eastward (future WAT when inverted). Other features can be followed throughout the proposed evolution: (1) Strong converging regions of the continental crust, identified in the forearc and cratonic sides (light violet). (2) The intervening softer region (shaded initially in shaded orange) being gradually incorporated into the Andean orogen (regions turning progressively into bright orange), tuned with the progressing occurrence of crustal shortening and structural inversion. (3) Propagation of deformation proceeding mostly eastward. (4) The overall divergent geometry and divergent growth process appearing as late features of the Andean orogen. For a full discussion, see Section 5 in the text. WAT denotes West Andean Thrust; EAT, East Andean Thrust; ECT, Eastern Cordillera Thrust; IAT, Interandean Thrust. For the present-day status, the bold red arrows indicate amounts of crustal shortening and trench retreat (tr). The modern post ~10 Ma divergent growth of the Andes–Altiplano Plateau is shown by smaller red arrows. The size of raining clouds is proportional to precipitation rates (in mm/yr, after Bookhagen and Strecker (2008)). (For interpretation of the references to colour in this figure legend, the reader is referred to the web version of this article.)

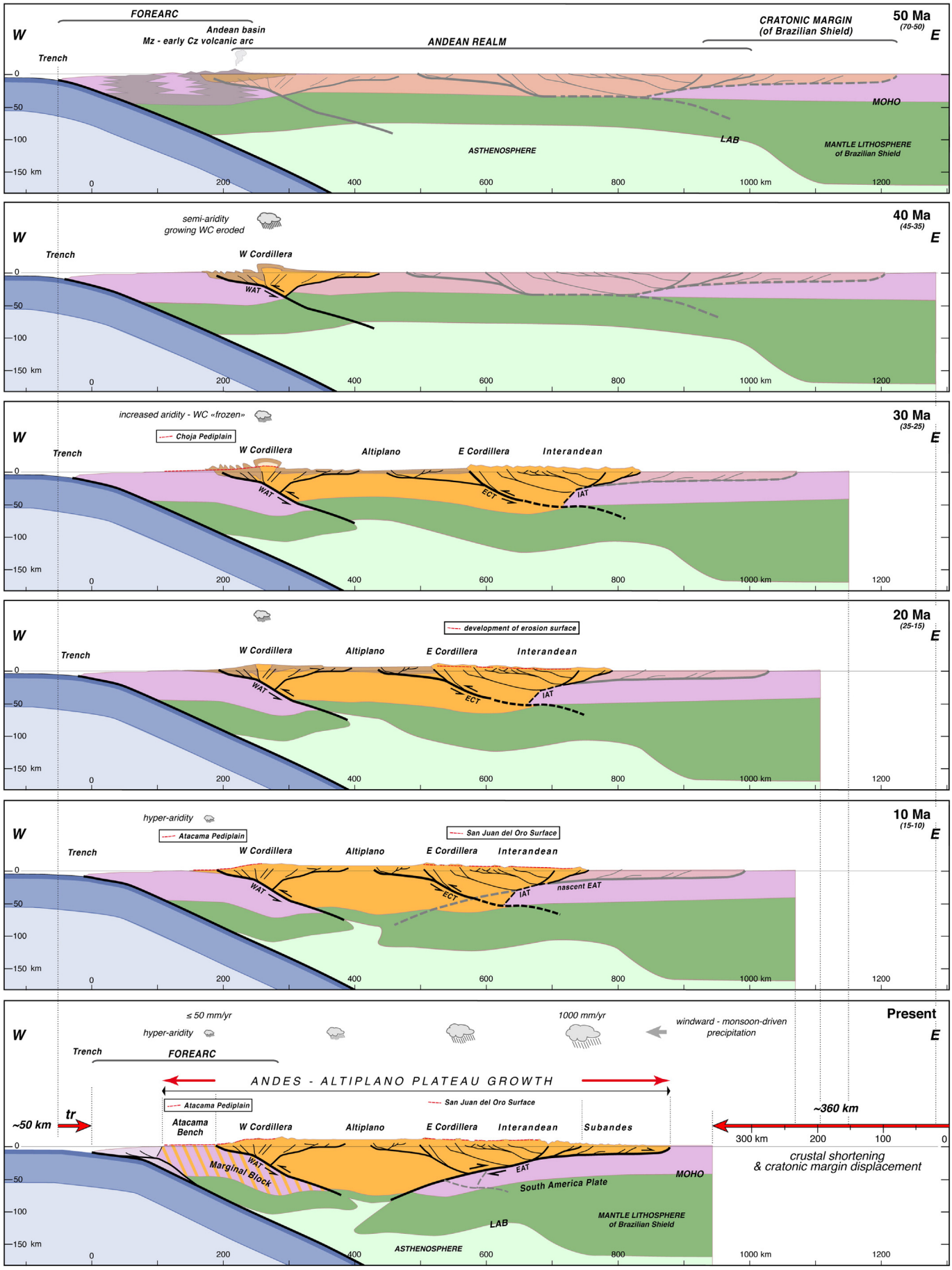
FOREARC
Andean basin
Mz - early Cz volcanic arc
ANDEAN REALM
CRATONIC MARGIN
(of Brazilian Shield)
50 Ma
(70-50)
W
E
Trench
MOHO
LAB
ASTHENOSPHERE
MANTLE LITHOSPHERE
of Brazilian Shield
semi-aridity
growing WC eroded
40 Ma
(45-35)
W Cordillera
WAT
increased aridity - WC «frozen»
Choja Pediplain
30 Ma
(35-25)
Altiplano
E Cordillera
Interandean
ECT
IAT
development of erosion surface
20 Ma
(25-15)
hyper-aridity
Atacama Pediplain
San Juan del Oro Surface
nascent EAT
10 Ma
(15-10)
≤ 50 mm/yr
1000 mm/yr
windward - monsoon-driven
precipitation
Present
ANDES - ALTIPLANO PLATEAU GROWTH
~50 km
tr
Atacama
Bench
Subandes
~360 km
crustal shortening
& cratonic margin displacement
Marginal Block
EAT
South America Plate
0
50
100
150 km
200
400
600
800
1000 km
1200
300 km

simplicity, the overall dip of the subducting slab remains constant (30°), but the kink at 20 km depth suggested by Contreras-Reyes et al. (2012) has formed gradually. We underscore that uncertainties in estimates of shortening, subduction erosion (and other embedded estimates) are large, but the values used here are reasonably safe for the large scale of our first-order synthesis.

(2) Concerning the chronology. Ages of deformation affecting the different structures are simplified as for Fig. 14 and are consistent with deformation ages and thermochronologically constrained exhumation as discussed by Sempere et al. (1990), Gubbels et al. (1993), Maksaev and Zentilli (1999), Muller et al. (2002), McQuarrie et al. (2005), Oncken et al. (2006), Scheuber et al. (2006), Ege et al. (2007), Arriagada et al. (2008), Barnes and Ehlers (2009), Charrier et al. (2013) and Eichelberger et al. (2013). Uncertainties and dispersion in those ages are large and difficult to quantify, so the "snapshots" here cover long durations of many Myr, so reasonable ranges of uncertainty can be bracketed. More importantly, the primary chronology and the succession of main Andean tectonic events are fully respected.

(3) Concerning the reconstruction technique. As the present-day structures of the Andean orogen are basically inherited from early structures (e.g. Elger et al. (2005); Barnes and Ehlers (2009); Oncken et al. (2012)), the evolution process is first simulated using the present-day geometry and an actualistic backward deformation approach. Then adjustments are obtained by forward deformation and so forth. That technique is applied to the main present-day crustal blocks, fault systems and associated crustal thickness structure (Yuan et al., 2000; Wölbern et al., 2009), as well as to long-lasting features of the mantle lithosphere structure (Heit et al., 2007) and flexure of the Brazilian Shield (Lyon-Caen et al., 1985) as specified in Fig. 14. As blocks, fault systems and other structures are stretched and displaced backwards gradually from the present, many important features of the present-day status (lower panel) can be readily identified since the initial status at 50 Ma.

(4) Concerning tectonic levels and styles. For the deep structure of the Eastern Cordillera and the Interandean belt, our schematic reconstruction of the present-day status (Figs. 14 and 15) is consistent with bivergent thick-skinned fold-thrust belt models with basement-involved crustal-scale faults and is inspired from tectonic interpretations by Kley (1996), Muller et al. (2002), Elger et al. (2005), Oncken et al. (2006), Scheuber et al. (2006) and Ege et al. (2007). However, for the early (>15–10 Ma) development of the bivergent Eastern Cordillera–Interandean fold-thrust belt, we adopt upper thrusts controlled by a lowermost crustal-scale west-vergent thrust. That choice is consistent with the significant earlier development of west-vergent thrusting at the western front of the Eastern Cordillera facing the Altiplano region, denoted here Eastern Cordillera Thrust (ECT), which is equivalent of the Coniri–Huarina Thrust defined by Sempere et al. (1990) and to the San Vicente Thrust of Muller et al. (2002). The thin-skinned deformation in the Subandes belt is consistent with seismic and borehole data as described by Baby et al. (1992), Baby et al. (1995) and Dunn et al. (1995). Shortening is accounted for by shear and displacement (simple shear) where large faults or thrust systems are gradually defined: in order of appearance, first the West Andean Thrust (WAT), then west-vergent East Cordillera Thrust (ECT) followed by the east-vergent Interandean Thrust (IAT). Finally, for the late (<15–10 Ma) period of development of the overall orogen, the conjugate shortening effects of the East Andean Thrust (EAT), associated with westward subduction of the Brazilian shield, and the underthrusting processes in the forearc beneath the Marginal Block, associated with subduction of the Nazca plate. The EAT concept used here encompasses in part the Subandean Thrust concept used, among others, by Kley (1996). Importantly, within intervening regions between main faults and in larger regions where deep fault structures cannot be specified, like in the deeper crust of the Altiplano, shortening and thickening processes are assumed to be diffuse (pure shear, see Fig. 14).

5.3. Initial status

The snapshot at 50 Ma (~70–50 Ma) captures the initial geology of the western margin of South America at latitude 21°S, just before failure of the crust and lithosphere of South America and definite inception of Andean orogeny (see previous discussion in section 3), so topographic relief appears restricted to the volcanic arc and the Altiplano region is nearly at sea level (Sempere et al., 1997). This happens after the end of the early and transitional periods of the Andean cycle, so the cross section shows mostly an extensional fabric of the back-arc close to the subduction zone, as well as a broader extensional region of continental South America, whose formation is probably associated with fragmentation of Pangaea, Gondwana, and the opening of the Atlantic. The uncertainty in age for the initial status is due to the suggestion of contraction already since the Maastrichtian–Danian (70–64 Ma) (Sempere et al., 1997; Mpodozis et al., 2005; Arriagada et al., 2006; Charrier et al., 2007; Amilibia et al., 2008). The continental crust includes two thicker strong regions (both in light violet): at the forearc (future Marginal Block) and at the cratonic margin of South America (Brazilian Shield). Between those two strong regions is a wide region with attenuated crust (≥400 km wide, shaded in orange), which is close to sea level and corresponds to the future shortened and thickened crust of the Andean orogen (compare with present-day stage in lower panel). That wide region includes: (1) the back-arc region, close to the subduction contact, which corresponds to the future Western Cordillera; (2) farther into the continent, the extensional region of the Tupiza, Estarca and Tres Cruces basins (not identified specifically in this panel), which appear to be important northern branches of the intra-continental Salta Rift extensional province (Grier et al., 1991; Kley et al., 1997; Kley et al., 2005; Insel et al., 2012). That overall continental region corresponds to the future Altiplano, Eastern Cordillera and Interandean belt and (3) the possibly extensional margin of the craton (Brazilian Shield), which corresponds to the future Subandes (Baby et al., 1995). Strikingly, the structure of the mantle lithosphere appears to bear the signature of the cratonic margin, as suggested by the present-day shape of the lithosphere–asthenosphere boundary (labelled LAB: Heit et al. (2007)). Backward to the initial status at 50 Ma in the reconstruction, the dramatic change in lithospheric thickness beneath the restored Subandes highlights the importance of pre-existent crustal and lithospheric thinning in the nascent Andean orogeny realm (bracketed), which is conversely characterized by its over-thickened crust in the present-day status. This feature clearly suggests that the pre-existent Andean fractured realm was attenuated, as well as structurally damaged and thermally softened during the early and transitional periods of the Andean cycle (see discussion by Sempere et al. (2002)). Therefore, during those periods a lithospheric-scale process zone may have been created, preparing the future deformation locus and style of the later Andean orogeny.

5.4. Snapshot at 40 Ma: deformation localized in Western Cordillera

The snapshot at 40 Ma (~45–35 Ma) shows the first effects of the Andean orogeny. Crustal shortening, thickening and basin inversion are localized only in the Western Cordillera, producing dominant west-vergent folding and thrusting of the Andean back-arc deposits observed in Cordillera Domeyko, as well as the beginning of exhumation of the basement backbone of the Western Cordillera and creation of the nascent Andean topographic relief (compare with Fig. 13). All those features are associated with the initiation of the so-called "Incaic phase" of deformation (see section 3.3.3). The deforming wedge (basement, in

orange, adorned with folded deposits, in brown) is rooted in the crustal-scale, west-vergent, West Andean Thrust (WAT). At 40 Ma, the style of dominant west-vergent deformation may have been similar to that observed for the present-day stage along a section of the Andes at the latitude of Santiago (33.5°S) (compare with Fig. 8 in Armijo et al. (2010a)).

5.5. Snapshot at 30 Ma

The snapshot at 30 Ma (~35–25 Ma) shows deformation nearly stopped in the Western Cordillera (associated with occurrence of the Choja Pediplain) and the consequent continuation of the Andean orogeny with a substantial widening of the mountainous region. This widening occurs by incorporation of inversion tectonics to the east of the Western Cordillera into the westernmost (future) Altiplano region and, more importantly, initiation of deformation in the bivergent wedge formed by the Eastern Cordillera and the Interandean belt (McQuarrie et al., 2005; Eichelberger et al., 2013), between the west-vergent Eastern Cordillera Thrust (ECT) and the east-vergent main Interandean Thrust (denoted IAT).

5.5.1. Completion of Choja Pediplain over Western Cordillera: tectonic vs. climatic forcing

Topping the Western Cordillera and its west piedmont is the Choja Pediplain (Galli-Olivier, 1967) (dashed red line), which truncates the exhumed basement forming the hidden "Incaic" backbone of the Western Cordillera and the west-vergent fold-thrust structure associated with the WAT (compare with Figs. 4, 8 and 11). Consequently, the period of possible semi-aridity during which the Choja Pediplain formed (between ~50 Ma and ~30 Ma) was characterized by sufficient precipitation and fluvial erosion over the whole Western Cordillera structural backbone, a process that may have substantially reduced tectonic relief. However, since ~30 ± 5 Ma, age of the first units deposited over the basal unconformity, the Central Depression Basin was starved of sediments, while the lack of precipitation and erosion appears to have inhibited further exhumation, so "freezing" tectonic activity over the Western Cordillera (see Figs. 4 and 11; Sections 2.3 and 3.3.3), similar to processes discussed by Dahlen and Suppe (1988) and Beaumont et al. (1992). We consider the geological evidence throughout the Pacific seaboard of South America to be compelling, indicative of a sharp increase of aridity, which argues for a climate change at continental scale. Consequently, the onset of Andean orogeny in the Western Cordillera at 50 Ma (or earlier) precedes an intensification of aridity and desertification since ~30 Ma. Intensification of aridity in the Atacama Desert following formation of the Choja Pediplain appears to occur in phase with the Early Oligocene cooling phase of climate associated with the onset of continental-scale glaciation over Antarctica (e.g. Zachos et al. (2001); Zachos et al. (2008); Barker et al. (2007); DeConto et al. (2008)). So we hypothesize: (1) That both the intensification of aridity in Atacama and the onset of glaciation in Antarctica may have shared a common cause. (2) Conversely, plate boundary conditions (forcing mechanisms) causing initiation of Andean orogeny since ~50 Ma may have also contributed to Cenozoic long-term climate cooling. Those two hypotheses are discussed in Section 6 (see Figs. 15, 17 and 18).

It has been suggested that global Cenozoic climate cooling may have triggered and sustained Andean orogeny by imposing increasingly dryer conditions in the central South America margin, which would have caused sediment starvation in the trench and increased shear stresses at the subduction interface (Lamb and Davis, 2003). However, the scenario by Lamb and Davis (2003) is inconsistent with the chronology of the most apparent climatic and tectonic events: the intensification of aridity in Atacama since ~30 Ma as documented by the Choja Pediplain has clearly followed the intense 50 Ma–30 Ma "Incaic" phase of shortening, upheaval and exhumation of the basement backbone of the North Chile Western Cordillera.

5.5.2. Late Eocene–Early Oligocene Andean growth by widening

The reduction of erosive power associated with a virtual shutoff of rain supply over the Western Cordillera, marked by the Choja Pediplain (post "Incaic" unconformity) may have inhibited (or "frozen") further deformation and upheaval of the Western Cordillera and instead fostered propagation of orogeny eastward to the Eastern Cordillera and the Interandean belt. However, the shortening process there appears again dominantly west-vergent, consistent with the onset of the Eastern Cordillera Thrust system (ECT) at the western front of the Eastern Cordillera, as defined by Sempere et al. (1990) and Muller et al. (2002), as well as with interpretation of seismic sections and thermochronology data documenting exhumation starting at ~40 Ma in the Eastern Cordillera and at ~30 Ma in the Interandean belt (Muller et al., 2002; Elger et al., 2005; Oncken et al., 2006; Scheuber et al., 2006; Ege et al., 2007; Barnes and Ehlers, 2009; Eichelberger et al., 2013). Significant west-vergent under-thrusting of the Altiplano basement beneath the Eastern Cordillera is also consistent with evolution of deposition and sediment transport conditions from the Eocene–Oligocene Potoco Formation to the Coniri Formation (represented together in brown) and development of an internally drained Altiplano basin, as discussed by Sempere et al. (1990), Sempere et al. (1997), Horton et al. (2001) and Charrier et al. (2013). Overall, the newly formed wedge made of deforming crust in the Eastern Cordillera–Interandean belt region between the ECT and the IAT with dominant west vergence appears similar to the tectonic wedge already formed under the Western Cordillera. However, initial uplift and exhumation of rocks in the centre of the Altiplano would be at ~30 Ma, as deduced from thermochronology (Ege et al., 2007), indicating that the tectonic thickening processes had already encompassed by ~30 Ma the broad region from the Western Cordillera to the Interandean belt (orange in Fig. 15).

5.6. Snapshot at 20 Ma: continuing deformation between Western Cordillera and Interandean belt

The snapshot at 20 Ma (~25–15 Ma) shows mainly the continuation of shortening and thickening processes throughout the region of the Altiplano and the Eastern Cordillera–Interandean belt wedge. According to current interpretations of basin evolution in the area (Horton, 2005), most of the shortening of the Eastern Cordillera and the Interandean belt, between the ECT and the IAT, had already been achieved by this time, which is consistent with continuing exhumation in the region, as documented by thermochronology (Scheuber et al., 2006; Ege et al., 2007; Barnes and Ehlers, 2009; Eichelberger et al., 2013). Those processes appear concomitant with development of a widespread erosion surface that progressively truncated the structure of the Eastern Cordillera, which is known as the San Juan del Oro Surface (Servant et al., 1989; Gubbels et al., 1993; Kennan et al., 1997).

5.7. Snapshot at 10 Ma: preparation for subduction of the Brazilian Shield

The snapshot at 10 Ma (~15–10 Ma) shows the situation on the eve of a radical change in the Andean evolution, when deformation of the Subandean belt was triggered by the onset of massive westward subduction of the Brazilian Shield under the Andes (e.g. Gubbels et al. (1993); Elger et al. (2005); Oncken et al. (2012)). Our reconstruction seeks to "capture" that instant, when a substantial flip of tectonic polarity, from bi-vergence with dominantly west-vergence to dominantly east-vergence, occurred under the Eastern Cordillera–Interandean belt wedge.

Apatite fission track cooling ages in the Eastern Cordillera and the Interandean belt suggest internal shortening in that region has been modest since ~20 Ma and that slip would have started to be transferred to a lower basement thrust by ~18–15 Ma, with some upheaval persisting in the frontal parts of the Interandean belt until 10 Ma (Eichelberger et al., 2013). Those ages span the completion of the San Juan del Oro Surface by erosion, reduction of internal relief and pedimentation (Servant

et al., 1989; Gubbels et al., 1993; Kennan et al., 1997). Today, the San Juan del Oro Surface appears as a composite succession of nearly undeformed erosion surfaces partly covered with volcanic and relatively starved sedimentary layers, much like the climatically-controlled Atacama Pediplain (Evenstar et al., 2009; Hartley and Evenstar, 2010) topping the Atacama Bench (Fig. 8). Our reconstruction suggests the foregoing features are associated with the nascent main East Andean Thrust (in gray, denoted EAT), which was in the process of being formed (see discussion by Oncken et al. (2012)). That process may have involved deformation localization by truncation of earlier west-vergent structures like the Eastern Cordillera Thrust across the already significantly thickened Andean crust (see deep structures crossed by the downward extension of EAT in dashed gray). Accordingly, the truncating structure of the nascent Eastern Cordillera Thrust at depth could have used the earlier east-vergent Interandean Thrust at middle depth to join the near-surface interface between Palaeozoic cover and Brazilian Shield basement. Although our reconstruction is schematic and far from being unique, we retain that a kinematic configuration of that sort is necessary to resolve simply the flip, from the dominant initial west vergence of the wedge Eastern Cordillera–Interandean belt, to the decided east vergence imposed later by the westward subduction of the Brazilian Shield under the Andes.

We note also that this critical moment of Andean evolution is marked by roughly coeval completion of the San Juan del Oro Surface by ~15–10 Ma and the completion of the Atacama Pediplain topping the Atacama Bench on the subduction margin, as discussed earlier (Evenstar et al., 2009) (see section 2 and Fig. 8), processes in turn appearing roughly coeval with the onset of hyper-aridity on the Pacific seaboard of central South America (Alpers and Brimhall, 1988; Gregory-Wodzicki, 2000; Jordan et al., 2014).

5.8. Present-day status: Late Miocene Andean growth by widening

The present-day status reflects mostly the bivergent widening growth of the Andean topography, by incorporating since ~10–7 Ma the Subandes belt to the east, as well as most of the forearc region to the west (the Marginal Block, now adorned with orange stripes in Fig. 15), so a total width of ~200 km added to the earlier mountain ranges. The present-day status also illustrates the prevalent precipitation conditions since the Andean orogen attained maturity. Those conditions constrain any further discussion on climate.

According to our reconstruction, the westward subduction of the Brazilian Shield under the Andes would be a relatively late feature of the orogenic evolution (see Oncken et al. (2006); Oncken et al. (2012)), after a crucial polarity flip of tectonic vergence under the Eastern Cordillera–Interandean belt wedge. Some clear effects of that event are the eventual establishment of the East Andean Thrust (EAT) involving massive thin-skinned detachment of the Palaeozoic–Tertiary cover of the Subandes from Cambrian and Pre-Cambrian basement of the Brazilian craton (Baby et al., 1992; Baby et al., 1995; Allmendinger and Zapata, 2000) associated with shortening of at least ~80 km in the Subandes fold-thrust belt (Dunn et al., 1995; Baby et al., 1997; McQuarrie et al., 2005), rapid cooling by rock exhumation beginning by ~10–5 Ma (Eichelberger et al., 2013) and significant flexure of the Brazilian Shield (Lyon-Caen et al., 1985; Heit et al., 2007; Wölbern et al., 2009) under the loading effect exerted by the already thickened Eastern Cordillera–Interandean belt region. Although with a significantly different thick-skinned style, the timing of crustal deformation at the eastern flank of the Puna Plateau between 24°S and 28°S (located southward, in continuity with the flank of the Altiplano Plateau) suggests a younger process of eastward widening (post 6–5 Ma; e.g. Strecker et al. (2009); Carrapa et al. (2011)). That younger widening could be indicative of a southward propagation along the EAT of incipient subduction of the Brazilian craton under the Puna, possibly involving deep-seated mechanisms at lithospheric scale similar to those described here for 21°S.

The decided westward subduction of the continental Brazilian craton since 10–7 Ma appears to have also contributed to initiating a new style of tectonic shortening, thickening and uplift processes throughout the width of the Andean orogen (e.g. Oncken et al. (2006); Norton and Schlunegger (2011); Oncken et al. (2012)), including (as discussed earlier Sections 4 and 5.1) possible thickening processes at the complex eastward subduction plate contact of the oceanic Nazca Plate. The latter inference would be consistent with the earlier suggestion of a bi-vergent kinematic coupling across the orogen (Elger et al., 2005). The mostly coeval late Neogene (post ~10 Ma) uplift and incision of low-relief surfaces on both flanks of the orogen (namely, the Atacama (Thouret et al., 2007; Schildgen et al., 2007) and San Juan del Oro surfaces (Servant et al., 1989; Gubbels et al., 1993; Kennan et al., 1997; Barke and Lamb, 2006)) appear to corroborate the occurrence of that new style. It follows that the inferred uplift and abandonment of those distant low-relief surfaces must have been concomitant with uplift of the wholesale transect at ~21°S of the Andean orogen (Hoke and Garzione, 2008), which would be consistent with the hypothesis of rapid average uplift of this part of the Altiplano since the late Miocene (see discussions by Garzione et al. (2006); Garzione et al. (2008); Barnes and Ehlers (2009); Ehlers and Poulsen (2009); Insel et al. (2010); Whipple and Gasparini (2014)). Importantly, the onset of the new style of Andean deformation by bivergent propagation follows the middle Miocene increase of aridity (passage to hyper-aridity) in the Atacama Desert (Alpers and Brimhall, 1988; Sillitoe and McKee, 1996; Jordan et al., 2014) coinciding with a major global cooling event (Gregory-Wodzicki, 2000) (see discussion in section 2.2). Therefore, for similar reasons as for the "frozen" deformation in the western Cordillera at ~30 Ma after formation of the Choja Pediplain (section 5.5.1), the flip to eastward vergence as well as the triggering of decided subduction of the Brazilian craton at ~10 Ma could have followed a reduction of erosive power "freezing" progressively exhumation in the Eastern Cordillera–Interandean belt wedge at ~15–10 Ma, which appears coeval with completion of the San Juan del Oro surface. If that were the case, then the possible post 10–7 Ma rapid uplift of the Andes and the Altiplano (Ghosh et al., 2006) could be an effect of average rapid Andean shortening at ~12 mm/yr since 10–7 Ma associated with bivergent propagation (and massive subduction of the Brazilian Shield under the Andes), which therefore could have been triggered as a feedback effect of the ~15–10 Ma (post-Middle Miocene) climate cooling (see Fig. 17 and further discussion in section 6.2). So, the possible rapid uplift of the Andes-Altiplano region since the late Miocene would not necessarily be an effect triggered by a short event of rapid lithospheric thinning, as suggested by (Garzione et al., 2006; Molnar and Garzione, 2007; Garzione et al., 2008; Hoke and Garzione, 2008).

5.9. Comparison of our interpreted section with earlier models

In Fig. 16, the model of Andean evolution developed here (Figs. 14 and 15) is compared with two fairly accepted, although competing, models. The three models share similarities. They are all established close to the axis of the Andean Orocline, or across the northernmost part of its southern limb, close to latitude 21°S, and they emphasize crustal thickening processes associated with tectonic shortening. Similarly, they share basically the same geological constraints on amounts of shortening and chronology, as well as geophysical large-scale constraints on crustal thickness (including a weak lower crust under the Altiplano) and mantle lithosphere structure (including flexure of strong Brazilian lithosphere and gradually thinned or catastrophically delaminated continental lithosphere under the orogen). However, the three models differ significantly in the interpretation of important features of geometry defining tectonic style of Andean evolution and its mechanical implications.

The model by McQuarrie et al. (2005) (top panel of Fig. 16) emphasizes east vergent thrusting throughout the Andes, with thin-skinned deformation of the Paleozoic through Tertiary cover strata detached

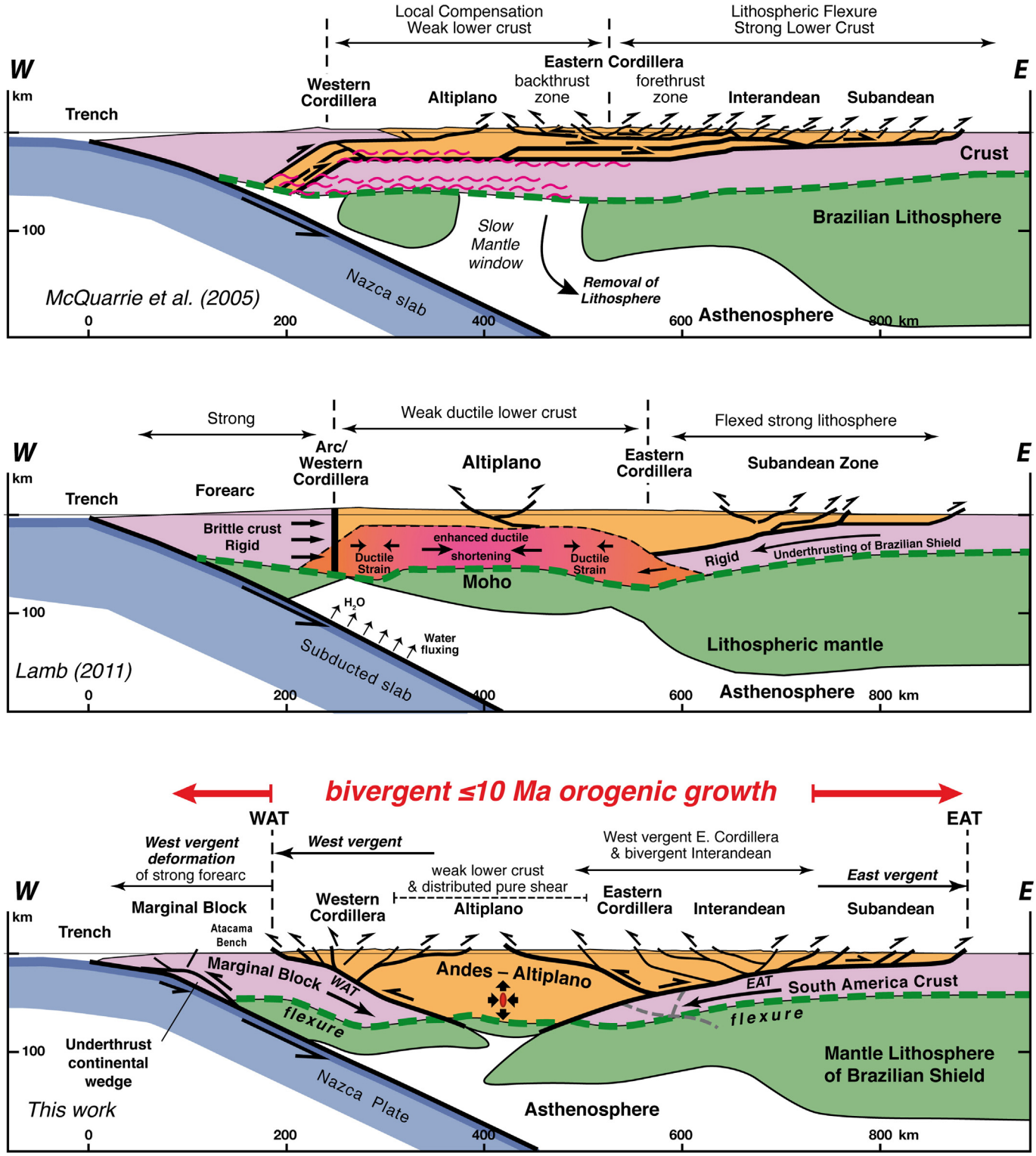

Fig. 16. Models of Andean orogeny. The interpretations of McQuarrie et al. (2005) (upper panel), based on McQuarrie (2002), and that of Lamb (2011) (middle panel), which follows basically the earlier interpretation of Isacks (1988), are redrawn from the originals (Fig. 4 in McQuarrie et al. (2005) and Fig. 6 in Lamb (2011)), to be compared with ours (lower panel), based on Figs. 14 and 15 in this paper. The three models are near the axis of the Andean Orocline, or across its northernmost southern limb close to latitude 21°S: model by McQuarrie et al. (2005) at ~20°S; model by Lamb (2011) at ~18°S. For a full discussion, see Section 5.9 in the text. WAT & EAT as in Fig. 14.

from a couple of horizontally stacked basement thrusts at no more than ~40 km depth. These units are in turn detached from a nearly undeformed lower crust (despite its weakness) and interpreted to be responsible for the major changes in crustal thickness and structural elevation between the Eastern Cordillera, the Interandean belt and the Subandean belt throughout the Andean Orocline. The upper detachment of cover beneath the western part of the Eastern Cordillera is west vergent, and east vergent beneath its eastern part. The sole (lower) detachment at mid-crustal depth extends horizontally for ~350 km under the Eastern Cordillera and the Altiplano, to ramp down westward with

~45° dip under the Western Cordillera, forming a large duplex structure eventually meeting the Moho under the forearc, close to the subduction zone. There are serious kinematic compatibility problems though, as for example, in the region of the lower crust beneath the forearc, near the intersection between the duplex and the Moho, which should have absorbed about ~300–400 km of shortening or thrust displacement transferred from the wholesale crustal shortening accommodated to the east in the Altiplano, Eastern Cordillera, Interandean belt and Subandean regions. That kind of problem is inherent of any model with east-vergent thrust detachments of crust throughout the Andes, rooted into lower crust and mantle, close to the subduction zone.

The model by Lamb (2011) (middle panel of Fig. 16) follows closely the earlier mechanical interpretation of Isacks (1988), but it also incorporates some details of more recent geological and geophysical constraints. As the model by McQuarrie et al. (2005), it emphasizes primary east vergent thrusting throughout the Andes. The mechanism distributing shortening in a ductile manner in the lower crust is steered by the underthrust Brazilian Shield serving as a "hydraulic ram" (or "piston"). That mechanism enhances shortening strain beneath the Altiplano, where the lithosphere is weaker because it is thinner and hotter, with an influx of water from the subducted slab. The rigid brittle crust of the forearc acts as a vertical wall that impedes flow farther westward and as a consequence localizes crustal thickening and uplift of the Western Cordillera, Altiplano and Eastern Cordillera. That vertical boundary between crustal regions with contrastingly different rheology may appear an unlikely geological feature, but it has the advantage of solving the kinematic problem of models like the previous one (McQuarrie et al., 2005), by conveniently distributing thickening processes throughout the Andes. However, that type of model has serious problems as well: (1) the proposed rheology contrast fails to explain the characteristic 50–10 Ma eastward propagation of deformation across the orogen, and (2) the model would have produced the whole Andean orogeny and its shortening of ~300–400 km since 10 Ma, only after the Subandes were active, with the underthrusting Brazilian Shield piston in operation to "pump" the thickening process.

In our model (lower panel of Fig. 16), the Andes are sustained by large bivergent thrust systems (WAT and EAT) and by tilt or flexure of relatively strong lithosphere of the Marginal Block and the Brazilian Shield on the two sides. That configuration explains the symmetrical location of deep crustal roots under the Western Cordillera and the Eastern Cordillera, and similarly as Lamb (2011), the diffuse shortening and thickening in the weaker lower crust over attenuated and weakened lithospheric mantle sustaining the Altiplano. Two dominantly west-vergent orogenic wedges, formed by thick-skinned, fully crustal-scale structures in the Western Cordillera and the Eastern Cordillera-Interandean belt, have evolved with time and progressive deformation toward bivergent geometries. The establishment of the East Andean Thrust, involving massive thin-skinned detachment of Subandean cover and onset of westward subduction of the Brazilian Shield under the Andes, would be a late feature of Andean Orogeny. Perhaps the most important difference between our model and earlier ones is that it appears kinematically and mechanically viable, while keeping consistency with the bulk of available geologic and chronologic constraints (Fig. 15).

6. Andean orogeny in concert with plate tectonics and Cenozoic climate change

The foregoing description of Andean orogeny and its tectonic–climatic timing foster reconsidering possible forcing and feedback mechanisms mediating Andean orogeny with climate change (Fig. 17). However, a preliminary question is the adequacy of the selected section at 21°S for that discussion. It is clear that the global Cenozoic climate cooling processes have produced their maximum drying effects in South America on its Pacific margin and centred at the middle latitudes of the Atacama Desert, which is coincident with the Central Andes and the Andean orocline, core of the Andean orogen. There, the increasing aridity caused erosion surfaces and pediments to form over the evolving Andean structure. As a consequence, the tectonic–climatic timing of Andean orogeny, such as defined in our section at 21°S (Figs. 14 and 15), would be appropriate to establish a comparison with global climate change.

However, tectonic effects propagated diachronically from the Pacific margin of the Central Andes to the hinterland and sideways along strike, toward higher and lower latitudes. Consequently, the tectonic timing captured with some time delay at any other point of the Andean orogen, away from the Central Andes margin, would be more difficult to correlate with global climate changes. The tectonic signal could be also perturbated by latitudinal variations of the pre-existent tectonic fabric, which has dictated modulations in tectonic style and timing of deformation. An important departure of the simple evolution at 21°S is documented in the Puna Plateau and its foreland, between 24°S and 28°S, which is associated with a thick-skinned, broken style of crustal deformation. In that region, the widening of the orogen started eastward from the "Incaic" (Eocene) Western Cordillera, but in contrast with 21°S, its propagation from the Puna eastern flank into the broken foreland is more complex and much less systematic from west to east (see Strecker et al. (1989); Carrapa et al. (2005); Mortimer et al. (2007); Hain et al. (2011); del Papa et al. (2013)). The climatic signal could also be perturbated as well, for example by latitudinal variations of precipitation carried by the monsoon winds. At 24°S–28°S, on the eastern flank of the Puna Plateau, the Oligo-Miocene climate conditions appear relatively arid, whereas higher available moisture has prevailed since monsoon intensification in the late Miocene (see Starck and Anzótegui (2001); Uba et al. (2007)). Nevertheless, the synchronous record of a similar combined tectonic–climatic events in distant places at the same latitude – like the abandonment and uplift of the Atacama pediplain and the abandonment and uplift of the San Juan del Oro Surface – suggests that the climate change toward dryer conditions would be almost synchronously driving the tectonic response throughout the Andean orogen near latitude 21°S.

Summarizing, for the purpose of discussing Andean orogeny vs. climate change the section at 21°S appears more adequate than sections at significantly lower or higher latitude. Indeed, that section is well constrained by abundant climatic, morphological, geological and geophysical data. The two main results concerning the Andean tectonic–climatic timing at 21°S are the following (see Fig. 17):

(1) There is a possible correlation of the long-term overall Andean growth process since ~50 Ma with the Cenozoic global process of

Fig. 17. Andean orogeny coupled with Cenozoic climate change. Correlation of global climate evolution (redrawn from Fig. 2 in Zachos et al. (2008), lower panel) with Andean growth (shortening in km) since ~50 Ma as described in this paper (bold red arrow labelled Andean Orogeny). Onset of "ramp-shaped" growth of Andean orogeny is synchronous with onset of the "ramp-shaped" temperature decrease since the Early Eocene climatic optimum (see text, Section 6, and Fig. 18). Onset of eastward propagation of deformation from the Western Cordillera to the Eastern Cordillera-Interandean wedge (marked by separation of growth curves labelled WC and EC-I$^+$) appears roughly synchronous with completion of Choja Pediplain, with onset of deposition of starved CDB at ~30–34 Ma, and follows the Late Eocene cooling period after the Mid-Eocene climatic optimum, which is in turn followed by formation of the Antarctic ice sheet. Triggering of subduction of the Brazilian craton (marked by separation of growth curves labelled EC-I$^+$ and SA$^+$) appears roughly synchronous with completion of Atacama Pediplain, with onset of hyper-aridity in Atacama Desert at ~15–10 Ma, and follows the Middle Miocene cooling period, after the Mid-Miocene climatic optimum. To enhance growth pulses (roughly between 40 and 30 Ma and since 10 Ma), the overall shortening curve for Andean Orogeny (bold red) is decomposed into shortening curves obtained by addition of shortening in different units in chronologic order of appearance: shortening of Western Cordillera alone (WC, segmented orange), cumulative shortening in WC plus Eastern Cordillera–Interandean belt wedge (WC + EC-I = EC-I$^+$, segmented green), cumulative shortening in EC-I$^+$ plus Subandes (WC + EC-I + SA = SA$^+$, segmented black). Note contrasting steady shortening rate of ~4 mm/yr since 30 Ma in EC-I$^+$, compared with the accelerated shortening rate of ~12 mm/yr since 10 Ma in SA$^+$, which is consistent with present-day GPS convergence rates across the East Andean Thrust (Brooks et al., 2003, 2011). (For interpretation of the references to colour in this figure legend, the reader is referred to the web version of this article.)

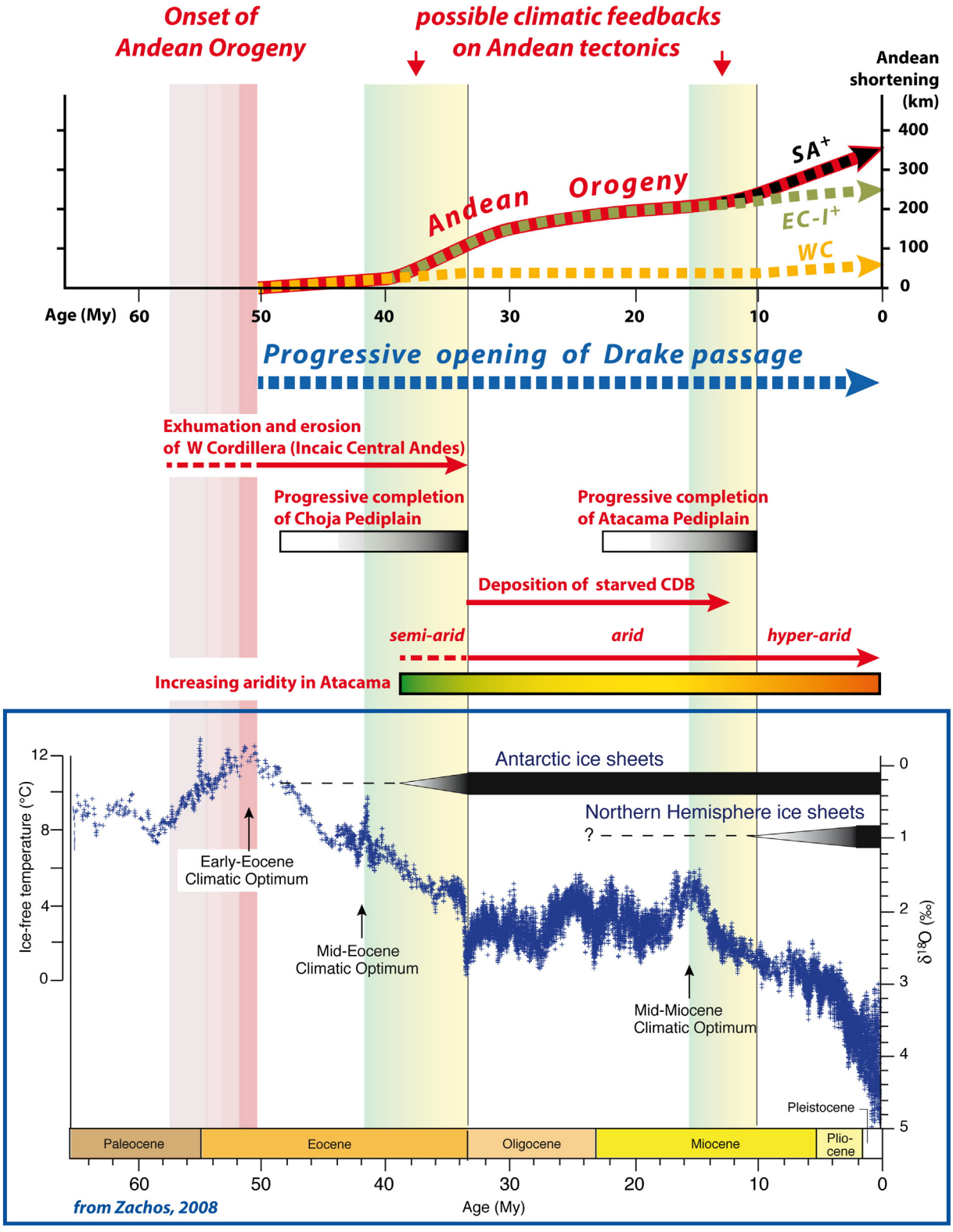

temperature ($\delta^{18}O$ variation) and CO_2 decrease since the early Eocene climatic optimum. During the same time period our planet has been led from ice-free conditions to, ultimately, a bipolar glaciation (transition from a 'greenhouse' to an 'icehouse' climate) (Zachos et al., 2001; Zachos et al., 2008).

(2) The stepwise growth process of Andean orogeny by two pulses of erosion-driven widening since 50 Ma appears synchronized with the similarly stepwise development of tectonic landscape over the Pacific seaboard of South America and the Atacama Desert. The main characteristics of the interplay between Andean tectonics and climate (see Figs. 3–4) are primarily constrained by the chronology of aggradation and pedimentation processes associated with the genesis of the stepped landscape over the Atacama Bench and the Western Cordillera (see Figs. 5–8). In turn, that process appears to be associated with formation of

the Choja and Atacama Pediplains, and with two events of rapid aridity increase (lasting ~ ≤ 5 Myr), which are probably controlled by cooling events of global climate, in the Late Eocene and in the Middle Miocene.

6.1. Plate tectonics as possible long-period forcing of Andean orogeny and global cooling

6.1.1. Climate, plate tectonics and Andean tectonics

Possible links of various type have been envisioned for the complex interactions between climate and tectonics (e.g. see review by Hay (1996)). Particularly, the examination of relationships between tectonic vertical uplift with Cenozoic climate has created controversy on which of these factors would be forcing one another, exemplified in a "chicken and egg" problem (Molnar and England, 1990; Raymo and Ruddiman, 1992; Hay et al., 2002). It has been suggested that the Cenozoic uplift of the Himalaya–Tibet Plateau may have contributed to drive, over the long-term, the overall Cenozoic climate cooling, mostly via chemical weathering and erosion of the newly-created mountain relief resulting in a decrease of atmospheric CO_2. In that case, the chicken and egg problem would be explained by positive feedbacks of cooling climate driving discrete increases of weathering and erosion and further tectonic uplift (Molnar and England, 1990; Raymo and Ruddiman, 1992).

Another possible influence of plate tectonics on global climate appears to be the long-lived horizontal displacement of plates and distribution of continental and oceanic crust in our planet (see discussions by DeConto (2009); Lee et al. (2013)). It is admitted that Palaeozoic aggregation of supercontinents (Pangaea, Gondwana) may have favoured Carboniferous glaciation (DeConto, 2009). Similarly, climatic conditions may have changed with Mesozoic continental spreading associated with fragmentation and dispersal of Gondwana (e.g. Lee et al. (2013)).

As discussed earlier (see section 3), the Andean structural cycle associated with the Andean subduction process starting at ~190 Ma is roughly correlated with dispersal of Gondwana and opening of the Atlantic. The first ~70% of that period (between 190 Ma and 50 Ma), which is associated with dominant margin-perpendicular tectonic extension in western South America, appears grossly overlapping the period of Mesozoic–Paleogene warmth (Jenkyns, 2003) and particularly the Cretaceous to early Paleogene (~140–50 Ma) period under greenhouse conditions (Hallam, 1984, 1985; Haq et al., 1987; Lee et al., 2013). The rest of the Andean structural cycle corresponds to the Andean orogeny properly, associated with margin-perpendicular tectonic shortening of continental South America, which as noted above, appears to have started synchronously with the onset of the temperature fall since 51–53 Ma (Zachos et al., 2001). Andean orogeny in the Western Cordillera starting at ~50 Ma apparently followed in the earliest Oligocene (~30 Ma) by a virtual shutoff of precipitation (marked by the Choja Pediplain and the post "Incaic" unconformity) suggests two main issues: (1) Andean orogeny cannot have been caused by climate change, as suggested earlier (Lamb and Davis, 2003), because that scenario is inconsistent with that chronology (see section 5.1.1). (2) More importantly, the apparent correlation of the long-term Andean growth process since ~50 Ma with global Cenozoic cooling (see Fig. 17) suggests that Cenozoic climate change could have been caused by the same tectonic boundary conditions as Andean orogeny.

Lee et al. (2013) suggested that long-term (>50 Myr) greenhouse–icehouse and CO_2 content oscillations may be associated with long-term tectonic fluctuations between island arc- and continental arc-dominated states, which ultimately depend on plate tectonic changes. In that scenario, the icehouse conditions of the Mid-Cenozoic to present would correspond to a return to an arc-dominated state. We explore an alternative hypothesis hereafter.

6.1.2. Effects of plate tectonic evolution and possible boundary conditions since 50 Ma

The long-term contraction and progressive mountain building across the Andean subduction margin during Andean orogeny (see Sections 3.3.3, 5 and Fig. 15) must be driven by deep-seated processes in the Earth's lithosphere and asthenosphere. Over the past 50 Myr, the boundary between the Nazca and South American plates has been submitted to positive trench rollback velocity (trench advance toward the continent) (e.g. Husson et al. (2008)) and rapid margin-orthogonal convergence (Pardo-Casas and Molnar, 1987). The trench advance and fast convergence appear to result from a reorganization of plate motion driven by the progressive collision of India and Africa against Eurasia and the consequent diversion of mantle flow westward, which would have accelerated the westward drift of South America (e.g. Silver et al. (1998); Husson et al. (2008); Faccenna et al. (2013)). Nevertheless, the establishment of trench advance conditions surpassing the average yield strength of continental lithosphere and provoking its failure requires tectonic changes to scale with the triggering of the bivergent and bilateral growth of the Andean orogen and formation of the Andean Orocline (Figs. 1 and 18). The idea of virtual "collision" of the South America continent against the Nazca Plate since ~50 Ma appears consistent with observations of shear-wave splitting resulting from deformation-induced mantle anisotropy (Russo and Silver, 1994, 1996). The model proposed by Russo and Silver (1994, 1996) predicts trench-parallel mantle flow beneath the subducting Nazca plate along the Andean margin, away from a central stagnation point, and corner flow around the northern and southern ends of the continent (see Fig. 18). Three-dimensional numerical simulations of subduction performed later by Schellart et al. (2007) suggest that the large slab (>6000 km) subducting along the entire west margin of South America may have caused slow trench advance at its centre and consequently would have developed a convex geometry consistent with the Andean Orocline.

The separation of Australia, Africa and South America from Antarctica by opening of the Southern Ocean allowed the establishment of the Antarctic Circumpolar Current and development of the Polar Frontal Zone, reducing poleward ocean heat transport and favouring glaciation over Antarctica (Kennett, 1977; Sijp and England, 2004; Barker et al., 2007; DeConto, 2009). Opening of the Tasmania passage since the Eocene is crucial to this process (e.g. Lawver and Gahagan (2003)). However, the Antarctic Circumpolar Current could not have been established without the long-lasting opening process of the Drake passage since 50 Ma by rupture of the South America–Antarctica continental bridge, its fragmentation into blocks, gradual opening of basins and accretion of lineated oceanic floor in the Scotia Sea, and overall 2000-km eastward drift of the Scotia Arc (Dalziel, 1981; Barker, 2001; Lawver and Gahagan, 2003; Barker and Thomas, 2004; Sijp and England, 2004; Livermore et al., 2005; Eagles et al., 2006; Scher and Martin, 2006; Livermore et al., 2007; Lagabrielle et al., 2009; Dalziel et al., 2013a; Dalziel et al., 2013b; Carter et al., 2014; Eagles and Jokat, 2014). The subduction-induced upper-mantle flow around the slab-edge predicted by models of Russo and Silver (1994, 1996) and Schellart et al. (2007) could be a long-lived driver of that chain of processes (Fig. 18).

6.2. Possible climatic feedbacks on Andean growth process

Present-day climate conditions in the Atacama Desert at the Pacific seaboard of central South America are arid to hyper-arid. Those conditions are primarily associated with almost complete lack of winter precipitation carried by westerly winds from the Pacific, driven by the SE Pacific anticyclone and the cold upwelling Peru–Chile Current, as well as, to the dry zone and associated cold sea surface temperature tongue entering from the coast of South America into the inter-tropical convergence zone (Takahashi and Battisti, 2007a; Takahashi and Battisti, 2007b; Garreaud et al., 2009). They are also associated with prevalence of easterly monsoon winds carrying relatively scarce summer precipitation from the Atlantic through the Amazonian region (e.g. Houston and Hartley (2003); Strecker et al. (2007); Garreaud et al. (2009)) (see Fig. 15). According to data from the Tropical Rainfall Measurement

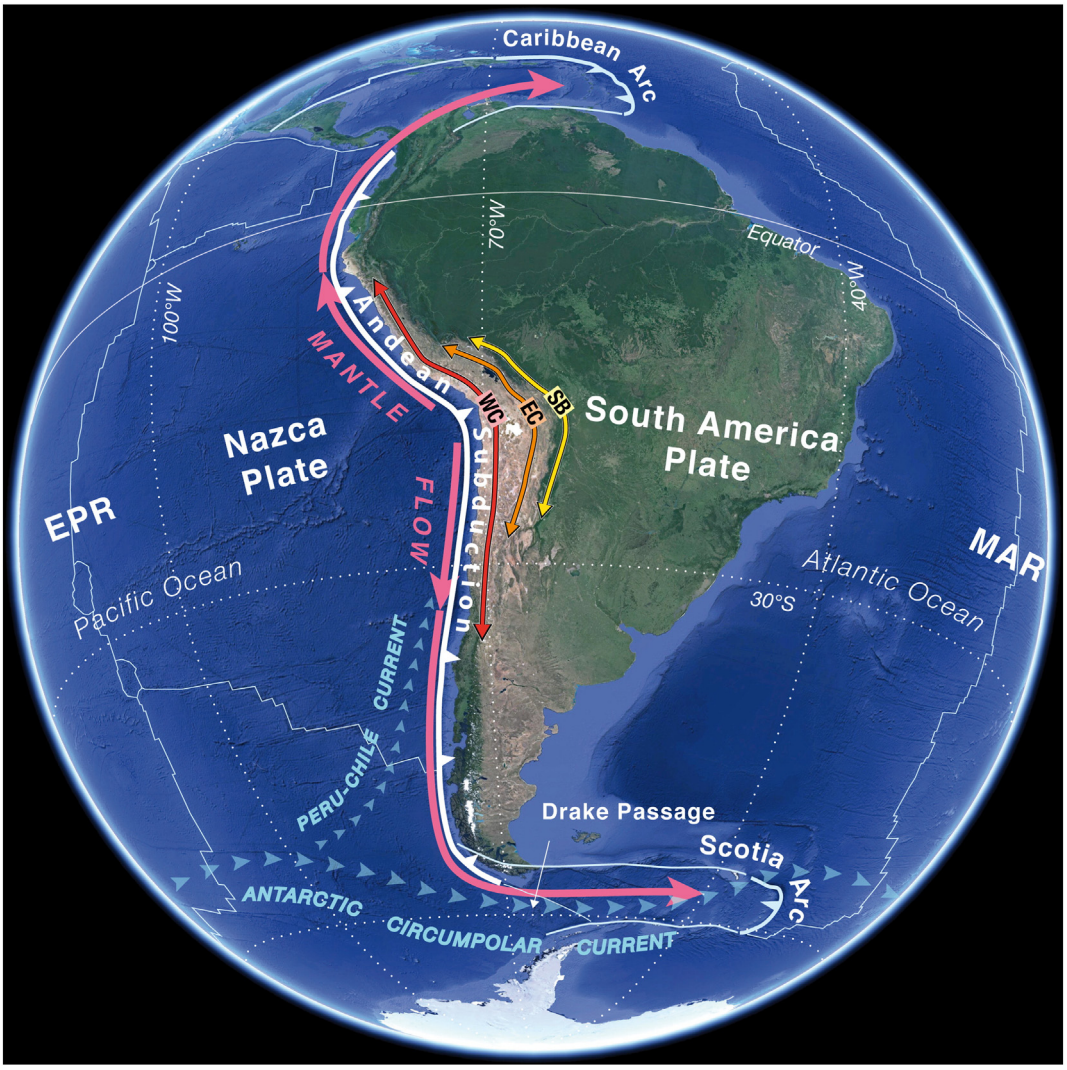

Fig. 18. Possible long-period tectonic forcing. Evolution of Andean orogeny by bivergent and bilateral growth since 50 Ma is consistent with deep-seated tectonic forcing at three levels (see discussion in text, Section 6): 1. At global scale (not represented here), trench advance and rapid margin-perpendicular plate-boundary Nazca–South America convergence (Pardo-Casas and Molnar, 1987) driven by a global-scale plate motion reorganization associated with India and Africa collision against Eurasia, which propels westward mantle flow and accelerated westward drift of South America (Silver et al., 1998; Husson et al., 2008). 2. At plate scale (depicted here), trench-parallel mantle flow beneath the subducting Nazca plate along the Andean margin, away from a central stagnation point (from Russo and Silver (1994, 1996)). 3. The same model predicts that corner flow around the southern end of South America has caused rupture of the South America–Antarctica continental bridge and opening of a seaway (Drake Passage) since ~50 Ma between South America and Antarctica (Livermore et al., 2005; Eagles et al., 2006; Livermore et al., 2007). Those rupture and opening have been ensued by overall 2000-km eastward drift of Scotia arc since 40 Ma (Barker, 2001; Barker and Thomas, 2004), critical for progressive establishment of coherent Antarctic Circumpolar and Peru–Chile Currents (ACC and PCC, respectively, in blue), which possibly contributed to cause Antarctic glaciation. Distance between distant plate boundaries, East Pacific Rise (EPR) and Middle Atlantic Ridge (MAR), about 90° of longitude apart (or about a quarter of our planet), give the scale of the deep-seated mantle convection processes involved in the forcing mechanism proposed here. Other abbreviations are as in Fig. 1.

Mission (TRMM) (Strecker et al., 2007; Bookhagen and Strecker, 2008), precipitation at the windward flank of the Andean orogen at the latitude of our section (21°S) over the Subandes belt attains a maximum of ~1000 mm/yr (represented by big clouds in Fig. 15), grading to semi-arid to arid over the Altiplano Plateau, then to the hyper-arid conditions ≤50 mm/yr (small clouds) on the leeward Andean flank (Atacama Desert). That present-day precipitation decrease across the Andes may be associated with the rain-shadow effect exerted by the growing mountain belt on moisture carried by the monsoon winds (Houston and Hartley, 2003; Strecker et al., 2009).

During the Cenozoic, the aridity increase over the Western Cordillera and the Atacama Desert was recorded in the landscape by two pivotal events of erosion power decrease, probably associated with a stepwise precipitation decrease: the first event is marked by formation of the Choja Pediplain, the second by formation of the Atacama Pediplain. Those events correspond schematically to the passage from semi-aridity to aridity at ~30 ± 5 Ma and from aridity to hyper-aridity at 15–10 Ma, respectively (see Fig. 15). The latter event being roughly coeval with formation of the San Juan del Oro surface over the Eastern Cordillera suggests the corresponding aridity increase has widespread expression in the landscape over of the Andes. As discussed earlier (section 5.8.1), the two steps of aridity increase in Andean climate appear to precede and possibly trigger the two main pulses of orogenic growth, by widening the Andean relief. Similar processes of erosion-driven tectonic changes were discussed, among others, by Willett (1999) and Norton and Schlunegger (2011). To explain the foregoing features, the hypothesis of a post-50 Ma gradual increase of the orographic shadow blocking the easterlies (similar to the present-day pattern) can be considered, because it is consistent with an overall gradual aridity increase in the Atacama Desert during the same time period.

However, a gradually increasing rain shadow would not explain the stepwise occurrence of the two events of rapid aridity increase. Chronologically (see Fig. 17), those relatively sharp events follow the well-known global cooling periods in the Late Eocene (after the Mid-Eocene climatic optimum) and in the Middle Miocene (after the Mid-Miocene climatic optimum) (Zachos et al., 2008), which appear associated with the intensification of cold Peru–Chile Current upwelling and accelerated reduction of moisture carried by the westerlies (e.g. Houston and Hartley (2003)). As a consequence, those two global cooling periods emerge as likely forcing factors for modulating aridity over the Pacific seaboard of South America and the subsequent tectonic evolution of the Andean orogen. Therefore, in contrast with the possible forcing of global climate cooling since ~50 Ma by viscous mantle flow and a long-period plate-tectonic reorganization (suggested in the previous section), the stepwise virtual "freezing" of tectonic activity in the Western Cordillera promoting two phases of widening of the Andean orogen by eastward propagation of deformation from the subduction margin into more continental areas of South America (see Sections 2.3, 5.5 and 5.8; Figs. 15 and 17) was possibly caused by stepwise increases of aridity in Atacama, which appear to be feedback effects from global climate cooling. The mechanism of positive feedbacks on the Andes by reducing erosion processes, tectonic activity and vertical uplift, which promote growth by widening horizontally the region of high-relief (e.g., Willett (1999); Norton and Schlunegger (2011)) is different from the hypothesized climate feedbacks on the Himalayas–Tibet Plateau, which by contrast would directly enhance erosion and rock exhumation processes, so accelerating tectonic activity and vertical uplift (Molnar and England, 1990).

Summarizing, the Andes can be seen as an orogen where an increasingly drying climate driven by the global Cenozoic cooling would have hampered significant erosion and rock exhumation (at most ~5–6 km of rock column removed in the Eastern Cordillera–Interandean Belt). That process would have impeded efficient crustal shortening during periods of relatively slow shortening rate, as illustrated by the steady ~4 mm/yr of shortening rate in the growth curve of Andean orogeny between 30 and 10 Ma (see Fig. 17, curve EC-I$^+$). That process would have also fostered crustal failure elsewhere and prepared fault propagation. As a consequence, the Andean orogen would widen by stepwise growth pulses into wetter regions of the continent, where faster erosion and thrust deformation can occur, as illustrated by the ~12 mm/yr of average shortening in the growth curve of Andean orogeny since 10 Ma (see Fig. 17, SA$^+$ curve). Large efficient fault systems like the East Andean Thrust (EAT, which sustains westward subduction of the continental Brazilian craton since 10–7 Ma) appear to be characterized by a high degree of localization of deformation associated with a large-scale structural continuity. So we speculate that the possible shortening rate variation during Andean orogeny (Fig. 17) could be explained by a fault-propagation process in an inhomogeneous visco-elastic lithosphere, with dampening of its surface modulated by discrete feedbacks from climate change acting on erosion efficiency.

7. Conclusions

The Atacama Bench at the Pacific seaboard of South America is a unique large-scale geomorphological expression of interplaying Andean tectonics and climate evolution during the Cenozoic. Analysing that interplay allows us to unravel some primary features of Andean orogeny and climate over South America. The keystone of that interplay is the concomitant development of west-vergent thrust tectonics, associated with creation of the largest relief on Earth at the Andean subduction margin, and pedimentation processes over the west flank of the Andes, associated with increasing aridity in the Atacama Desert.

We find that the vertical tectonic relief of 13 km at the Andean margin is the result of the evolution over the past 50 Myr of two parallel flat-ramp thrust systems of similar geometry and scale, at the West Andean Thrust and at the subduction interface. That style of tectonic process represents progressive collision and substantial underthrusting of the marginal Mesozoic arc and its basement (designated Marginal Block) beneath the adjacent more internal continental basement of the Western Cordillera, sustaining its high relief and thickness. We consider that particular feature of Andean tectonics comparable with continental collision processes elsewhere (e.g. the Himalaya) and basic to our understanding of Andean orogeny.

We infer that thrust splay structures and other fault complexities may control seismic loading processes at the subduction plate interface and explain occurrence and distribution of asperities under the oceanward forearc (Song and Simons, 2003; Wells et al., 2003), down-dip segmentation of coupling and seismicity (Béjar-Pizarro et al., 2013) and occurrence of megathrust earthquake rupture (Vigny et al., 2011).

Total shortening across the west-vergent fold-thrust belt in North Chile under the Western Cordillera is not less than ~20–30 km and may attain ~30–50 km, which is up to an order of magnitude larger than earlier estimates. Most of that shortening is associated with exhumation by erosion during the earlier period of strong uplift and mountain building in the Western Cordillera (50–30 Ma period, also called "Incaic" deformation). The later process of breakage of the forearc and addition of light continental material under the Atacama Bench (causing crustal thickening and its observed uplift) indicates overall trenchward growth of the Central Andes by relatively recent incorporation of the Marginal Block to the elevated land since ~10 Ma.

We find that the increasing aridity in the Atacama Desert during the Cenozoic is marked in the landscape by two events of erosion power decrease over the growing Western Cordillera. Those events are probably associated with a stepwise decrease of precipitation contributing in turn to steps in aridity increase and desertification, which correspond schematically to the passage from semi-aridity to aridity at ~30–33 Ma and from aridity to hyper-aridity at 15–10 Ma, respectively. The first event is marked by completion of the Choja Pediplain; the second by completion of the Atacama Pediplain.

Incorporating our results with a critical revision of published knowledge (geological, geomorphological, geophysical) allows us to construct a complete 2D tectonic section throughout the core of the Andean orogen. We also draw up the pertinent structural evidence to reconstruct a first-order evolution of Andean orogeny over the past 50 Myr. The Andean orogen results from protracted processes of bivergent crustal shortening and thickening in a wide, previously stretched and mechanically weakened region of continental South America, squeezed since 50 Ma between the rigid Marginal Block and the South America Plate (Brazilian Shield). The growth process of Andean orogeny has involved two main propagation pulses of tectonic deformation and crustal shortening eastward into continental South America. The first pulse has transferred dominant west-vergent thrust activity from the Western Cordillera (50–30 Ma) to dominant bi-vergent activity in the Eastern Cordillera and the Interandean belt (40–10 Ma). The last pulse since 10 Ma involves polarity flip to east-vergent thrusting and initiation of deformation of the Subandean belt, triggered by onset of massive westward subduction of the Brazilian Shield under the Andes. The last pulse involves also west-vergent trenchward growth of orogeny by incorporation of the Marginal Block. The bi-vergent growth process has caused rapid uplift of the Atacama Pediplain (topping the Atacama Bench), coevally with uplift of the San Juan del Oro surface (topping the Eastern Cordillera), so throughout the ≥600-km-wide region of the high Andes–Altiplano.

The overall "ramp-shaped" growth curve of Andean orogeny over the past 50 Myr is synchronous with onset of the "ramp-shaped" temperature decrease since the Early Eocene climatic optimum, leading our planet from ice-free conditions to, ultimately, a bipolar glaciation (Zachos et al., 2008). Thus, Andean growth and global cooling may have operated under the same long-period forcing mechanism at plate-scale, involving stable viscous flow in the Earth's mantle.

However, Andean growth appears modulated by two climatic feedbacks causative of stepwise reductions of erosive power and precipitation over the Andean margin. The first erosive power reduction is coeval with the Late Eocene cooling period after the Mid-Eocene (~42 Ma) climatic optimum, leading to completion of the Choja Pediplain close to the Eocene-Oligocene boundary and promoting the eastward propagation of deformation from the Western Cordillera to the Eastern Cordillera-Interandean belt wedge. The second erosive power reduction is coeval with the Late Miocene cooling period after the Mid-Miocene (~15 Ma) climatic optimum and appears associated with establishment of hyper-aridity in the Atacama Desert, leading to completion of the Atacama Pediplain at ~10 Ma. Those conditions appear to be responsible of a tectonic "freezing" in the Middle-Late Miocene which may have promoted since the triggering of subduction of the Brazilian craton and the bivergent growth with rapid uplift throughout the Andes–Altiplano region.

The concomitant bivergent and bilateral growth processes away from the Andean core appears fundamental for our understanding of Andean orogeny and its interplay with global climate. That growth pattern is consistent with three-dimensional subduction models involving trench-parallel mantle flow beneath the subducting Nazca plate along the Andean margin, away from a central stagnation point, and corner flow around the northern and southern ends of the continent (Russo and Silver, 1994, 1996; Schellart et al., 2007). Corner flow may have contributed to the gradual opening process of the Drake passage since 50 Ma by rupture of the South America–Antarctica continental bridge, which has allowed the establishment of the Antarctic Circumpolar Current (ACC) and favoured glaciation over Antarctica (Kennett, 1977; Sijp and England, 2004; Barker et al., 2007; DeConto, 2009).

The virtual collision of the Marginal Block with continental South America since ~50 Ma requires changes in boundary conditions, specifically a global-scale reorganization of plate motion causing trench advance across the plate boundary, surpassing the average yield strength of continental lithosphere and provoking its failure. Those conditions have been attained after the progressive collision of India and Africa against Eurasia and the consequent diversion of mantle flow westward, which has accelerated the westward drift of South America and initiated fast convergence and trench advance at the subduction margin of South America, as suggested by Silver et al. (1998), Husson et al. (2008) and Faccenna et al. (2013).

Altogether, the above offers possible forcing mechanisms of plate tectonics and orogeny on climate, without mediation by surface process as chemical weathering, erosion, etc. The global plate reorganization leading to critical plate-boundary conditions of mantle flow around South America has probably driven both, Andean orogeny in South America and opening of Drake passage between South America and Antarctica. Conversely, the suggested long-period plate-scale tectonic forcing of Andean orogeny and global Cenozoic climate appears punctuated by possible short-period climatic feedbacks on Andean growth, so it also offers altogether an alternative solution for the chicken and egg problem opposing tectonic vs. climatic driving mechanisms (Molnar and England, 1990).

Acknowledgements

This work has been supported by INSU-CNRS project "Diachronism of West Andean Thrust", LABEX UnivEarthS (Sorbonne Paris Cité), and ANR MegaChile. Over years we have benefited from enlightening discussions on orogeny with many colleagues and friends, among which we wish to mention J.-P. Avouac, R. Charrier, P. Cobbold, C. Galli-Olivier, J. Malavieille, M. Mattauer, B. Meyer, P. Molnar, O. Oncken, V. Ramos, T. Sempere, M. Strecker, P. Tapponnier, R. Thiele, and S. Willett. We also benefited from a crucial assessment of an earlier manuscript by P. Molnar. We wish to thank constructive thorough reviews by two anonymous reviewers and wise suggestions by Editor M. Strecker.

References

Adam, J., Reuther, C.-D., 2000. Crustal dynamics and active fault mechanics during subduction erosion. Application of frictional wedge analysis on to the North Chilean Forearc. Tectonophysics 321, 297–325. http://dx.doi.org/10.1016/S0040-1951(00)00074-3.

Allmendinger, R., Zapata, T., 2000. The footwall ramp of the Subandean decollement, northernmost Argentina, from extended correlation of seismic reflection data. Tectonophysics 321 (1), 37–55.

Allmendinger, R.W., Jordan, T., Kay, S., Isacks, B.L., 1997. The evolution of the Altiplano–Puna Plateau of the Central Andes. Annu. Rev. Earth Planet. Sci. 25, 139–174.

Allmendinger, R.W., González, G., Yu, J., Hoke, G., Isacks, B., 2005. Trench-parallel shortening in the Northern Chilean Forearc: tectonic and climatic implications. Geol. Soc. Am. Bull. 117 (1–2), 89–104.

Alpers, C.N., Brimhall, G.H., 1988. Middle Miocene climatic-change in the Atacama Desert, northern Chile — evidence from supergene mineralization at La Escondida. Geol. Soc. Am. Bull. 100 (10), 1640–1656. http://dx.doi.org/10.1130/0016-7606(1988)100<1640:mmccit>2.3.co;2.

Amilibia, A., Sabat, F., McClay, K.R., Munoz, J.A., Roca, E., Chong, G., 2008. The role of inherited tectono-sedimentary architecture in the development of the central Andean mountain belt: insights from the Cordillera de Domeyko. J. Struct. Geol. 30 (12), 1520–1539. http://dx.doi.org/10.1016/j.jsg.2008.08.005.

Amundson, R., Dietrich, W., Bellugi, D., Ewing, S., Nishiizumi, K., Chong, G., Owen, J., Finkel, R., Heimsath, A., Stewart, B., 2012. Geomorphologic evidence for the late Pliocene onset of hyperaridity in the Atacama Desert. Geol. Soc. Am. Bull. 124 (7–8), 1048–1070.

Arancibia, G., Matthews, S., de Arce, C.P., 2006. K–Ar and 40Ar/39Ar Geochronology of supergene processes in the Atacama Desert, northern Chile: tectonic and climatic relations. J. Geol. Soc. 163 (1), 107–118.

Ardill, J., Flint, S., Chong, G., Wilke, H., 1998. Sequence stratigraphy of the Mesozoic Domeyko Basin, northern Chile. J. Geol. Soc. 155, 71–88. http://dx.doi.org/10.1144/gsjgs.155.1.0071.

Armijo, R., Thiele, R., 1990. Active faulting in northern Chile: ramp stacking and lateral decoupling along a subduction plate boundary? Earth Planet. Sci. Lett. 98 (1), 40–61. http://dx.doi.org/10.1016/0012-821X(90)90087-E.

Armijo, R., Rauld, R., Thiele, R., Vargas, G., Campos, J., Lacassin, R., Kausel, E., 2010a. The West Andean Thrust, the San Ramón Fault and the seismic hazard for Santiago, Chile. Tectonics 29, TC2007. http://dx.doi.org/10.1029/2008TC002427.

Armijo, R., Rauld, R., Thiele, R., Vargas, G., Campos, J., Lacassin, R., Kausel, E., 2010b. Reply to the comment by R. A. Astini and F. M. Dávila on "The West Andean Thrust, the San Ramón Fault, and the seismic hazard for Santiago, Chile". Tectonics 29, TC4010. http://dx.doi.org/10.1029/2010TC002692 (doi:4010.1029/2010TC002692).

Arriagada, C., Cobbold, P.R., Roperch, P., 2006. Salar de Atacama basin: a record of compressional tectonics in the central Andes since the mid-Cretaceous. Tectonics 25 (1). http://dx.doi.org/10.1029/2004tc001770.

Arriagada, C., Roperch, P., Mpodozis, C., Cobbold, P.R., 2008. Paleogene building of the Bolivian Orocline: tectonic restoration of the central Andes in 2-D map view. Tectonics 27 (6). http://dx.doi.org/10.1029/2008tc002269.

Astini, R.A., Dávila, F.M., 2010. Comment on "The West Andean Thrust, the San Ramón Fault, and the seismic hazard for Santiago, Chile" by Armijo et al. Tectonics 29, TC4009. http://dx.doi.org/10.1029/2009TC002647 (doi:4010.1029/2009TC002647).

Aubouin, J., Borrello, A.V., Cecioni, G., Charrier, R., Chotin, P., Frutos, J., Thiele, R., Vicente, J.-C., 1973. Esquisse paléogéographique et structurale des Andes Méridionales. Rev. Géogr. Phys. Géol. Dyn. Paris 15 (1–2), 11–72.

Avouac, J.P., 2003. Mountain building, erosion, and the seismic cycle in the Nepal Himalaya. In: Dmowska, R. (Ed.), Advances in Geophysics vol. 46. Elsevier Academic Press Inc., San Diego, pp. 1–80. http://dx.doi.org/10.1016/s0065-2687(03)46001-9.

Baby, P., Herail, G., Salinas, R., Sempere, T., 1992. Geometry and kinematic evolution of passive roof duplexes deduced from cross-sections balancing — Example from the foreland thrust system of Southern Bolivian Subandean Zone. Tectonics 11 (3), 523–536.

Baby, P., Moretti, I., Guillier, B., Limachi, R., Mendez, E., Oller, J., Specht, M., 1995. Petroleum system of the northern and central Bolivian sub-Andean zone. In: Tankard, A.J., Suárez, R., Welsink, H.J. (Eds.), Petroleum Basins of South America. AAPG Memoir 62, pp. 445–458.

Baby, P., Rochat, P., Mascle, G., Herail, G., 1997. Neogene shortening contribution to crustal thickening in the back arc of the Central Andes. Geology 25 (10), 883–886. http://dx.doi.org/10.1130/0091-7613(1997)025<0883:nsctct>2.3.co;2.

Bahlburg, H., Hervé, F., 1997. Geodynamic evolution and tectonostratigraphic terranes of northwestern Argentina and northern Chile. Geol. Soc. Am. Bull. 109 (7), 869–884. http://dx.doi.org/10.1130/0016-7606(1997)109<0869:geatto>2.3.co;2.

Barke, R., Lamb, S., 2006. Late Cenozoic uplift of the Eastern Cordillera, Bolivian Andes. Earth Planet. Sci. Lett. 249 (3–4), 350–367. http://dx.doi.org/10.1016/j.epsl.2006.07.012.

Barker, P.F., 2001. Scotia Sea regional tectonic evolution: implications for mantle flow and palaeocirculation. Earth-Sci. Rev. 55 (1–2), 1–39. http://dx.doi.org/10.1016/S0012-8252(01)00055-1.

Barker, P.F., Thomas, E., 2004. Origin, signature and palaeoclimatic influence of the Antarctic Circumpolar Current. Earth-Sci. Rev. 66 (1–2), 143–162. http://dx.doi.org/10.1016/j.earscirev.2003.10.003.

Barker, P.F., Filippelli, G.M., Florindo, F., Martin, E.E., Scher, H.D., 2007. Onset and role of the Antarctic Circumpolar Current. Deep-Sea Res. II Top. Stud. Oceanogr. 54 (21–22), 2388–2398. http://dx.doi.org/10.1016/j.dsr2.2007.07.028.

Barnes, J.B., Ehlers, T.A., 2009. End member models for Andean Plateau uplift. Earth-Sci. Rev. 97 (1–4), 105–132. http://dx.doi.org/10.1016/j.earscirev.2009.08.003.

Beaumont, C., Fullsack, P., Hamilton, J., 1992. Erosional control of active compressional orogens. In: McClay, K.R. (Ed.), Thrust Tectonics. Springer, Netherlands, pp. 1–18 http://dx.doi.org/10.1007/978-94-011-3066-0_1.

Becker, J.J., et al., 2009. Global Bathymetry and Elevation Data at 30 Arc Seconds Resolution: SRTM30_PLUS. Mar. Geod. 32 (4), 355–371. http://dx.doi.org/10.1080/01490410903297766.

Béjar-Pizarro, M., et al., 2010. Asperities and barriers on the seismogenic zone in North Chile: state of the art after the 2007 Mw 7.7 Tocopilla earthquake inferred by GPS and InSAR data. Geophys. J. Int. 183 (1). http://dx.doi.org/10.1111/j.1365-246X.2010.04748.x.

Béjar-Pizarro, M., Socquet, A., Armijo, R., Carrizo, D., Genrich, J., Simons, M., 2013. Andean structural control on interseismic coupling in the North Chile subduction zone. Nat. Geosci. http://dx.doi.org/10.1038/NGEO1802.

Bookhagen, B., Strecker, M.R., 2008. Orographic barriers, high-resolution TRMM rainfall, and relief variations along the eastern Andes. Geophys. Res. Lett. 35 (6). http://dx.doi.org/10.1029/2007gl032011.

Brooks, B.A., Bevis, M., Smalley, R., Kendrick, E., Manceda, R., Lauría, E., Maturana, R., Araujo, M., 2003. Crustal motion in the Southern Andes (26–36 S): do the Andes behave like a microplate? Geochem. Geophys. Geosyst. 4 (10), 1085. http://dx.doi.org/10.1029/2003GC000505.

Brooks, B.A., et al., 2011. Orogenic-wedge deformation and potential for great earthquakes in the central Andean backarc. Nat. Geosci. 4. http://dx.doi.org/10.1038/NGEO1143.

Carrapa, B., Adelmann, D., Hilley, G.E., Mortimer, E., Sobel, E.R., Strecker, M.R., 2005. Oligocene range uplift and development of plateau morphology in the southern central Andes. Tectonics 24 (4). http://dx.doi.org/10.1029/2004tc001762.

Carrapa, B., Trimble, J.D., Stockli, D.F., 2011. Patterns and timing of exhumation and deformation in the Eastern Cordillera of NW Argentina revealed by (U–Th)/He thermochronology. Tectonics 30 (3), TC3003. http://dx.doi.org/10.1029/2010TC002707.

Carter, A., Curtis, M., Schwanenthal, J., 2014. Cenozoic tectonic history of the South Georgia microcontinent and potential as a barrier to Pacific-Atlantic through flow. Geology http://dx.doi.org/10.1130/G35091.1.

Casquet, C., Fanning, C.M., Galindo, C., Pankhurst, R.J., Rapela, C.W., Torres, P., 2010. The Arequipa Massif of Peru: new SHRIMP and isotope constraints on a Paleoproterozoic inlier in the Grenvillian orogen. J. S. Am. Earth Sci. 29 (1), 128–142. http://dx.doi.org/10.1016/j.jsames.2009.08.009.

Charrier, R., Pinto, L., Rodríguez, M.P., 2007. Tectonostatigraphic evolution of the Andean Orogen in Chile. In: Moreno, T., Gibbons, W. (Eds.), The Geology of Chile. The Geological Society, London, pp. 21–114.

Charrier, R., Herail, G., Pinto, L., Garcia, M., Riquelme, R., Farias, M., Munoz, N., 2013. Cenozoic tectonic evolution in the Central Andes in northern Chile and west central Bolivia: implications for paleogeographic, magmatic and mountain building evolution. Int. J. Earth Sci. 102 (1), 235–264. http://dx.doi.org/10.1007/s00531-012-0801-4.

Clift, P.D., Hartley, A.J., 2007. Slow rates of subduction erosion and coastal underplating along the Andean margin of Chile and Peru. Geology 35 (6), 503–506.

Coira, B., Davidson, J., Mpodozis, C., Ramos, V., 1982. Tectonic and magmatic evolution of the Andes of northern Argentina and Chile. Earth-Sci. Rev. 18 (3–4), 303–332. http://dx.doi.org/10.1016/0012-8252(82)90042-3.

Collins, W., 2003. Slab pull, mantle convection, and Pangaean assembly and dispersal. Earth Planet. Sci. Lett. 205 (3), 225–237.

Contreras-Reyes, E., Jara, J., Grevemeyer, I., Ruiz, S., Carrizo, D., 2012. Abrupt change in the dip of the subducting plate beneath north Chile. Nat. Geosci. 5, 342–345. http://dx.doi.org/10.1038/ngeo1447.

Coulbourn, W.T., Moberly, R., 1977. Structural evidence of evolution of fore-arc basins off South-America. Can. J. Earth Sci. 14 (1), 102–116.

Dahlen, F.A., Suppe, J., 1988. Mechanics, growth, and erosion of mountain belts. Geol. Soc. Am. Spec. Pap. 218, 161–178. http://dx.doi.org/10.1130/SPE218-p161.

Dalziel, I., 1981. Back-arc extension in the southern Andes: a review and critical reappraisal. Philos. Trans. R. Soc. London, Ser. A Math. Phys. Sci. 300 (1454), 319–335.

Dalziel, I.W., Forsythe, R.D., 1985. Andean evolution and the terrane concept. In: AAPG (Ed.), Tectonostratigrahic Terranes of the Circum-Pacific Region, Circum Pacific Council Publications, Earth Science Series.

Dalziel, I.W.D., Lawver, L.A., Pearce, J.A., Barker, P.F., Hastie, A.R., Barfod, D.N., Schenke, H.W., Davis, M.B., 2013a. A potential barrier to deep Antarctic circumpolar flow until the late Miocene? Geology 41 (9), 947–950. http://dx.doi.org/10.1130/g34352.1.

Dalziel, I.W.D., Lawver, L.A., Norton, I.O., Gahagan, L.M., 2013b. The Scotia Arc: Genesis, Evolution, Global Significance. In: Jeanloz, R. (Ed.), Annual Review of Earth and Planetary Sciences. vol. 41, pp. 767–793. http://dx.doi.org/10.1146/annurev-earth-050212-124155.

DeConto, R.M., 2009. Plate Tectonics and Climate Change. Encyclopedia of Paleoclimatology and Ancient Environments. Springer, pp. 784–798 (edited).

DeConto, R.M., Pollard, D., Wilson, P.A., Palike, H., Lear, C.H., Pagani, M., 2008. Thresholds for Cenozoic bipolar glaciation. Nature 455 (7213), 652-U652. http://dx.doi.org/10.1038/nature07337.

Decou, A., von Eynatten, H., Mamani, M., Sempere, T., Worner, G., 2011. Cenozoic forearc basin sediments in Southern Peru (15–18 degrees S): stratigraphic and heavy mineral constraints for Eocene to Miocene evolution of the Central Andes. Sediment. Geol. 237 (1–2), 55–72. http://dx.doi.org/10.1016/j.sedgeo.2011.02.004.

Dekens, P.S., Ravelo, A.C., McCarthy, M.D., 2007. Warm upwelling regions in the Pliocene warm period. Paleoceanography 22 (3), PA3211. http://dx.doi.org/10.1029/2006PA001394.

del Papa, C., Hongn, F., Powell, J., Payrola, P., Do Campo, M., Strecker, M., Petrinovic, I., Schmitt, A., Pereyra, R., 2013. Middle Eocene–Oligocene broken-foreland evolution in the Andean Calchaqui Valley, NW Argentina: insights from stratigraphic, structural and provenance studies. Basin Res. 25 (5), 574–593.

DeMets, C., Gordon, R.G., Argus, D.F., Stein, S., 1994. Effect of recent revisions to the geomagnetic reversal time scale on estimates of current plate motions. Geophys. Res. Lett. 21, 2191–2194.

Dunn, J.F., Hartshorn, K.G., Hartshorn, P.W., 1995. Structural styles and hydrocarbon potential of the Sub-Andean thrust belt of southern Bolivia. In: Tankard, A.J., Suárez, R., Welsink, H.J. (Eds.), Petroleum Basins of South America. AAPG Memoir 62, pp. 523–543.

Eagles, G., Jokat, W., 2014. Tectonic reconstructions for paleobathymetry in Drake Passage. Tectonophysics 611, 28–50.

Eagles, G., Livermore, R., Morris, P., 2006. Small basins in the Scotia Sea: the Eocene Drake Passage gateway. Earth Planet. Sci. Lett. 242 (3–4), 343–353. http://dx.doi.org/10.1016/j.epsl.2005.11.060.

Ege, H., Sobel, E.R., Scheuber, E., Jacobshagen, V., 2007. Exhumation history of the southern Altiplano plateau (southern Bolivia) constrained by apatite fission track thermochronology. Tectonics 26 (1). http://dx.doi.org/10.1029/2005tc001869.

Ehlers, T.A., Poulsen, C.J., 2009. Influence of Andean uplift on climate and paleoaltimetry estimates. Earth Planet. Sci. Lett. 281 (3), 238–248.

Eichelberger, N., McQuarrie, N., Ehlers, T.A., Enkelmann, E., Barnes, J.B., Lease, R.O., 2013. New constraints on the chronology, magnitude, and distribution of deformation within the central Andean orocline. Tectonics 32 (5), 1432–1453. http://dx.doi.org/10.1002/tect.20073.

Elger, K., Oncken, O., Glodny, J., 2005. Plateau-style accumulation of deformation: Southern Altiplano. Tectonics 24 (4).

Evenstar, L.A., Hartley, A.J., Stuart, F.M., Mather, A.E., Rice, C.M., Chong, G., 2009. Multiphase development of the Atacama Planation Surface recorded by cosmogenic 3He exposure ages: implications for uplift and Cenozoic climate change in western South America. Geology 37 (1), 27–30. http://dx.doi.org/10.1130/G25437A.1.

Faccenna, C., Becker, T.W., Conrad, C.P., Husson, L., 2013. Mountain building and mantle dynamics. Tectonics 32 (1), 80–93. http://dx.doi.org/10.1029/2012tc003176.

Farías, M., Charrier, R., Comte, D., Martinod, J., Hérail, G., 2005. Late Cenozoic deformation and uplift of the western flank of the Altiplano: evidence from the depositional, tectonic, and geomorphologic evolution and shallow seismic activity (northern Chile at 19°30′S). Tectonics 24, TC4001 (4010.1029/2004TC001667).

Fuller, C.W., Willett, S.D., Brandon, M.T., 2006. Formation of forearc basins and their influence on subduction zone earthquakes. Geology 34 (2), 65–68. http://dx.doi.org/10.1130/G21828.1.

Galli-Olivier, C., 1967. Pediplain in northern Chile and the Andean uplift. Science 158 (3801), 653–655 (0.1126/science.158.3801.653).

García, M., Hérail, G., 2005. Fault-related folding, drainage network evolution and valley incision during the Neogene in the Andean Precordillera of Northern Chile. Geomorphology 65, 279–300.

García, M., Riquelme, R., Farías, M., Hérail, G., Charrier, R., 2011. Late Miocene–Holocene canyon incision in the western Altiplano, northern Chile: tectonic or climatic forcing? J. Geol. Soc. Lond. 168, 1047–1060. http://dx.doi.org/10.1144/0016-76492010-134.

Garreaud, R.D., Vuille, M., Compagnucci, R., Marengo, J., 2009. Present-day South American climate. Palaeogeogr. Palaeoclimatol. Palaeoecol. 281 (3–4), 180–195. http://dx.doi.org/10.1016/j.palaeo.2007.10.032.

Garreaud, R.D., Molina, A., Farias, M., 2010. Andean uplift, ocean cooling and Atacama hyperaridity: a climate modeling perspective. Earth Planet. Sci. Lett. 292 (1–2), 39–50. http://dx.doi.org/10.1016/j.epsl.2010.01.017.

Garzione, C.N., Molnar, P., Libarkin, J.C., MacFadden, B.J., 2006. Rapid late Miocene rise of the Bolivian Altiplano: evidence for removal of mantle lithosphere. Earth Planet. Sci. Lett. 241 (3), 543–556.

Garzione, C.N., Hoke, G.D., Libarkin, J.C., Withers, S., MacFadden, B., Eiler, J., Ghosh, P., Mulch, A., 2008. Rise of the Andes. Science 320 (5881), 1304–1307.

Ghosh, P., Garzione, C.N., Eiler, J.M., 2006. Rapid uplift of the Altiplano revealed through 13C–18O bonds in paleosol carbonates. Science 311 (5760), 511–515.

Grandin, R., Doin, M.P., Bollinger, L., Pinel-Puyssegur, B., Ducret, G., Jolivet, R., Sapkota, S.N., 2012. Long-term growth of the Himalaya inferred from interseismic InSAR measurement. Geology 40 (12), 1059–1062. http://dx.doi.org/10.1130/g33154.1.

Gregory-Wodzicki, K.M., 2000. Uplift history of the Central and Northern Andes: a review. Geol. Soc. Am. Bull. 112 (7), 1091–1105. http://dx.doi.org/10.1130/0016-7606(2000)112<1091:uhotca>2.3.co;2.

Grier, M.E., Salfity, J.A., Allmendinger, R.W., 1991. Andean reactivation of the Cretaceous Salta Rift, northwestern Argentina. J. S. Am. Earth Sci. 4 (4), 351–372. http://dx.doi.org/10.1016/0895-9811(91)90007-8.

Gubbels, T.L., Isacks, B.L., Farrar, E., 1993. High-level surfaces, plateau uplift, and foreland development, Bolivian Central Andes. Geology 21 (8), 695–698. http://dx.doi.org/10.1130/0091-7613(1993)021<0695:hlspua>2.3.co;2.

Hain, M., Strecker, M., Bookhagen, B., Alonso, R., Pingel, H., Schmitt, A., 2011. Neogene to Quaternary broken foreland formation and sedimentation dynamics in the Andes of NW Argentina (25 S). Tectonics 30 (2).

Hall, S.R., Farber, D.L., Audin, L., Finkel, R.C., 2012. Recently active contractile deformation in the forearc of southern Peru. Earth Planet. Sci. Lett. 337, 85–92. http://dx.doi.org/10.1016/j.epsl.2012.04.007.

Hallam, A., 1984. Pre-Quaternary sea-level changes. Annu. Rev. Earth Planet. Sci. 12, 205–243. http://dx.doi.org/10.1146/annurev.ea.12.050184.001225.

Hallam, A., 1985. A review of Mesozoic climates. J. Geol. Soc. 142 (3), 433–445. http://dx.doi.org/10.1144/gsjgs.142.3.0433.

Haq, B.U., Hardenbol, J., Vail, P.R., 1987. Chronology of fluctuating sea levels since the Triassic. Science 235 (4793), 1156–1167. http://dx.doi.org/10.1126/science.235.4793.1156.

Hartley, A.J., Chong, G., 2002. Late Pliocene age for the Atacama Desert: implications for the desertification of western South America. Geology 30 (1), 43–46.

Hartley, A.J., Evenstar, L., 2010. Cenozoic stratigraphic development in the north Chilean forearc: implications for basin development and uplift history of the Central Andean margin. Tectonophysics 495 (1–2), 67–77. http://dx.doi.org/10.1016/j.tecto.2009.05.013.

Hartley, A.J., Chong, G., Houston, J., Mather, A.E., 2005. 150 million years of climatic stability: evidence from the Atacama Desert, northern Chile. J. Geol. Soc. 162, 421–424. http://dx.doi.org/10.1144/0016-764904-071.

Haschke, M., Gunther, A., 2003. Balancing crustal thickening in arcs by tectonic vs. magmatic means. Geology 31 (11), 933–936. http://dx.doi.org/10.1130/g19945.1.

Hay, W., 1996. Tectonics and climate. Geol. Rundsch. 85 (3), 409–437.

Hay, W.W., Soeding, E., DeConto, R.M., Wold, C.N., 2002. The Late Cenozoic uplift–climate change paradox. Int. J. Earth Sci. 91 (5), 746–774.

Heit, B., Sodoudi, F., Yuan, X., Bianchi, M., Kind, R., 2007. An S receiver function analysis of the lithospheric structure in South America. Geophys. Res. Lett. 34 (14). http://dx.doi.org/10.1029/2007gl030317.

Hoke, G.D., Garzione, C.N., 2008. Paleosurfaces, paleoelevation, and the mechanisms for the late Miocene topographic development of the Altiplano plateau. Earth Planet. Sci. Lett. 271 (1), 192–201.

Hoke, L., Lamb, S., 2007. Cenozoic behind-arc volcanism in the Bolivian Andes, South America: implications for mantle melt generation and lithospheric structure. J. Geol. Soc. 164, 795–814. http://dx.doi.org/10.1144/0016-76492006-092.

Hoke, G.D., Isacks, B.L., Jordan, T.E., Blanco, N., Tomlinson, A.J., Ramezani, J., 2007. Geomorphic evidence for post-10 Ma uplift of the western flank of the central Andes 18°30′–22°S. Tectonics 26, TC5021. http://dx.doi.org/10.1029/2006TC002082.

Hoke, G.D., Graber, N.R., Mescua, J.F., Giambiagi, L.B., Fitzgerald, P.G., Metcalf, J.R., 2014. Near pure surface uplift of the Argentine Frontal Cordillera: insights from (U–Th)/He thermochronometry and geomorphic analysis. In: Sepúlveda, S.A., et al. (Eds.), Geodynamic Processes in the Andes of Central Chile and Argentina. Geological Society, London, Special Publications http://dx.doi.org/10.1144/SP399.4.

Horton, B.K., 2005. Revised deformation history of the central Andes: inferences from Cenozoic foredeep and intermontane basins of the Eastern Cordillera, Bolivia. Tectonics 24 (3).

Horton, B.K., Hampton, B.A., Waanders, G.L., 2001. Paleogene synorogenic sedimentation in the Altiplano plateau and implications for initial mountain building in the central Andes. Geol. Soc. Am. Bull. 113 (11), 1387–1400.

Houston, J., Hartley, A.J., 2003. The central andean west-slope rainshadow and its potential contribution to the origin of hyper-aridity in the Atacama desert. Int. J. Climatol. 23 (12), 1453–1464. http://dx.doi.org/10.1002/joc.938.

Hubert-Ferrari, A., King, G.C.P., Manighetti, I., Armijo, R., Meyer, B., Tapponnier, P., 2003. Long-term elasticity in the continental lithosphere; modelling the Aden Ridge Propagation and the Anatolian Extrusion Process. Geophys. J. Int. 153, 111–132.

Husson, L., Conrad, C.P., Faccenna, C., 2008. Tethyan closure, Andean orogeny, and westward drift of the Pacific Basin. Earth Planet. Sci. Lett. 271 (1), 303–310.

Insel, N., Poulsen, C.J., Ehlers, T.A., 2010. Influence of the Andes Mountains on South American moisture transport, convection, and precipitation. Clim. Dyn. 35 (7–8), 1477–1492.

Insel, N., Grove, M., Haschke, M., Barnes, J.B., Schmitt, A.K., Strecker, M.R., 2012. Paleozoic to early Cenozoic cooling and exhumation of the basement underlying the eastern Puna plateau margin prior to plateau growth. Tectonics 31. http://dx.doi.org/10.1029/2012tc003168.

Instituto Geológico Minero y Metalúrgico (INGEMMET), 2001. Mapa Geológico, quadrangles of Caravelí, Chuquibamba, Huambo, Chivay, Ocoña, La Yesera, Aplao, Arequipa, Camaná, Mollendo, La Joya, Puquina, Punta Bombom and Clemesí. Instituto Geológico Minero y Metalúrgico. Scale 1:100,000.

Isacks, B.L., 1988. Uplift of the central Andean plateau and bending of the Bolivian orocline. J. Geophys. Res. 93 (B4), 3211–3231.

Jeffery, M.L., Ehlers, T.A., Yanites, B.J., Poulsen, C.J., 2013. Quantifying the role of paleoclimate and Andean Plateau uplift on river incision. J. Geophys. Res. Earth Surf. 118 (2), 852–871.

Jenkyns, H.C., 2003. Evidence for rapid climate change in the Mesozoic–Palaeogene greenhouse world. Philos. Trans. R. Soc. Lond. Ser. A Math. Phys. Eng. Sci. 361 (1810), 1885–1916. http://dx.doi.org/10.1098/rsta.2003.1240.

Jordan, T.E., Mpodozis, C., Munoz, N., Blanco, N., Pananont, P., Gardeweg, M., 2007. Cenozoic subsurface stratigraphy and structure of the Salar de Atacama Basin, northern Chile. J. S. Am. Earth Sci. 23 (2–3), 122–146. http://dx.doi.org/10.1016/j.jsames.2006.09.024.

Jordan, T.E., Nester, P.L., Blanco, N., Hoke, G.D., Dávila, F., Tomlinson, A.J., 2010. Uplift of the Altiplano-Puna plateau: a view from the west. Tectonics 29, TC5007. http://dx.doi.org/10.1029/2010TC002661.

Jordan, T.E., Kirk-Lawlor, N.E., Blanco, N., Rech, J.A., Cosentino, N.J., 2014. Landscape modification in response to repeated onset of hyperarid paleoclimate states since 14 Ma, Atacama Desert, Chile. Geol. Soc. Am. Bull. B30978, 30971.

Kennan, L., Lamb, S.H., Hoke, L., 1997. High-altitude palaeosurfaces in the Bolivian Andes: evidence for late Cenozoic surface uplift. Geol. Soc. Lond., Spec. Publ. 120 (1), 307–323. http://dx.doi.org/10.1144/gsl.sp.1997.120.01.20.

Kennett, J.P., 1977. Cenozoic evolution of Antarctic glaciation, the circum-Antarctic Ocean, and their impact on global paleoceanography. J. Geophys. Res. Oceans Atmos. 82 (27), 3843–3860. http://dx.doi.org/10.1029/JC082i027p03843.

Kirk-Lawlor, N.E., Jordan, T.E., Rech, J.A., Lehmann, S.B., 2013. Late Miocene to Early Pliocene paleohydrology and landscape evolution of Northern Chile, 19 to 20 S. Palaeogeogr. Palaeoclimatol. Palaeoecol. 387, 76–90.

Kley, J., 1996. Transition from basement-involved to thin-skinned thrusting in the Cordillera Oriental of southern Bolivia. Tectonics 15 (4), 763–775. http://dx.doi.org/10.1029/95tc03868.

Kley, J., 1999. Geologic and geometric constraints on a kinematic model of the Bolivian orocline. J. S. Am. Earth Sci. 12 (2), 221–235.

Kley, J., Monaldi, C., 1998. Tectonic shortening and crustal thickness in the Central Andes: how good is the correlation? Geology 26 (8), 723–726.

Kley, J., Müller, J., Tawackoli, S., Jacobshagen, V., Manutsoglu, E., 1997. Pre-Andean and Andean-age deformation in the Eastern Cordillera of southern Bolivia. J. S. Am. Earth Sci. 10 (1), 1–19.

Kley, J., Monaldi, C., Salfity, J., 1999. Along-strike segmentation of the Andean foreland: causes and consequences. Tectonophysics 301 (1–2), 75–94. http://dx.doi.org/10.1016/S0040-1951(98)90223-2.

Kley, J., Rossello, E.A., Monaldi, C.R., Habighorst, B., 2005. Seismic and field evidence for selective inversion of Cretaceous normal faults, Salta rift, northwest Argentina. Tectonophysics 399 (1–4), 155–172. http://dx.doi.org/10.1016/j.tecto.2004.12.020.

Kukowski, N., Oncken, O., 2006. Subduction Erosion – the "Normal" Mode of Fore-Arc Material Transfer along the Chilean Margin? In: Oncken, O., et al. (Eds.), The Andes, Active Subduction Orogeny. Springer, Berlin, pp. 217–236 http://dx.doi.org/10.1007/978-3-540-48684-8_10

Lagabrielle, Y., Godderis, Y., Donnadieu, Y., Malavieille, J., Suarez, M., 2009. The tectonic history of Drake Passage and its possible impacts on global climate. Earth Planet. Sci. Lett. 279 (3–4), 197–211. http://dx.doi.org/10.1016/j.epsl.2008.12.037.

Lamb, S., 2011. Did shortening in thick crust cause rapid Late Cenozoic uplift in the northern Bolivian Andes? J. Geol. Soc. 168 (5), 1079–1092. http://dx.doi.org/10.1144/0016-76492011-008.

Lamb, S., Davis, P., 2003. Cenozoic climate change as a possible cause for the rise of the Andes. Nature 425 (6960), 792–797. http://dx.doi.org/10.1038/nature02049.

Lawver, L.A., Gahagan, L.M., 2003. Evolution of Cenozoic seaways in the circum-Antarctic region. Palaeogeogr. Palaeoclimatol. Palaeoecol. 198 (1–2), 11–37. http://dx.doi.org/10.1016/s0031-0182(03)00392-4.

Lee, C.-T.A., Shen, B., Slotnick, B.S., Liao, K., Dickens, G.R., Yokoyama, Y., Lenardic, A., Dasgupta, R., Jellinek, M., Lackey, J.S., 2013. Continental arc–island arc fluctuations, growth of crustal carbonates, and long-term climate change. Geosphere 9 (1), 21–36.

Livermore, R., Nankivell, A., Eagles, G., Morris, P., 2005. Paleogene opening of Drake Passage. Earth Planet. Sci. Lett. 236 (1–2), 459–470. http://dx.doi.org/10.1016/j.epsl.2005.03.027.

Livermore, R., Hillenbrand, C.D., Meredith, M., Eagles, G., 2007. Drake Passage and Cenozoic climate: an open and shut case? Geochem. Geophys. Geosyst. 8. http://dx.doi.org/10.1029/2005gc001224.

Loewy, S.L., Connelly, J.N., Dalziel, I.W.D., 2004. An orphaned basement block: the Arequipa–Antofalla basement of the central Andean margin of South America. Geol. Soc. Am. Bull. 116 (1–2), 171–187. http://dx.doi.org/10.1130/b25226.

Lucassen, F., Becchio, R., Wilke, H.G., Franz, G., Thirlwall, M.F., Viramonte, J., Wemmer, K., 2000. Proterozoic–Paleozoic development of the basement of the Central Andes (18–26°S) — a mobile belt of the South American craton. J. S. Am. Earth Sci. 13 (8), 697–715.

Lyon-Caen, H., Molnar, P., Suarez, G., 1985. Gravity anomalies and flexure of the Brazilian Shield beneath the Bolivian Andes. Earth Planet. Sci. Lett. 75 (1), 81–92. http://dx.doi.org/10.1016/0012-821x(85)90053-6.

Maksaev, V., Zentilli, M., 1999. Fission track thermochronology of the Domeyko Cordillera, northern Chile; implications for Andean tectonics and porphyry copper metallogenesis. Explor. Min. Geol. 8 (1–2), 65–89.

Marquardt, C., Lavenu, A., Ortlieb, L., Godoy, E., Comte, D., 2004. Coastal neotectonics in Southern Central Andes: uplift and deformation of marine terraces in Northern Chile (27 S). Tectonophysics 394 (3), 193–219.

McQuarrie, N., 2002. The kinematic history of the central Andean fold-thrust belt, Bolivia: implications for building a high plateau. Geol. Soc. Am. Bull. 114 (8), 950–963. http://dx.doi.org/10.1130/0016-7606(2002)114<0950:tkhotc>2.0.co;2.

McQuarrie, N., Horton, B.K., Zandt, G., Beck, S., DeCelles, P.G., 2005. Lithospheric evolution of the Andean fold-thrust belt, Bolivia, and the origin of the central Andean plateau. Tectonophysics 399 (1–4), 15–37. http://dx.doi.org/10.1016/j.tecto.2004.12.013.

Mégard, F., 1984. The Andean orogenic period and its major structures in central and northern Peru. J. Geol. Soc. 141 (5), 893–900. http://dx.doi.org/10.1144/gsjgs.141.5.0893.

Melnick, D., Bookhagen, B., Echtler, H.P., Strecker, M.R., 2006. Coastal deformation and great subduction earthquakes, Isla Santa María, Chile (37°S). Geol. Soc. Am. Bull. 118 (11–12), 1463–1480. http://dx.doi.org/10.1130/b25865.1.

Molnar, P., Cane, M.A., 2007. Early Pliocene (pre-Ice Age) El Nino-like global climate: which El Nino? Geosphere 3 (5), 337–365. http://dx.doi.org/10.1130/ges00103.1.

Molnar, P., England, P., 1990. Late Cenozoic uplift of mountain ranges and global climate change: chicken or egg? Nature 346 (6279), 29–34. http://dx.doi.org/10.1038/346029a0.

Molnar, P., Garzione, C.N., 2007. Bounds on the viscosity coefficient of continental lithosphere from removal of mantle lithosphere beneath the Altiplano and Eastern Cordillera. Tectonics 26 (2).

Molnar, P., Lyon-Caen, H., 1988. Some simple physical aspects of the support, structure, and evolution of mountain belts. Geol. Soc. Am. Spec. Pap. 218, 179–207.

Montgomery, D.R., Balco, G., Willett, S.D., 2001. Climate, tectonics, and the morphology of the Andes. Geology 29 (7), 579–582. http://dx.doi.org/10.1130/0091-7613(2001)029<0579:ctatmo>2.0.co;2.

Mortimer, C., 1973. The Cenozoic history of the southern Atacama Desert, Chile. J. Geol. Soc. 129 (5), 505–526. http://dx.doi.org/10.1144/gsjgs.129.5.0505.

Mortimer, C., Saric, N., 1975. Cenozoic studies in northernmost Chile. Geol. Rundsch. 64 (1), 395–420.

Mortimer, E., Carrapa, B., Coutand, I., Schoenbohm, L., Sobel, E.R., Gomez, J.S., Strecker, M.R., 2007. Fragmentation of a foreland basin in response to out-of-sequence basement uplifts and structural reactivation: El Cajón–Campo del Arenal basin, NW Argentina. Geol. Soc. Am. Bull. 119 (5–6), 637–653.

Mpodozis, C., Ramos, V.A., 1989. The Andes of Chile and Argentina. In: Ericksen, G.E., Cañas Pinochet, M.T., Reinemund, J.A. (Eds.), Geology of the Andes and its Relation to Hydrocarbon and Mineral Resources. Circum-Pacific Council for Energy and Mineral Resources Earth Sciences Series, Houston, Texas, pp. 59–90.

Mpodozis, C., Ramos, V.A., 2008. Tectónica jurásica en Argentina y Chile: extensión, subducción oblicua, rifting, deriva y colisiones? Rev. Asoc. Geol. Argent. 63 (4), 481–497.

Mpodozis, C., Arriagada, C., Basso, M., Roperch, P., Cobbold, P., Reich, M., 2005. Late Mesozoic to Paleogene stratigraphy of the Salar de Atacama Basin, Antofagasta, Northern Chile: implications for the tectonic evolution of the Central Andes. Tectonophysics 399 (1), 125–154.

Muller, J.P., Kley, J., Jacobshagen, V., 2002. Structure and Cenozoic kinematics of the Eastern Cordillera, southern Bolivia (21 degrees S). Tectonics 21 (5). http://dx.doi.org/10.1029/2001tc001340.

Muñoz, N., Charrier, R., 1996. Uplift of the western border of the Altiplano on a west-vergent thrust system, Northern Chile. J. S. Am. Earth Sci. 9 (3–4), 171–181.

Nester, P., 2008. Basin and Paleoclimate Evolution of the Pampa del Tamarugal Forearc Valley, Atacama Desert, Northern Chile, 253 pp. Cornell Univ, Ithaca, N. Y.

Noble, D.C., McKee, E.H., Megard, F., 1979. Early Tertiary Incaic tectonism, uplify, and volcanic activity, Andes of Central Peru. Geol. Soc. Am. Bull. 90 (10), 903–907. http://dx.doi.org/10.1130/0016-7606(1979)90<903:etitua>2.0.co;2.

Norton, K., Schlunegger, F., 2011. Migrating deformation in the Central Andes from enhanced orographic rainfall. Nat. Commun. 2, 584.

Oncken, O., Kley, J., Elger, K., Victor, P., Schemmann, K., et al., 2006. Deformation of the Central Andean upper plate system — facts, fiction, and constraints for plateau models. In: Oncken, O. (Ed.), The Andes, Active Subduction Orogeny. Springer, Berlin, pp. 3–27 http://dx.doi.org/10.1007/978-3-540-48684-8_1.

Oncken, O., Boutelier, D., Dresen, G., Schemmann, K., 2012. Strain accumulation controls failure of a plate boundary zone: linking deformation of the Central Andes and lithosphere mechanics. Geochem. Geophys. Geosyst. 13, 22. http://dx.doi.org/10.1029/2012gc004280.

Ortlieb, L., Zazo, C., Goy, J., Hillaire-Marcel, C., Ghaleb, B., Cournoyer, L., 1996. Coastal deformation and sea-level changes in the northern Chile subduction area (23 S) during the last 330 ky. Quat. Sci. Rev. 15 (8), 819–831.

Ouimet, W.B., Cook, K.L., 2010. Building the central Andes through axial lower crustal flow. Tectonics 29 (3).

Pardo-Casas, F., Molnar, P., 1987. Relative motion of the Nazca (Farallon) and South-American plates since Late Cretaceous time. Tectonics 6 (3), 233–248. http://dx.doi.org/10.1029/TC006i003p00233.

Picard, D., Sempere, T., Plantard, O., 2008. Direction and timing of uplift propagation in the Peruvian Andes deduced from molecular phylogenetics of highland biotaxa. Earth Planet. Sci. Lett. 271 (1), 326–336.

Pinto, L., Hérail, G., Charrier, R., 2004. Sedimentación sintectónica asociada a las estructuras neógenas en la Precordillera de la zona de Moquella, Tarapacá (19° 15′ S, norte de Chile). Rev. Geol. Chile 31 (1), 19–44.

Pinto, L., Herail, G., Charrier, R., 2010. Syntectonic sedimentation associated with Neogene structures in the Precordillera of Moquella Zone, Tarapacá (19° 15′S, northern Chile). Andean Geol. 31 (1).

Ramos, V.A., 1988. Late Proterozoic–Early Paleozoic of South America: a collisional history. Episodes 11, 168–174.

Ramos, V.A., 2008. The basement of the central Andes: the Arequipa and related terranes. Annu. Rev. Earth Planet. Sci. 36, 289–324 (210.1146/annurev.earth.1136.031207.124304).

Ramos, V.A., 2010. The tectonic regime along the Andes: present-day and Mesozoic regimes. Geol. J. 45 (1), 2–25. http://dx.doi.org/10.1002/gj.1193.

Ramos, V.A., Aleman, A., 2000. Tectonic evolution of the Andes. In: Cordani, U., Milani, E.J., Thomaz Filho, A., Campos Neto, M.C. (Eds.), Tectonic Evolution of South America, pp. 635–685 (31st Int. Geol. Congr., Rio de Janeiro).

Ramos, V.A., Jordan, T.E., Allmendinger, R.W., Mpodozis, C., Kay, S.M., Cortes, J.M., Palma, M., 1986. Paleozoic terranes of the central Argentine–Chilean Andes. Tectonics 5 (6), 855–880. http://dx.doi.org/10.1029/TC005i006p00855.

Rapela, C.W., Pankhurst, R.J., Casquet, C., Baldo, E., Saavedra, J., Galindo, C., 1998. Early evolution of the Proto-Andean margin of South America. Geology 26 (8), 707–710. http://dx.doi.org/10.1130/0091-7613(1998)026<0707:eeotpa>2.3.co;2.

Raymo, M., Ruddiman, W.F., 1992. Tectonic forcing of late Cenozoic climate. Nature 359 (6391), 117–122.

Rech, J.A., Currie, B.S., Michalski, G., Cowan, A.M., 2006. Neogene climate change and uplift in the Atacama Desert, Chile. Geology 34 (9), 761–764.

Rech, J.A., Currie, B.S., Shullenberger, E.D., Dunagan, S.P., Jordan, T.E., Blanco, N., Tomlinson, A.J., Rowe, H.D., Houston, J., 2010. Evidence for the development of the Andean rain shadow from a Neogene isotopic record in the Atacama Desert, Chile. Earth Planet. Sci. Lett. 292 (3), 371–382.

Regard, V., Saillard, M., Martinod, J., Audin, L., Carretier, S., Pedoja, K., Riquelme, R., Paredes, P., Hérail, G., 2010. Renewed uplift of the Central Andes Forearc revealed by coastal evolution during the Quaternary. Earth Planet. Sci. Lett. 297 (1–2), 199–210. http://dx.doi.org/10.1016/j.epsl.2010.06.020.

Roperch, P., Sempere, T., Macedo, O., Arriagada, C., Fornari, M., Tapia, C., Garcia, M., Laj, C., 2006. Counterclockwise rotation of late Eocene–Oligocene fore-arc deposits in southern Peru and its significance for oroclinal bending in the central Andes. Tectonics 25 (3). http://dx.doi.org/10.1029/2005tc001882.

Russo, R.M., Silver, P.G., 1994. Trench-parallel flow beneath the Nazca Plate from seismic anisotropy. Science 263 (5150), 1105–1111. http://dx.doi.org/10.1126/science.263.5150.1105.

Russo, R.M., Silver, P.G., 1996. Cordillera formation, mantle dynamics, and the Wilson cycle. Geology 24 (6), 511–514. http://dx.doi.org/10.1130/0091-7613(1996)024<0511:CFMDAT>2.3.CO;2.

Sáez, A., Cabrera, L., Jensen, A., Chong, G., 1999. Late Neogene lacustrine record and palaeogeography in the Quillagua–Llamara basin, Central Andean fore-arc (northern Chile). Palaeogeogr. Palaeoclimatol. Palaeoecol. 151 (1), 5–37.

Schellart, W.P., Freeman, J., Stegman, D.R., Moresi, L., May, D., 2007. Evolution and diversity of subduction zones controlled by slab width. Nature 446, 308–311. http://dx.doi.org/10.1038/nature05615.

Scher, H.D., Martin, E.E., 2006. Timing and climatic consequences of the opening of Drake Passage. Science 312 (5772), 428–430.

Scheuber, E., Mertmann, D., Ege, H., Silva-González, P., Heubeck, C., Reutter, K.-J., Jacobshagen, V., 2006. Exhumation and basin development related to formation of the central Andean plateau, 21° S. in The Andes, Active Subduction Orogeny. In: Oncken, O., et al. (Eds.), Springer, Berlin, pp. 285–301 http://dx.doi.org/10.1007/978-3-540-48684-8_13.

Schildgen, T.F., Hodges, K.V., Whipple, K.X., Reiners, P.W., Pringle, M.S., 2007. Uplift of the western margin of the Andean plateau revealed from canyon incision history, southern Peru. Geology 35 (6). http://dx.doi.org/10.1130/G23532A.1.

Schildgen, T.F., Hodges, K.V., Whipple, K.X., Pringle, M.S., van Soest, M.C., Cornell, K., 2009. Late Cenozoic structural and tectonic development of the western margin of the central Andean Plateau in southwest Peru. Tectonics 28, TC4007. http://dx.doi.org/10.1029/2008TC002403.

Schildgen, T.F., Balco, G., Shuster, D.L., 2010. Canyon incision and knickpoint propagation recorded by apatite He-4/He-3 thermochronometry. Earth Planet. Sci. Lett. 293 (3–4), 377–387. http://dx.doi.org/10.1016/j.epsl.2010.03.009.

Schlunegger, F., Zeilinger, G., Kounov, A., Kober, F., Hüsser, B., 2006. Scale of relief growth in the forearc of the Andes of Northern Chile (Arica latitude, 18°S). Terra Nova 18, 217–223. http://dx.doi.org/10.1111/j.1365-3121.2006.00682.x.

Schlunegger, F., Kober, F., Zeilinger, G., vonRotz, R., 2010. Sedimentology-based reconstructions of paleoclimate changes in the Central Andes in response to the uplift of the Andes, Arica region between 19 and 21°S latitude, northern Chile. Int. J. Earth Sci. 99 (Supplement 1), 123–137. http://dx.doi.org/10.1007/s00531-010-0572-8.

Sébrier, M., Lavenu, A., Fornari, M., Soulas, J., 1988. Tectonics and uplift in Central Andes (Peru, Bolivia and northern Chile) from Eocene to present. Géodynamique 3 (1–2), 85–106.

Sempere, T., Herail, G., Oller, J., Bonhomme, M.G., 1990. Late Oligocene-early Miocene major tectonic crisis and related basins in Bolivia. Geology 18 (10), 946–949. http://dx.doi.org/10.1130/0091-7613(1990)018<0946:loemmt>2.3.co;2.

Sempere, T., Butler, R.F., Richards, D.R., Marshall, L.G., Sharp, W., Swisher, C.C., 1997. Stratigraphy and chronology of upper Cretaceous lower Paleogene strata in Bolivia and northwest Argentina. Geol. Soc. Am. Bull. 109 (6), 709–727.

Sempere, T., et al., 2002. Late Permian-Middle Jurassic lithospheric thinning in Peru and Bolivia, and its bearing on Andean-age tectonics. Tectonophysics 345 (1–4), 153–181. http://dx.doi.org/10.1016/s0040-1951(01)00211-6.

Servant, M., Sempere, T., Argollo, J., Bernat, M., Feraud, G., Lobello, P., 1989. Cenozoic landsacpe and uplift evolution of the Eastern Cordillera of the Bolivian Andes. C. R. Acad. Sci. II 309 (4), 417–422.

Shackleton, R.M., Ries, A.C., Coward, M.P., Cobbold, P.R., 1979. Structure, metamorphism an geochronology of the Arequipa Massif of coastal Peru. J. Geol. Soc. 136 (2), 195–214. http://dx.doi.org/10.1144/gsjgs.136.2.0195.

Sheffels, B.M., 1990. Lower bound on the amount of crustal shortening, in the central Bolivian Andes. Geology 18 (9), 812–815.

Sijp, W.P., England, M.H., 2004. Effect of the Drake Passage throughflow on global climate. J. Phys. Oceanogr. 34 (5), 1254–1266. http://dx.doi.org/10.1175/1520-0485(2004)034<1254:eotdpt>2.0.co;2.

Sillitoe, R.H., McKee, E.H., 1996. Age of supergene oxidation and enrichment in the Chilean porphyry copper province. Econ. Geol. Bull. Soc. Econ. Geol. 91 (1), 164–179.

Silver, P.G., Russo, R.M., Lithgow-Bertelloni, C., 1998. Coupling of South American and African Plate motion and Plate deformation. Science 279 (5347), 60–63. http://dx.doi.org/10.1126/science.279.5347.60.

Song, T.-R.A., Simons, M., 2003. Large trench-parallel gravity variations predict seismogenic behavior in subduction zones. Science 301 (630). http://dx.doi.org/10.1126/science.1085557.

Starck, D., Anzótegui, L., 2001. The late Miocene climatic change—persistence of a climatic signal through the orogenic stratigraphic record in northwestern Argentina. J. S. Am. Earth Sci. 14 (7), 763–774.

Stern, R.J., 2002. Subduction zones. Rev. Geophys. 40 (4). http://dx.doi.org/10.1029/2001rg000108.

Strecker, M., Cerveny, P., Bloom, A., Malizia, D., 1989. Late Cenozoic tectonism and landscape development in the foreland of the Andes: northern Sierras Pampeanas (26–28 S), Argentina. Tectonics 8 (3), 517–534.

Strecker, M.R., Alonso, R.N., Bookhagen, B., Carrapa, B., Hilley, G.E., Sobel, E.R., Trauth, M.H., 2007. Tectonics and climate of the southern central Andes. Annu. Rev. Earth Planet. Sci. 35, 747–787. http://dx.doi.org/10.1146/annurev.earth.35.031306.140158.

Strecker, M.R., Alonso, R., Bookhagen, B., Carrapa, B., Coutand, I., Hain, M.P., Hilley, G.E., Mortimer, E., Schoenbohm, L., Sobel, E.R., 2009. Does the topographic distribution of the central Andean Puna Plateau result from climatic or geodynamic processes? (vol 37, pg 643, 2009). Geology 37 (9), 790-790.

Suárez, G., Molnar, P., Burchfiel, B.C., 1983. Seismicity, fault plane solutions, depth of faulting, and active tectonics of the Andes of Peru, Ecuador, and southern Colombia. J. Geophys. Res. 88 (B12), 10403–10428.

Takahashi, K., Battisti, D.S., 2007a. Processes controlling the mean tropical pacific precipitation pattern. Part I: The Andes and the eastern Pacific ITCZ. J. Clim. 20 (14), 3434–3451. http://dx.doi.org/10.1175/jcli4198.1.

Takahashi, K., Battisti, D.S., 2007b. Processes controlling the mean tropical pacific precipitation pattern. Part II: The SPCZ and the southeast pacific dry zone. J. Clim. 20 (23), 5696–5706. http://dx.doi.org/10.1175/2007jcli1656.1.

Thouret, J.-C., Wörner, G., Gunnell, Y., Singer, B., Zhang, X., Souriot, T., 2007. Geochronologic and stratigraphic constraints on canyon incision and Miocene uplift of the Central Andes in Peru. Earth Planet. Sci. Lett. 263 (3–4), 151–166. http://dx.doi.org/10.1016/j.epsl.2007.07.023.

Tomlinson, A.J., Blanco, N., Maksaev, V., Dilles, J., Grunder, A., Ladino, M., 2001. Geología de la Cordillera Andina de Quebrada Blanca–Chuquicamata, Regiones I y II (20°30′–22°30′). Servicio Nacional de Geología y Minería (Chile).

Tosdal, R.M., Clark, A.H., Farrar, E., 1984. Cenozoic polyphase landscape and tectonic evolution of the Cordillera Occidental, southernmost Peru. GSA Bull. 95 (11) (1318-1133, 10.1130/0016-7606(1984)95 < 1318:CPLATE > 2.0.CO;2).

Uba, C.E., Strecker, M.R., Schmitt, A.K., 2007. Increased sediment accumulation rates and climatic forcing in the central Andes during the late Miocene. Geology 35 (11), 979–982.

Uyeda, S., Kanamori, H., 1979. Back-Arc opening and the mode of subduction. J. Geophys. Res. 84 (B3), 1049–1061.

Vergara, H., and A. Thomas (1984), Hoja Collacagua, Región de Tarapacá, scale 1:250.000, Carta Geológica de Chile - Servicio Nacional de Geología y Minería, Santiago, Chile.

Victor, P., Oncken, O., Glodny, J., 2004. Uplift of the western Altiplano plateau: evidence from the Precordillera between 20° and 21°S (northern Chile). Tectonics 23, TC4004 (4010.1029/2003TC001519).

Vigny, C., et al., 2011. The 2010 Mw 8.8 Maule Megathrust Earthquake of Central Chile, Monitored by GPS. Science 332 (1417). http://dx.doi.org/10.1126/science.1204132.

von Huene, R., Ranero, C., 2003. Subduction erosion and basal friction along the sediment-starved convergent margin off Antofagasta, Chile. J. Geophys. Res. Solid Earth (1978–2012) 108 (B2).

Wells, R.E., Blakely, R.J., Sugiyama, Y., Scholl, D.W., Dinterman, P.A., 2003. Basin-centered asperities in great subduction zone earthquakes: a link between slip, subsidence, and subduction erosion? J. Geophys. Res. 108 (B10), 2507. http://dx.doi.org/10.1029/2002JB002072.

Whipple, K.X., Gasparini, N.M., 2014. Tectonic control of topography, rainfall patterns, and erosion during rapid post-12 Ma uplift of the Bolivian Andes. Lithosphere 6 (4), 251–268. http://dx.doi.org/10.1130/l325.1.

Willett, S.D., 1999. Orogeny and orography: the effects of erosion on the structure of mountain belts. J. Geophys. Res. Solid Earth 104 (B12), 28957–28981. http://dx.doi.org/10.1029/1999jb900248.

Wölbern, I., Heit, B., Yuan, X., Asch, G., Kind, R., Viramonte, J., Tawackoli, S., Wilke, H., 2009. Receiver function images from the Moho and the slab beneath the Altiplano and Puna plateaus in the Central Andes. Geophys. J. Int. 177 (1), 296–308. http://dx.doi.org/10.1111/j.1365-246X.2008.04075.x.

Yuan, X., et al., 2000. Subduction and collision processes in the Central Andes constrained by converted seismic phases. Nature 408, 958–961. http://dx.doi.org/10.1038/35050073.

Zachos, J., Pagani, M., Sloan, L., Thomas, E., Billups, K., 2001. Trends, rhythms, and aberrations in global climate 65 Ma to present. Science 292 (5517), 686–693. http://dx.doi.org/10.1126/science.1059412.

Zachos, J.C., Dickens, G.R., Zeebe, R.E., 2008. An early Cenozoic perspective on greenhouse warming and carbon-cycle dynamics. Nature 451 (7176), 279–283. http://dx.doi.org/10.1038/nature06588.